UNIVERSIDADE DA BEIRA INTERIOR
Engenharia

Dynamic Behavior of a Single Droplet Impinging onto a Sloped Surface

Inês Alexandra dos Santos Ferrão

Dissertação para obtenção do Grau de Mestre em
Engenharia Aeronáutica
(ciclo de estudos integrado)

Orientador: Prof. Doutor André Resende Rodrigues da Silva

Covilhã, outubro de 2018

Acknowledgments

Firstly, I would like to express my sincere gratitude to my supervisor, Professor André Resende Rodrigues da Silva for providing me with this opportunity. I also want to thank for his guidance, dedication and knowledge. It was an honor to work under his supervision.

I also sincerely thank Professor Jorge Manuel Martins Barata, president of AeroG – Aeronautics and Astronautics Research Center for the opportunity to participate in their activities and to improve the scientific research. There are no words to thank all the colleagues who belong to AeroG, for the support, friendship and for all the good times. Especially, to the PhD student Daniela Ribeiro for always listening and giving me encouragement words. I would like to acknowledge the endless help, generous advices, and all the support during the study.

I would like to thank Professor António Mendes and PhD student Francisco Braga who aided me with the measurement of the surface roughness. Thanks for the help and availability.

My acknowledgments are also going to the lab technician, Mr. Rui Manuel Tomé Paulo, who has been helpful and for the support given in the building of the experimental facility.

To my dear friends, I want to thank for their friendship, support, unforgettable and unique moments. Especially to Gonçalo, who supported me with love and not letting me give up. Thank you for your understanding and patience throughout this journey.

Lastly, I would like to take this opportunity to express my gratitude to my family who always inspired me and believed in me. Particularly to my parents and brother, for their unconditional support throughout the last difficult years. Without them, nothing of this would be possible.

Resumo

O impacto de gotas é um fenómeno frequente que ocorre em diversas aplicações, tais como na injeção de combustível em motores de combustão interna, processos de pintura que envolvem spray e resfriamento de equipamentos eletrónicos. Devido ao avanço tecnológico, torna-se possível observar detalhadamente a dinâmica do impacto de gotas. No estudo do impacto de gotas os parâmetros que influenciam são: os fluídos, juntamente com as suas propriedades físicas, a superfície de impacto, o ambiente circundante e ainda a aceleração gravítica. A combinação desses termos leva a efeitos diferentes e únicos.

Verificou-se que os estudos sobre o comportamento dinâmico dos impactos oblíquos são escassos e não estão completamente compreendidos. Consequentemente decidiu-se aprofundar o respetivo tema através do desenvolvimento do presente trabalho.

O principal objetivo do presente trabalho é uma comparação entre dois estudos experimentais. Um dos trabalhos é referente ao impacto de gotas sobre uma superfície seca com um escoamento cruzado e o outro corresponde ao impacto de gotas sobre uma superfície inclinada, usando duas placas secas de alumínio com uma dada rugosidade média (Ra = 0,19μm e Ra = 0,13μm). Devido ao escoamento cruzado, a gota não tem a mesma direção da aceleração gravítica e sofre uma certa deformação que parece influenciar a condição de impacto. Para a superfície inclinada, a gota é esférica ao longo da trajetória e tanto a aceleração gravítica como o movimento da gotícula têm a mesma direção. Neste estudo foi considerada uma velocidade de escoamento cruzado de $7m/s$ e foi projetado um mecanismo que tem a possibilidade de variar os ângulos da superfície. Foram utilizados quatro fluidos: 100% Jet-Fuel, 75%JF - 25% HVO, 50%JF - 50%HVO e H_2O (água pura) como referência. Considerou-se uma combinação de um combustível de aviação convencional, Jet A-1 e um biocombustível (HVO - Óleo Vegetal Hidroprocessado) mais especificamente e NEXBTL. Com o objetivo de implementar novas alternativas para reduzir os níveis de poluição. É através destas inovações que é possível melhorar vários sistemas, tais como motores a pistão ou turbinas a gás com combustíveis alternativos. A fim de manter a coerência dos resultados entre os dois trabalhos experimentais, a velocidade de impacto e o ângulo de incidência foram mantidos aproximadamente os mesmos nas duas atividades. Devido às diferentes condições de impacto, apenas dois fenómenos eram esperados: deposição e splash. Foi desenvolvido um algoritmo em MATLAB para determinar os diâmetros de gotas e as velocidades de impacto.

Os dados experimentais obtidos permitem comparar os limites de splash disponíveis na literatura. O objetivo dessas correlações empíricas é prever a transição entre deposição e splash. Desta forma, para o impacto normal também foi estudado e analisado o limite splash/non-splash para as duas superfícies de impacto.

Palavras-chave

Impacto de gotas, Impacto oblíquo, Superfície inclinada, Escoamento cruzado, Jet-Fuel, Biocombustível, Limite de Splash.

Abstract

Droplet impact is a common phenomenon that occurs frequently in several applications such as fuel injection in internal combustion engines, processes involving spray paints and cooling of electronic equipment. Due to the technological advance, it becomes possible to observe in detail the dynamic impingement. In the study of droplet impingement, the influencing parameters are the liquid, along with its physical properties, the impact surface, the surrounding environment, or by the action of gravity. The combination of these terms lead to different and unique effects.

The researches concerning the dynamic behavior of oblique impacts are scarce and not fully understood. Consequently, it was decided to deepen its theme through the development of this work.

The major goal of the present work is a comparison that involves an experimental study of the phenomena occurring during the impact of liquid droplets onto a dry surface with a cross flowing air and droplets impact onto a sloped surface, using two dry aluminum plates with mean roughness (Ra=$0.19\mu m$ and Ra=$0.13\mu m$). Due to the crossflow, the droplet does not have the same direction as the gravitational acceleration and suffers a certain deformation that seems to vary the condition. For the sloped surface, the droplet is spherical throughout the trajectory and both the gravitational acceleration and movement of the droplet have the same direction. In this study, it was considered a crossflow velocity of $7m/s$ and it was designed a mechanism that has the possibility to vary the surface angles. Four fluids were used: 100% Jet-Fuel, 75%JF - 25%HVO, 50%JF - 50%HVO and H_2O (pure water) as a reference. It was considered a combination of a conventional jet fuel and a biofuel (HVO – Hydroprocessed Vegetable Oil), more specifically Jet A-1 and NEXBTL, with the aim to implement new alternatives to reduce the pollution levels. It is through these innovations that it is possible to improve various systems such as piston engines or gas turbines with alternative fuels. In order to maintain the coherence of the results between the two experimental works, the impact velocity and incident angle were kept approximately the same, in the two activities. Due to the different impact conditions, only two phenomena were expected for this comparison: spreading and splash. A MATLAB algorithm was developed to achieve the different droplet diameters and impact velocities. The researches concerning the dynamic behavior of oblique impacts are scarce, and not fully understood.

The experimental data obtained allows comparing the splashing thresholds available in the literature. The purpose of this empirical correlations is to predict the transition between deposition and splash. Therefore, the normal impact was also studied and analyzed the splash/non-splash transition for the two impact surfaces analyzed.

Keywords

Droplet impact, Oblique impact, Sloped surface, Crossflow, Jet-Fuel, Biofuel, Splashing Threshold.

Index

List of Figures

List of Tables

Nomenclature

Symbol	Designation	Units
A, B	Surface Roughness Coefficient	–
Al	Aluminum	–
a, b, k	Dependent Constants	–
Bo	Bond Number	–
Ca	Capillary Number	–
D_0	Droplet Diameter	$[mm]$
D_{cs}	Deformed Droplet Characteristic Length in the Cross-Stream Direction	$[mm]$
D_{in}	Needle Inner Diameter	$[mm]$
D_{out}	Needle Outer Diameter	$[mm]$
Fr	Froude Number	–
g	Gravitational Acceleration Constant	$[ms^{-2}]$
K_c	Splashing Parameter	–
La	Laplace Number	–
m	Slope	$[^o]$
m	Mass of Substance	$[Kg]$
Oh	Ohnesorge Number	–
Ra	Mean Roughness Surface	$[\mu m]$
Re	Reynolds Number	–
U	Impact Velocity	$[ms^{-1}]$
U_{cf}	Crossflow Velocity	–
u_n	Normal Velocity Component	$[ms^{-1}]$
u_t	Tangential Velocity Component	$[ms^{-1}]$
u_{no}	Critical Velocity for Splashing at a Normal Angle of Incidence	$[ms^{-1}]$
V	Volume of Substance	$[m^3]$
We	Weber Number	–
We_c	Critical Weber Number	–
We_n	Normal Weber Number	–
We_t	Tangential Weber Number	–

Greek symbols

Symbol	Designation	Units
θ	Incident angle	$[^o]$
θ_{static}	Static contact angle	$[^o]$
μ	Dynamic Viscosity	$[mPa.s]$
ρ	Density	$[Kgm^{-3}]$
σ	Surface tension	$[mNm^{-1}]$
τ	Time after impact	$[ms]$

Subscripts

0	Related to the droplet
c	Critical value
cf	Crossflow
cs	Cross-stream direction
in	Inner diameter
n	Normal component
out	Outer diameter
t	Tangential component

List of Acronyms

fps	Frames per second
HEFA	Hydroprocessed Esters and Fatty Acids
HVO	Hydroprocessed Vegetable Oil
IC	Internal combustion
JF	Jet-Fuel
LED	Light Emitting Diode
PTFE	Polytetrafluoethylene
NEXTBL	Next Generation Biomass-to-Liquid
SHP	Superhydrophobic
ST	Splashing threshold

Chapter 1

1. Introduction

Firstly, in this chapter, the motivation will be presented in order to explain the importance of this experimental work. Thereafter, a literature review was elaborated to provide support, which includes the relevant studies for the present work. In the third section, the main objectives planned for this dissertation are presented. The last section regards the overview, where the organization of this work is explained.

1.1 Motivation

Throughout the years, the aeronautical industry has proved indispensable to society. In order to be as effective as possible, this industry has undergone several changes. One of the main dilemmas is the dependency of fuel, which is fundamentally derived from oil (figure 1.1). The constant changes in oil prices have greatly hampered the financial sector. However, the biggest problem is greenhouse gas emissions. Consequently, the aeronautical industry is pursuing new alternatives that contribute to the reduction of the environmental pollution.

This reality requires an immediate demand for other energy sources, so biofuels are an emerging alternative. In this manner, raising expectations about the generation of energy in the world in a sustainable way is necessary to protect the environment .

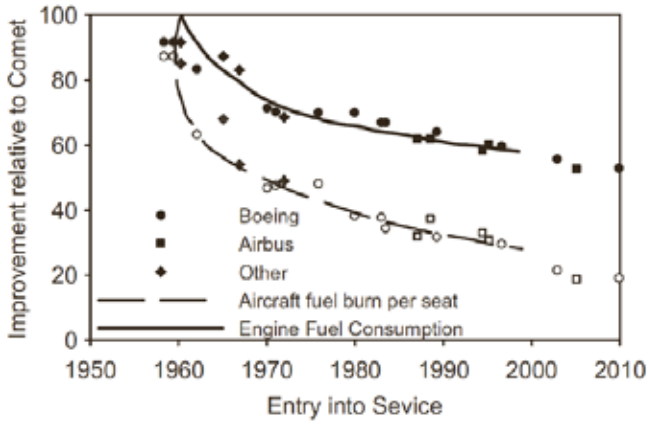

Figure 1.1- Diagram regarding fuel consumption reduction over the last 60 years adapted, The values are referred to the De Havilland Comet, the first civil jet airliner adapted from (Pizziol, 2017).

Currently, biofuels are intended as a substitute for conventional fuels. The difference between these two fluids is the process of production, cleanliness and quality. Conventional fuels are of fossil origin, so their resources are scarce and not renewable. On the contrary, biofuels are of biological origin, in particular, derived from plants and animals, hence can be easily replaced and, when burned have less impact on the environment. It is essential to study the addition of biofuels in the fuel mixture of aircraft engines, in order to operate adequately and with the desired effect. Spray-surface interaction is considered an important phenomenon in internal combustion engines. Analyzing the phenomena observed in this interaction using conventional fuel and biofuel is an advance in sustainable development. Several studies were done in order to improve and understand these processes. Silva (2007) analyzed experimentally and numerically the physical aspects of the fuel processes.

Regarding the oblique impacts, it can be noticed at fuel injection on combustion walls or onto airplane wings, when it is considered icing studies. Researches evolving oblique impacts are scarce and not fully understood.

The aim of the present work is to obtain enhanced knowledge about the behavior of droplet impingement onto sloped surfaces. Thus, a comparative study between a droplet impact onto a sloped surface and a droplet impact onto a surface with the influence of a crossflow was developed. Due to the issue that was mentioned before, in this experimental study Jet-Fuel and biofuel were the fluids considered. According to the current legislation, in civil aviation, it only allows fuel mixtures with at least 50% Jet-Fuel in volume. Due to this, in this work, it was only considered mixtures with 50% or less of biofuel. The alternative fuel chosen is the NEXBTL, an hydroprocessed vegetable oil known as HVO (Pizziol, 2017).

1.2 Literature Review

Over the past century, many studies have been done based on the collision between liquid droplets and a surface which could be dry or wetted, smooth or rough and even sloped. So, the phenomenon of droplet impingement on a surface has many applications such as spray cooling, inkjet printing, pesticide spraying and engine combustion, where the secondary droplet size distribution after impact is taken into consideration.

The outcomes of the impingement depend on the various impact conditions. So, the influencing parameters are the liquid along with its physical properties, the impact surface, the surrounding environment, or by the action of gravity. Relating all of these aspects and analyze the impact of the droplets it is possible to increase the knowledge regarding this theme.

Therefore, it is necessary to have knowledge about some details. The impingement governing parameters, impact regimes, oblique impact, surface roughness and splashing threshold will be addressed in the following subsections.

1.2.1 Impingement Governing Parameters

As already mentioned the phenomena observed due to droplet impact are conditioned by several parameters such as liquid properties or surface conditions. Through the recent advances in technology, the researchers were able to perform detailed experimental studies of droplet impact dynamics. The outcomes were grouped into categories and for a better understanding the dimensionless numbers were considered, presented below.

Weber number

This dimensionless number represents a measure of droplet kinetic energy and surface energy. The kinetic energy intends to deform the shape of the droplet, whereas the surface energy tries to keep the droplet geometrically compact. The viscous effects are neglected,

$$We = \frac{\rho U^2 D_0}{\sigma} \qquad (1.1)$$

where U corresponds to the droplet impact velocity and D_0 is the droplet diameter. So, ρ and σ are density and surface tension of the droplet fluid, respectively.

For an inclined impact, the droplet dynamics depend on two distinct Weber numbers, based on the velocity components normal and tangential to the surface. Therefore, these numbers are given by the expressions below. The expression (1.2) exhibits, the ratio of the *n*-direction (normal direction) collisional energy to the surface energy. Unlike this, the expression (1.3) exhibits, the ratio of the *t*-direction (tangential direction) collisional energy to the surface energy. The normal Weber number (We_n) is used to distinguish the regimes of deposition and splashing when the droplet impacts on an inclined surface (Zen et al, 2010). The expression for the tangential Weber number is represented by We_t.

$$We_n = \frac{\rho u_n^2 D_0}{\sigma} \qquad (1.2)$$

$$We_t = \frac{\rho u_t^2 D_0}{\sigma} \qquad (1.3)$$

Reynold number

This number expresses the ratio between inertial and viscous forces,

$$Re = \frac{\rho U D_0}{\mu} \qquad (1.4)$$

where μ is the dynamic viscosity of the droplet fluid.

Ohnesorge number

This number describes the relation between capillary and viscous forces and is important in the characterization of disintegration processes.

$$Oh = \frac{\mu}{\sqrt{\rho\sigma D_0}} = \frac{\sqrt{We}}{Re} \quad (1.5)$$

Capillary number

The capillary number establishes the relation between viscous forces and surface tension forces.

$$Ca = \frac{We}{Re} = \frac{\mu}{\sigma}U \quad (1.6)$$

Laplace number

This dimensionless number relates the surface tension and viscous forces action on the liquid.

$$La = \frac{\rho\sigma D_0}{\mu^2} = \frac{Re^2}{We} = \frac{We}{Ca^2} = \frac{Re}{Ca} = Oh^{-2} \quad (1.7)$$

Gravity-related effects are characterized by the *Bond number*, or by the *Froude number*.

Bond number

The Bond number, the is relation between the body (gravitational) forces and surface tension forces,

$$Bo = \frac{\rho g D_0^2}{\sigma} \quad (1.8)$$

where g corresponds to the gravitational acceleration.

Froude number

This number describes the ratio between inertial and gravitational forces. Dispense viscous effects. This is the dimensionless parameter that can show if gravity can be neglected.

$$Fr = \frac{U^2}{gD_0} = \frac{We}{Bo} \quad (1.9)$$

In general, gravity effects can be neglected for $Fr \geq 10^2$ (Deegan et al. 2008).

1.2.2 Impact Regimes

The resultant phenomenon of a droplet impacting onto a solid and liquid surface depend on the properties of the liquid, the characteristics of the target surface such as roughness, temperature, inclination, the influence of a crossflow, and the kinematics parameters such as velocity and momentum. The impact on dry surfaces is influence by the surface characteristics, such as wettability and roughness (Yarin, 2006). The behavior of a droplet impinging perpendicular to a surface has been studied in an intensive way using experimental or numerical methods and several discoveries were introduced in the scientific community. Nevertheless, studies in impact with an inclined surface are scarce so it is important to investigate in order to understand the parameters that most condition it. The desired outcome may vary according to the application. Thus, the deposition is requested in some applications like spray painting and metal sprays, whereas in inhalators and in engine combustions, the distribution of secondary droplet size after impacting is taken into consideration.

To be more specific, at the moment of impact, due to the shape oscillations, a droplet may be spherical or elliptical. The impact can be on the free surface of a liquid in a deep pool, on a thin liquid film or on a dry solid surface. As mentioned before, the impact may be normal (perpendicular) or oblique, in air or in vacuum. The liquid may be Newtonian or non-Newtonian. The liquids of the droplet and pool/film may be miscible or immiscible. The solid surface may be hard or soft, rough or smooth, chemically homogeneous or heterogeneous. It may also be porous, flat or curved, at the same temperature of the droplet or at a different one (Yarin, 2006).

Figure 1.2 demonstrates the different parameters that are important during droplet impact. It is shown the physiognomy of the liquid drop, the different types of impact and the most used target surfaces.

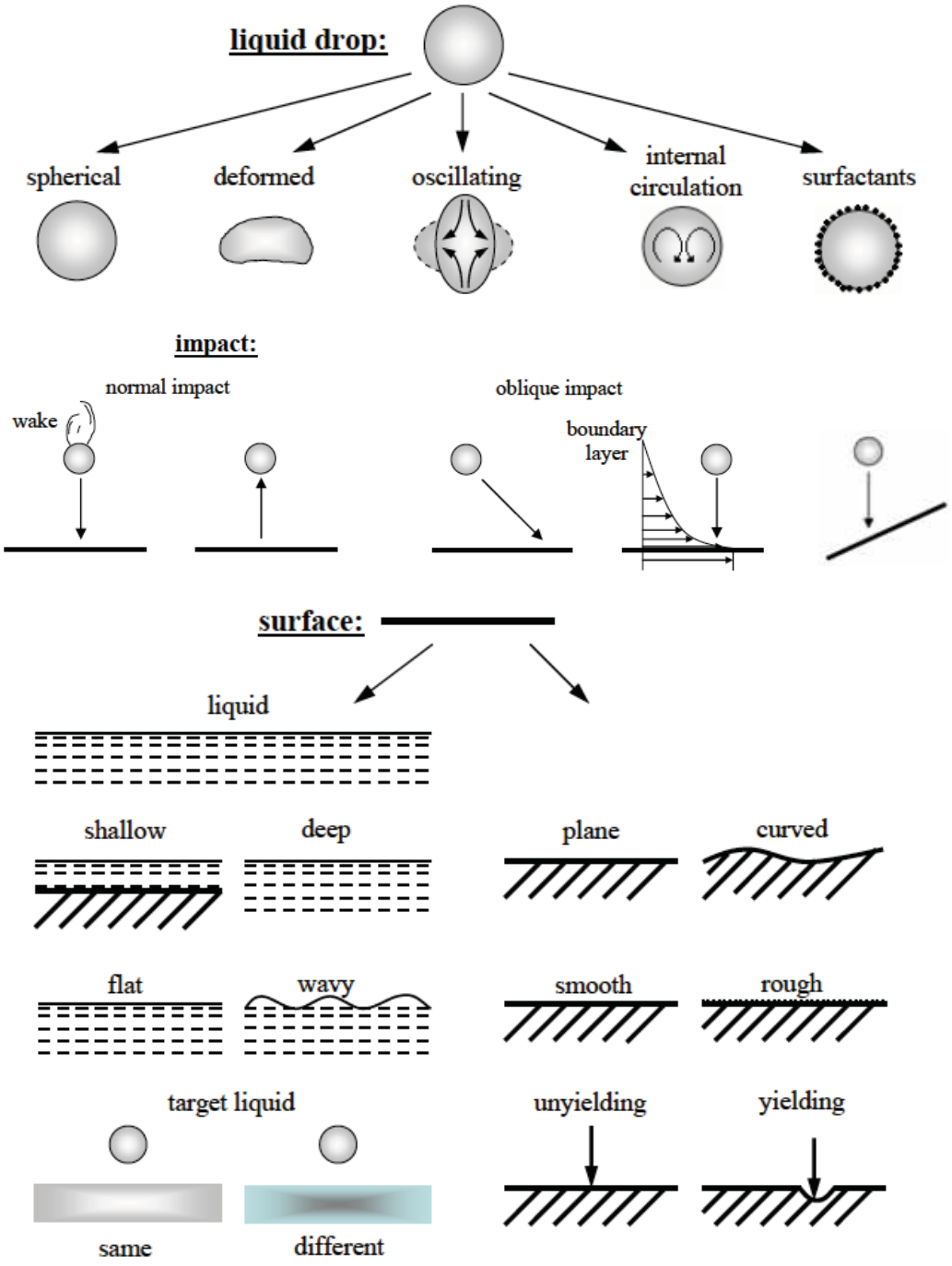

Figure 1.2 - Survey of parameters governing the impact of a liquid drop adapted from (Silva, 2007).

Worthington (1876) was the first trying to understand the droplet impingement. However, did not have advanced techniques to photograph, so the author developed a mechanism that captured the phenomenon a few moments after the impact. The purpose of the investigation was to observe the droplet standards of various liquids at different falling heights on a horizontal smoked glass plate, and through this, it was possible to distinguish spread and disintegration.

A few years later, through the technological advance and interest in executing more experimental activities to expand the knowledge about droplet impingement, Bai and Gosman (1995) described a model for the simulation of spray/surface interactions within the framework of the Lagrangian approach.

According to Bai and Gosman (1995) it can be found four basic different outcomes. They are denominated by stick, spread, rebound, and splash.

Stick

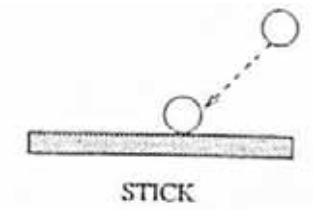

Figure 1.3 - Stick regime from Bai and Gosman (1995).

Stick happens when the impinging droplet adheres to the wall in nearly spherical form. The stick regime usually occurs at a very low Weber number (figure 1.3).

Spread

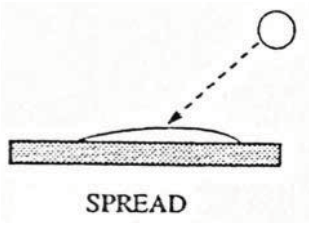

Figure 1.4 - Spread regime from Bai and Gosman (1995).

Spread occurs when the droplet impacts with a moderate velocity onto a dry or wetted wall and spreads out to form a wall film for a dry wall, or merges with the pre-existing liquid film for a wetted wall (figure 1.4), according Bai and Gosman (1995).

Rebound

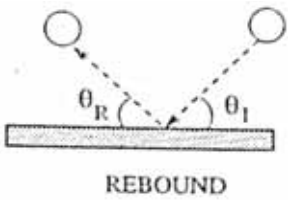

Figure 1.5 - Rebound regime from Bai and Gosman (1995).

Rebound is observed when the impinging droplet bounces off the wall after impact, Figure 1.5. Rebound occurs if the droplet owns sufficient kinetic energy transformed from the droplet surface energy, it can lift off the surface completely. The rebound is an outcome that may occur at the end of the recoiling phase (figure 1.5).

Splash

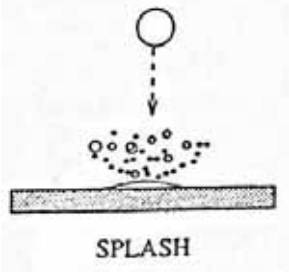

Figure 1.6 - Splash regime from Bai and Gosman (1995).

This phenomenon is observed when a droplet collide with a surface at a high impact energy, a crown is formed, jets develop on the periphery of the crown and these jets become unstable and break up into many fragments, figure 1.6.

A few years later, Rioboo et al. (2001) analyzed previous works, such as Cossali et al. (1997) and they investigated in more detail the classification of the outcomes. Their work was performed on dry surfaces and at a normal impact angle. They tested water, ethanol, glycol/water mixtures, and silicone droplets on surfaces with various degrees of wettability and roughness. It was observed six different outcomes: deposition, prompt splash, corona splash, receding break-up, partial rebound, and complete rebound. Some of them were reported by Bai and Gosman (1995), as already been demonstrated.

Deposition or Spread

Deposition or spread also observed previously in Bai and Gosman (1995), refers to the droplet deformation without any break-up and stays attached to the surface, as already referenced. The deposition refers to an impact in which the droplet simply spreads and retracts sticking to the surface, as can be seen in figure 1.7. According to Chen and Wang (2005) this phenomenon usually happens in low-energy impacts or impacts with a medium tangential Weber number. During the spread, it may occur fingering and at later stages, the droplet may rebound from the surface, that will be referenced later Moita (2009).

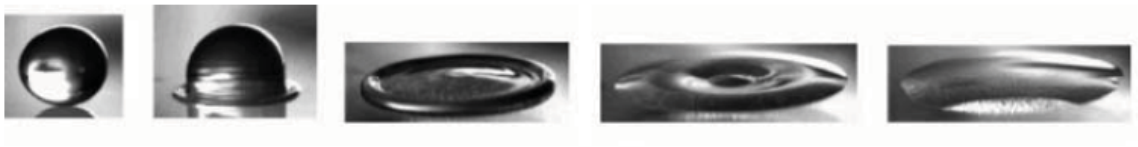

Figure 1.7 - Spreading according to Rioboo et al. (2001).

Prompt splash and Corona splash

Splash was reported by Bai and Gosman (1995). However, some authors divided this phenomenon in two: prompt and crown splash.

Prompt splash is observed when the Weber number is high enough to generate small droplets that are ejected from the impact region or the crown edge when it is still advancing. Thus, the prompt splash is characterized by the break-up of the main droplet into secondary droplets, right at the early instants after impact. They also noticed that this phenomenon only occurs in rough surfaces. However, it has been verified, in the most recent literature, that not only prompt splash is verified in this type of surface, but it is mostly influenced by the surface structure (figure 1.8).

Figure 1.8 - Prompt splash according to Rioboo et al. (2001).

Corona splash, also known as delayed or crown splash, usually occurs in impacts involving liquid films. This phenomenon produces droplets from crown fluid sheet and occurs near or after the stage of maximum expansion, show in figure 1.9.

Previously, this distinction between prompt and corona or delayed splash was referend by Cossali et al. (1997). It was also reported that respectively, to secondary droplets in prompt splash they are smaller than produced by delayed splash.

According to Yarin (2006), corona or crown can be understood as the crater surrounded by a rather thick rim of displaced liquid, for a better understanding of this effect.

More concretely, Josserand and Thoroddsen (2016) reported that splashing arises from the breakup of a fine liquid sheet that is ejected radially along the substrate.

Figure 1.9 - Crown splash according to Rioboo et al. (2001).

Receding break-up

Receding break-up occurs when the lamella starts to recede after reaching the maximum spreading diameter. So, if the dynamic contact angle reaches zero, that means that some drops are left behind by the receding lamella (figure 1.10).

Rioboo et al. (2001) reported that this outcome only occurs when a receding phase is observed and this is influenced by the maximum diameter reached by the spreading droplet and the receding contact angle.

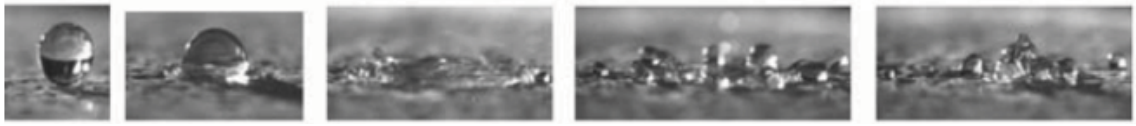

Figure 1.10 - Receding break-up according to Rioboo et al. (2001).

Partial rebound and Complete rebound

According to Ribeiro (2018), taking into consideration the surface properties, rebound only happen for the impact upon dry surfaces whereas, the partial rebound can happen in dry or liquid surfaces (figure 1.11) and (figure 1.12).

Figure 1.11 - Complete rebound from Rioboo et al. (2001).

Figure 1.12 - Partial rebound according to Rioboo et al. (2001).

Furthermore, Rioboo et al. (2001) concluded that the difference between partial and complete rebound is the dynamic receding contact angle. Therefore, low values of contact angle correspond to partial rebound and for high values, a complete rebound occurs. To understand the importance of the contact angle will be presented the concept of wettability.

Wettability describes the ability of a liquid to spread on a solid and it can be represented by the angle between the contour of the drop surface and the interface liquid/solid, denominated by the static contact angle (θ_{static}). Static contact angles are measured when the droplet is standing on the surface. The contact angle decreases as the wettability increases. High wettability corresponds to small contact angles ($\theta_{static} < 90^{\circ}$), while low wettability corresponds to large contact angles ($\theta_{static} > 90^{\circ}$), as shown in figure 1.13.

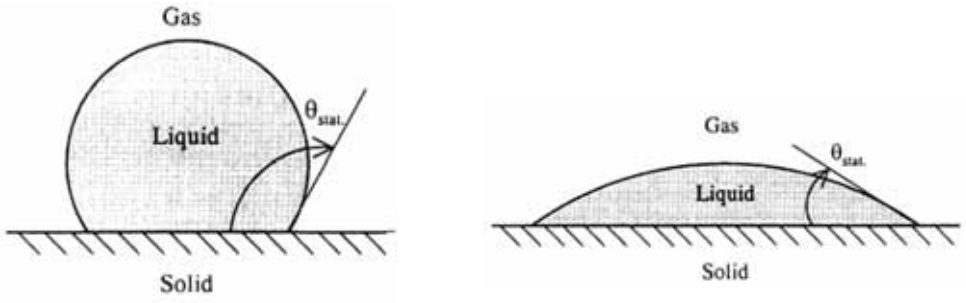

(a) (b)

Figure 1.13 - Definition of static contact angle: a) Non-wetting system; b) Highly wettable system.

The results obtained due to droplet impingement depend on the combination of several boundary conditions, such as the impact velocity, droplet diameter, viscosity, and others. Rioboo et al. (2001), agglutinated all of these phenomena in table 1.1 and demonstrated the effects of the various parameters.

Table 1.1 - Six outcomes influenced by several parameters adapted from Rioboo et al. (2001).

Increase of	Deposition	Prompt splash	Corona splash	Receding breakup	Partial rebound	Complete rebound
U	↓	↑	↑	↑	↑	
D_0	↓	↑				
σ		↓	↓	↑	↑	↑
μ	↑	↓	↓	↓		
θ_{static}				↑	↑	↑

The fingering was another observed outcome in droplet impingement and it was not referenced by Bai and Gosman (1995), and Rioboo et al. (2001). This outcome occurs when there is an instability in the rim of the lamella at the beginning of the spreading phase. Thus, at moderate impact velocities, it is visible some fingers-like shape structures growing ahead of the contact line and further break up during the last stages (Marmanis and Thoroddsen, 1996), as can be seen in figure 1.14. Thoroddsen and Sakakibara (1998), performed several studies in order to understand the evolution of the fingering pattern.

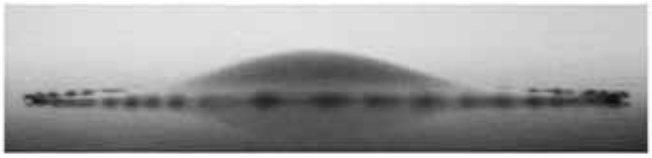

Figure 1.14 - Fingering from Thoroddsen and Sakakibara (1998).

Figure 1.15 shows an evolution of the frontal undulations during the spreading, seeing the lamellar expansion for a better understanding of fingering. This phenomenon was also reported by Yarin (2006).

Figure 1.15 - Frontal undulations during the spreading from Thoroddsen and Sakakibara (1998).

The focus of various researches were the characteristics of the impinging droplets and their outcomes taking into consideration the impact energy, shown on figure 1.16.

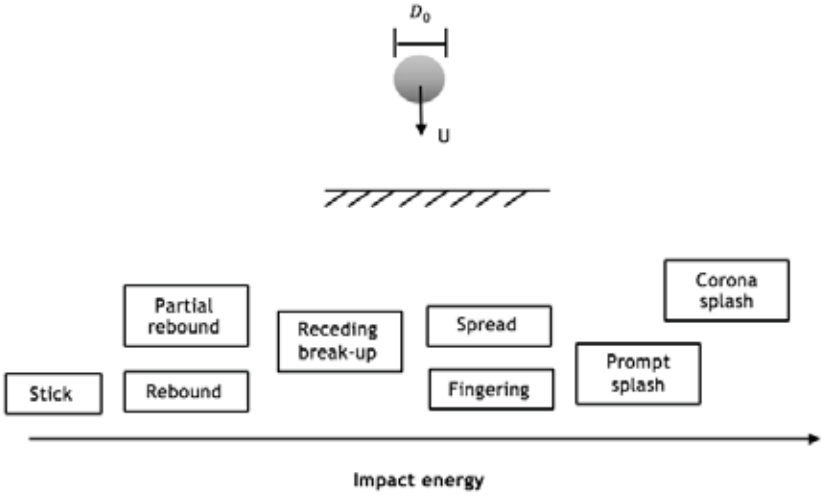

Figure 1.16 - Outcomes according to the impact energy.

1.2.3 Oblique impact

As can be seen, in Figure 1.17 there are clearly differences between the normal and oblique impacts. In normal impact, the droplet collides perpendicularly on the surface. Thus, the droplet can impact a stationary surface or a surface can impact a stationary droplet. However, the oblique impact occurs when a droplet collides usually with a surface, at an angle θ or due to a boundary layer. Usually, the droplet impacts upon a surface obliquely in real situations. An example of oblique impact is the fuel injection on combustion walls or droplets impacting onto airplane wings (icing studies) (Kind, 2001). When a droplet impacts onto a surface with a certain angle, the characteristics of the dynamic behavior may differ from the normal impact. Figure 1.17 shows two examples of oblique impact. Figure 1.17 a) refers to an oblique impact where the droplet describes a trajectory with a certain inclination. Figure 1.17 b) occurs when the impact surface describes a certain inclination with respect to the horizontal axis.

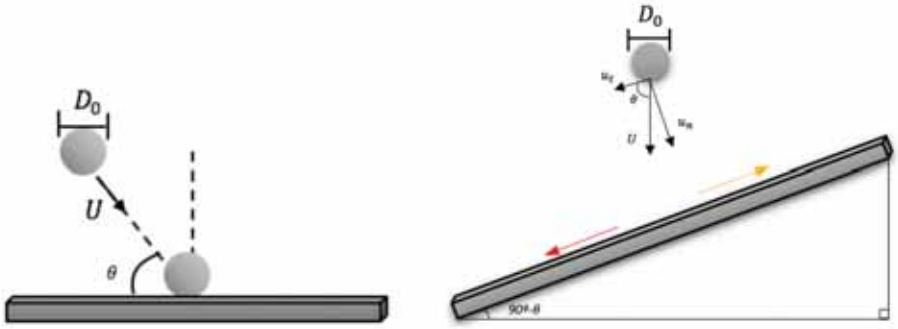

(a) (b)

Figure 1.17 - Oblique impact; a) stationary surface, b) stationary inclined surface.

The oblique impact of single drops distinguishes from the normal impact by exhibiting a different behavior and, hence, it is necessary to carry out investigations. It's important to highlight that the amount of studies investigating the impact of droplets onto inclined surfaces is very scarce.

Figure 1.17 b) shows the droplet impact velocity (U), which is composed of a normal (u_n) and tangential (u_t) components. In oblique impacts, the impact velocity has these two components. Some research focuses on the normal component of velocity. However, the effect of the velocity component parallel to the surface may not be neglected. This subject will be discussed in more detail below. The angle between the absolute velocity of the incident droplet and the impact surface is designated as incident angle (θ). Since the surface is inclined, gravity plays an important role during the droplet impact process, not only can promote the instability of the expanding film at downward flow but also can stabilize the film at upward flow during the drop impact, this observation is more detailed in Chapter 3. To provide a better understanding of this kind of impact, the upper side is symbolized by an orange arrow and the lower side by a red arrow. The outcome of onto an oblique impact also depends of on surface properties which play an important role in droplet-surface-interaction. Therefore, in previous developed activities due to different conditions, it is possible to observe different results. Some of the works previously performed and relevant for this dissertation will be presented in table 1.2.

Stow and Hadfield (1981), investigated the droplet impacting onto an inclined surface and the asymmetry of the expanding film was observed. Stow and Hadfield (1981) mentioned that the droplet deformation and splashing characteristics after impact on a dry solid surface can be conditioned by two parameters, the droplet velocity and, the surface roughness. It was also verified by Worthington (1876), one of the first to study the dynamic of impingements.

In order to more exhaustively examine the impact of droplets on an inclined surface, it was necessary to change some impact conditions. Consequently, Kang and Lee (1999) studied the dynamic behavior of a water droplet impinging upon an inclined heated surface. Through this investigation, was possible begin to understand which direction (normal or tangential) influence more the disintegration. So, it was found that in this case, the normal momentum would be more relevant, taking into account the influence of the impact surface temperature. Taking into consideration the heated inclined surface, Moreira et al. (2007) studied the secondary atomization which occurs at fuel injection in internal combustion engines. In this study was used water and isooctane droplets impacting at different angles on a stainless-steel surface. It was observed that at very small impact angles, less than *15º*, the component of the impact velocity parallel to the surface contributes to the significant asymmetry of the lamella and it also inhibits the growth rate of the crown. Jin et al. (2016) accomplished a study with a cold surface, and the temperature of the impact surface was considered *21.0ºC* to *-15.0ºC*.

They found that increasing the inclined angle, the gravity plays a bigger role on the droplet kinematics and the water droplet also had a larger tangent momentum at the early stage of the impact process.

Maintaining the surface temperature, another important parameter is the variation of the incident angle. According to Jayaratne and Mason (1964), the outcome depends largely on the impact angle, which also influences the direction of the secondary droplets for smooth surfaces. Liu et al. (2010) studied the effect of the incident angle also on the splashing phenomenon. They noticed that increasing oblique angles, the spreading velocity increases but splashing reduces. Relating the incident angle and the velocity component parallel to the surface, Yao and Cai (1988) reported that if θ is not 90^o, the tangential velocity component acts to destabilize the spreading liquid film, and hence to enhance the fragmentation of the droplet following its impingement. As mentioned before, the droplet impact velocity (U) has two components. These two velocity components could condition the impact in different ways.

Bird et al. (2009) investigated experimentally and via modelling, how tangential velocity affects splashing on a dry smooth surface. They noticed that based on the magnitude of the tangential velocity, there are three possible behaviors: the lamella will spread in all directions, splash in all directions, or asymmetrically splash. When there is no tangential velocity, the drops either spread or splash in all direction.

In order to study the tangential velocity, some authors used in their experiments a moving surface. Zen et al. (2010) investigated the combined effect of moving surface velocity and its inclination angle on impacting outcomes. Once the impact occurs onto an inclined surface, the splashing can be subdivided into two regimes. One regime is the splash toward the lower edge, namely splash-down, and the other is the splash in all directions, namely splash-around. This last one requires higher impact energy than the splash-down does and can be asymmetric. Therefore, the transition from splash-down to splash-around is observed by increasing the impact energy gradually. Similarly to Bird et al. (2009) considering the horizontal moving surface, the surface velocity excite the occurrence of splashing that is toward the opposite direction of the surface movement, whereas it suppresses the splashing in the same direction of surface movement. So, when the droplet impacts on a moving inclined surface, the surface velocity advances the splashing on the rear edge and eliminates the splashing on the front edge.

However, to simplify the studies Cui et al. (2009), exanimated the behavior of liquid droplets behaviors impacting on a dry inclined surface at low velocity. They reported that the maximum spread diameter increases with the Weber number when the incident angle is constant, once the higher impact kinetic energy leads to a larger maximum spread diameter. In the same conditions as the previous work, Šikalo et al. (2005) investigated drop impacts onto dry walls and liquid films at low impact angles and low normal Weber number focused on the deposition and rebound. In this study was considered droplets of water, isopropanol, and glycerine.

Whereas a droplet generally deposits on the surface for high incident angles, a rebound can occur at lower angles and for smooth or wetted surfaces. The water (low viscous liquid) will either rebound or deposit on smooth or wetted surfaces. Furthermore, it was also notable that when a droplet impacts onto an inclined surface, the shape of the droplet distorts, and it spreads asymmetrically relative to the point of impact. The difference in the spreading velocity of the lamellas on the downward and backward directions increases with a decrease of incident angle. With the purpose of study the phenomena of droplet-surface interactions more concretely spread, splash, partial rebound and rebound Šikalo and Ganić (2006) observed that the transition from deposition to splash happens with increasingly energetic impact onto smooth surfaces or with the influence of surface roughness. The splash occurs due to the instability of the lamella after it reaches a certain diameter. Consequently, at the impact onto an inclined smooth surface the lamella extends in forward direction, its rim become unstable and it disintegrates in droplets.

Likewise, Shen et al. (2016) studied the spreading dynamics of a droplet on an inclined surface and the results indicate that dominated by gravity and capillarity, the droplet experiences a complex asymmetric deformation and sliding motion after the droplet comes into contact with the inclined surfaces. Nevertheless, not all the impacts occur in a dry surface.

Liang et al. (2013) observed the spreading and splashing processes during a liquid drop impact on an inclined wetted surface. The results showed that both surface tension and viscosity could largely effect the spreading and splashing behaviors. Following the same methodology, Liang et al. (2014) studied in more detail spread, splash, rebound, and partial rebound, and they noticed that for the spreading extent, three primary influencing parameters are considered: the incident angle and Ohnesorge and Weber numbers. It was also notable that with the the incident angle reduction would be able to visualize rebound and partial rebound.

Considering the finish of the impact surface, some investigations used superhydrophobic surfaces. Yeong et al. (2014) used these impact surfaces characteristics and their results revealed that oblique and normal drop impact behaved similarly at low normal Weber numbers. However, at higher Weber numbers, normal and oblique impacts results diverged in terms of maximum spread, which could be related to asymmetric and more complex outcomes. In the same year, Antonini et al. (2014) reported an experimental study on water drop oblique impacts onto hydrophobic and superhydrophobic tilted surfaces, with the objective of understanding drop impact dynamics and conditions for drop rebound on low wetting surfaces.

Table 1.2 - Summary of researches regarding inclined surfaces.

Authors	Investigation	Experiment	Results	Observations
Stow and Hadfield (1981)	• Splash.	• Water; • Inclined surface (Smooth aluminum).	• Impacts with inclined planes suggest that the critical velocity will increase with the obliqueness of the impact.	• Asymmetry of the expanding film.
Kang and Lee (1999)	• Spread; • Splash.	• Water; • Inclined surface *[0º - 60º];* • D_0*= 2.17mm- 2.33mm;* • *We= 57 – 59.*	• The inclination of the surface might provide a much wider wetting than the horizontal surface even though the normal impact momentum is decreased. • Experimental results showed that droplet behavior after impact was greatly influenced by the normal momentum of the impinging droplet.	• The surface's inclination angle mostly affects the horizontal velocities of the disintegrated droplets.

Moreira et al (2007)	• Spread; • Splash.	• Water; • Isoctane; • Hot inclined surface [6^o - 90^o](Stainless steel); • D_0=2.53mm – 2.75mm; • *We*= 240 – 600; • We_N=16-600.	• The largest number of droplets is ejected during the period of more intense boiling during which the mean droplet size is larger; • The number of droplets ejected at the earlier stage of break-up is larger for the fluid with smaller surface tension, as surface tension plays a major role in sustaining pressure forces created by the vapor at the solid-liquid interface.	• The incident angle of fuel droplet/valve interactions in IC engines i.e $15^o<\theta<90^o$; • The spreading rate at earlier stages after impact is smaller on inclined surfaces due to the smaller normal velocity component, the lamella is largely expanded along the surface due to the increased parallel velocity.
Jin et al (2016)	• Spread.	• Water; • Inclined surface [0^o - 60^o], (Quartz); • *We*=155.3; • *Bo*=1.1; • *Oh*=0.002; • *Re*=5855.	• The higher inclined angle allowed the water droplet to have a larger momentum in the tangent direction of the early stage of the impact process. This tangent momentum together with gravity was believed to be the primary factor that increased inside the bulk water region.	• The surface was inclined, gravity also plays an important role during the droplet impact processes. The water droplet was found to go through five phases, kinetic, spreading, gliding, relaxation, and wetting phase. It is also noticed that the foremost point moved faster than the rearmost point.

Jayaratne and Mason (1964)	• Coalesce (Connection between drops or liquid film at low impact energies); • Rebound.	• Water; • D_0= *120μm - 4000μm*	• The outcome depends largely on the impact angle, which also influences the direction of the secondary droplets for smooth surfaces.	• Larger droplets coalesce with the plane surface at smaller impact angles.
Liu et al (2010)	• Splash.	• FC-72; • H_20; • Perfluorohexane; • Inclined surface *[28°-74.7°]* (Smooth Plexigas).	• Increasing oblique incident angles, spreading velocity increases, but splashing reduces. The decrease in splashing observed in oblique impacts is accounted for using u_n.	• The downhill velocity is larger than the uphill velocity for all the inclined surfaces.
Yao and Cai (1988)	• Breakup (Disintegration).	• Water; • Hot moving surface; • Surface temperature *[100°C-380°C];* • D_0=*0.6mm-3.5mm*.	• If θ is not *90°*, the tangential velocity component acts to destabilize the spreading liquid film, and hence to enhance the fragmentation of the droplet following its impingement.	• With the same vertical Weber number, the existence of a tangential velocity component destabilizes the drop; • As the droplet nears the surface, the entrained gas layer between the droplet and the surface increases the resistance of droplet-surface contact.

Bird et al. (2009)	• Splash.	• Ethanol; • Moving surface (Dry, smooth aluminum surface); • Inclined surface *[0º-50º]* (Dry, smooth aluminum surface) • u_t= *0 m/s - 21 m/s.*	• The experiments demonstrate that sufficient tangential velocity can either trigger or inhibit splashing on a portion of the drop; • When there is no tangential velocity, the drops either spread or splash in all directions.	• For the moving surface, when the tangential velocity is increased, the portion of the lamella moving in the same direction as the substrate continues to spread, whereas the portion of the lamella moving opposite to the substrate delaminates and splashes.
Zen et al. (2010)	• Spread; • Splash.	• Ethanol; • Moving inclined surface *[0º-50º]* (Silicon wafer disk); • D_0=*2.32mm – 2.58mm.*	• The component of gravity generates an opposite influence on the lower and upper edges; • Ethanol with the advantage of low surface tension not only emerges splashing in a high impacting energy but also easily induces the asymmetric splashing on an inclined or moving surface.	• The splashing severely occurs in the lower edge and it is meant that the instability of the lower edge is relatively higher than the upper edge; • The normal Weber number is used to distinguish the spread and splashing when the droplet impacts on an inclined surface.

Cui et al. (2009)	• Spread.	• Water; • Inclined surface *[13º - 90º]* (PVC); • *We=33 – 1200;* • D_0*=4mm – 5mm.*	• The maximum spread diameter increases with the Weber number when the incident angle is constant; • The higher impact kinetic energy leads to a larger maximum spread diameter.	• The impacting droplets spread on the surface until liquid surface tension and viscosity overcame inertial forces, after which they recoiled off the surface.
Šikalo et al. (2005)	• Spread; • Rebound; • Partial rebound.	• Water; • Isopropanol (C_3H_8O); • Glycerin; • Inclined surface *[2.5º - 35º]* (Smooth glass, rough glass and smooth wax); • *We=40 – 1063;* • *1 < We$_n$ < 16.5;* • *Re= 27 – 8880;* • D_0*=1.8mm – 3.3mm.*	• No rebound is observed for dry smooth wax and rough glass; • Water will either rebound or deposit on smooth or wetted surfaces; • The increase of impact velocity increases the spreading in both the forward and backward directions but also decreases the sliding of water droplet on wax; • The deformation of a droplet increases with an increase of the incident angle and the contact time of the droplet with the surface decreases.	• When a drop impacts onto an inclined surface, the shape of the droplet distorts, and it spreads asymmetrically relative to the point of impact; • Higher deformation corresponds to low surface tension and viscosity; • The drop generally deposits on the surface for large incident angles and rebound occurs at small angles for smooth surfaces.

Šikalo and Ganić (2006)	• Spread; • Splash; • Rebound; • Partial rebound.	• Water; • Isopropanol; • Glycerine; • Inclined surface *[0.5º - 3.5º]* (Smooth glass, rough glass and smooth wax); • *We= 50 – 1063;* • *We_n= 0.007 – 0.34.*	• The splash occurs due to the instability of the lamella after it reaches a certain diameter.	• The transition from deposition to splash happens with increasingly energetic impact onto smooth surfaces or with the influence of surface roughness.
Shen et al. (2016)	• Spread.	• Numerically (LBM - Lattice Boltzmann methods); • *Re =100.*	• Dominated by gravity and capillarityy, the droplet experiences a complex asymmetric deformation and sliding motion after the droplet comes into contact with the inclined surface; • The droplet spreading behavior on an inclined surface is also affected by the surface wettability.	• Increases in the inclination angle and equilibrium contact angle lead to a faster droplet motion and a smaller wetted area.

Liang et al. (2013)	• Spread; • Splash.	• *30 vol%* glycerol/water; • Butanol; • Heptane; • Inclined surface *[28° - 74,7°]* (Steel plate); • D_0*=1.58mm – 2.1mm.*	• The splashing process is unsymmetrical due to the incident angle, extending from the lower position to the higher position gradually; • Surface tension is the main resistance for splashing, while low viscosity results in prompt splashing and high viscosity should be responsible for delayed splashing.	• Increasing surface tension, the size of secondary drops and the duration of the liquid sheet can be increased.
Liang, et al. (2014)	• Spread; • Splash; • Rebound; • Partial rebound.	• *30 vol%* glycerol/water; • Butanol; • Heptane; • Inclined surface *[28° - 74,7°];* • D_0*=1.58mm, 1.59mm, 2.11mm.*	• The spreading factor in the normal direction can be decreased by reducing the incident angle, whereas the Weber number influence are minor; • The decrease of the incident angle leads to the increase of the front spreading factor whereas the back spreading appears the opposite trend, caused by the combinated effect of the inertia force and gravity; • The *Oh* increment is disadvantageous to the spreading	• Rebound and partial rebound can only be observed at a smaller incident angle, lower Weber and higher viscosity.

			process. However, the *Oh* effect becomes weak with the decrement in the impact angle.	
Yeong et al. (2014)	• Spread; • Splash.	• Water-glycerol mixtures; • Inclined surface with superhydrophobic coating *[15º - 60º];* • We_n*= 6 – 110;* • *Oh = 0.0018 – 0.028.*	• In oblique and normal impact the droplet behaved similarly (in terms of maximum drop spread as well as rebound dynamics) at low Weber numbers. However, at higher Weber numbers, the results diverged in terms of maximum spread which could be related to asymmetric and more complex outcomes.	• The impact of the drop on the superhydrophobic surface could be separated into six stages, i.e. preimpact, collision, maximum spread, rebound, disengagement, and pós-impact.
Antonini et al. (2014)	• Deposition; • Sliding; • Rolling; • Rebound; • Partial rebound.	• Water; • Inclined surface [*15º - 80º*] (Hydrophobic surface, A1-Teflon, SHS-1, SHS-2); • U*=0.8m/s – 4.1m/s;* • D_0*=2.40mm – 2.60mm;* • *We=25 – 585.*	• On the hydrophobic surface, the increase in both surface tilting and impact Weber number led to the transition from drop rebound, to partial rebound and sliding.	• On hydrophobic surfaces, rebound was never observed for tilt angles higher than 45º; • Complete rebound occurred with an angle of *10º* and *30º*.

It is important to mention that an oblique impact with a stationary surface does not necessarily provide the same results as a normal impact on a surface moving perpendicularly to the direction of impact. This fact happens due to the boundary layer. The presence of a boundary layer may originate the lift-off of a droplet.

Several studies noticed droplet deformation due to the presence of a crossflow before the impact. This means that the droplet experiences a deformation stage which affects the drag properties and, consequently the trajectory before impact (Rodrigues, 2016) as can be seen in Figure 1.18 and in figure 1.19.

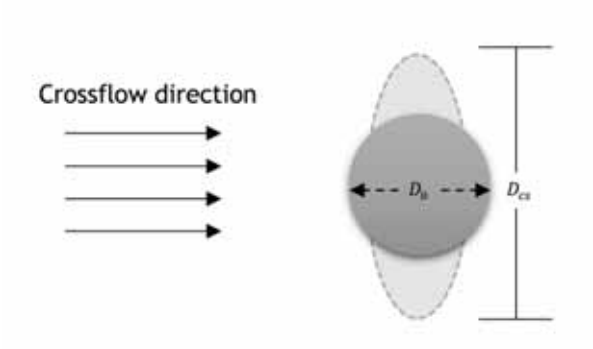

Figure 1.18 - Droplet deformation due to the crossflow adapted from (Rodrigues (2016)).

where, D_0 is the initial droplet diameter and D_{cs} can be defined as the deformed droplet characteristic length in the cross-stream direction. Due to aerodynamic forces acting on the distorted droplet reflected drops acquire a rotational velocity.

Several researchers were developed in order to understand the effect of the crossflow. It was studied the influence on droplet diameter, secondary atomization, the velocity of impinging spray and other subjects (Cunha et al., 2018), (Rodrigues, 2016), (Sinha et al. 2015), (Panão et al., 2013), (Lee and Park, 2018).

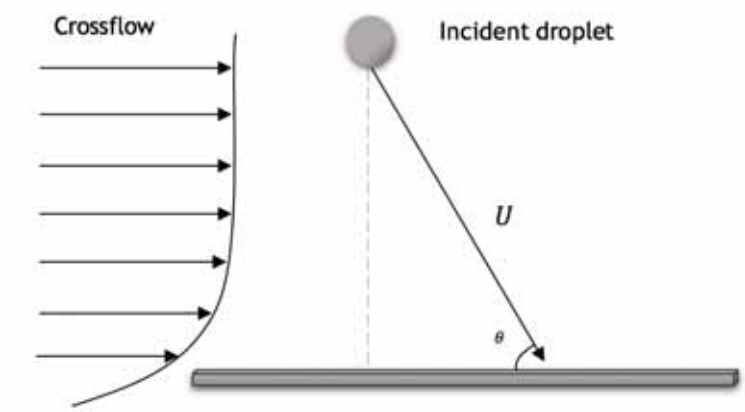

Figure 1.19 - Schematic diagram of droplet impact onto a solid surface with the influence of crossflow.

1.2.4 Surface roughness

Surface characteristics always had a huge relevance to the scientific community. The interest on these features is related to the phenomena observed from the droplet impingement onto a surface which affects the critical thresholds between impingement regimes.

Thus, several authors were interested in studying the roughness of a surface. Engel (1955) reported that the surface influences the phenomenon of the impact. Therefore, the splash is more notable when the surface roughness is increased. Furthermore, splashing occurs for less energetic impacts onto rough surfaces than to polished surfaces. These conclusions were also confirmed by Levin and Hobbs (1971). It is important to emphasize that the occurrence of splash has raised many questions, so the study on the roughness has been developed in this sense. Alterations in the surface roughness influence the number, the total volume and the size distribution of secondary droplets. Stow and Stainer (1977) studied the droplet impacts onto metallic surfaces and concluded that the number and size of droplets produced by the splash increase with the surface roughness.

In order to include more details to this research, few years later Stow and Hadfield (1981) tried to evaluate the size distribution of splashed droplets more precisely. Stow and Hadfield (1981), proposed a correlation, based on a "splashing parameter", K_c which predicts the threshold for droplet disintegration that depends on the roughness amplitude, (quantified by the mean roughness, Ra).

Mundo et al. (1995), was even more specific. They reported that the deformation, spreading and splashing of the droplets depends not only on the kinematics, fluid parameters of primary droplets, and also on the ratio of the surface roughness compared to the droplet diameter. Therefore, they noticed that the splash depends on the kinetic energy and that is independent of the kind of surface. If the impact has high kinetic energy and enough momentum normal to the surface to overcome the surface tension of the liquid the corona appears. On the contrary, if there is low kinetic energy and not enough momentum normal to the surface the droplet deposits on the surface. Regarding the kind of surface, the behavior of the droplet is not the same for smooth or rough surfaces. So, when the surface is rough the droplet distribution is more uniform, with smaller secondary droplets than for a smooth surface.

Recently, it was developed a study intended to understand the different outcomes of droplet-surface interaction. The authors of this research were Šikalo and Ganić (2006). They concluded that the transition from deposition to splash happens with increasingly energetic energic impact onto smooth surfaces or with the influence of surface roughness. They also investigated the droplet impingement upon a sloped surface.

Šikalo and Ganić (2006), changed the incident angle and the roughness of the surface and observed different phenomena.

1.2.5 Splashing Threshold

The fluid mechanics of droplets impinging on a surface has an enormous importance in many different technical applications. For each application different phenomena are desired. Splash is one of the most required which has a huge interest to researchers. Therefore, several transition criteria were developed.

The splashing threshold can be defined as a theoretical model that predicts the inception of the splash and should comprise various parameters which are responsible for each phenomenon specifically. Several researchers elaborated empirical correlations to achieve the transition between phenomena. Stow and Hadfield (1981) suggested a correlation in order to determine when splash occurs. So, it was introduced *(K_C)*, the splashing parameter, which takes into consideration the impact velocity and size of the incident drop on the dynamics of impact.

$$K_c = B.Oh^a.We^b \qquad (1.10)$$

where *a* and *b* depend on the experimental conditions. The dimensionless numbers are crucial to identify the regimes threshold. However, other parameters are also important such as the surface roughness. According to Moita (2009), the reported correlations do not completely account for the complex mechanisms arising at the liquid-solid interface, when the impact occurs onto a rough target. The discrepancies between the various criteria are compared and adapted to a diversity of experimental results. Most authors, such as Stow and Hadfield (1981) include the effect of the surface roughness with the mean roughness amplitude. They reported that rough surfaces exhibit a lower value of K_c, and therefore more splashing. Others, such as Bai and Gosman (1995) include the effect of surface roughness by varying the fitting parameters of the correlation. These authors studied the dynamic behavior of a single droplet impact onto a surface and relating to data from other researchers have established transition criteria for dry and wetted surfaces. The following equation is based on Stow and Hadfield (1981) experiments and represents the transition between spread and splash for dry walls. Considering We_c as the critical Weber number, the splash occurs if this value is reached.

$$We_c = A.La^{-0.18} \qquad (1.11)$$

where the coefficient *A* depends on the surface roughness, *Ra*. This relation is shown in table 1.3.

Table 1.3 - Typical values of the coefficient A depending on the surface roughness adapted from Bai and Gosman (1995).

Ra (μm)	*A*
0.05	5264
0.14	4534
0.84	2634
3.1	2056
12	1322

Mundo et al. (1995) developed an empirical correlation using a combination between Ohnesorge and Reynolds numbers. In this criterion the influence of surface roughness was not taken into account. Thus, several experimental studies of liquid spray droplets impinging on a flat surface have been performed with aim of formulating an empirical model describing the deposition and the splashing process. For the impact surface, it was considered two discs, one with a smooth surface and the other with a rough surface. In this threshold was only considered the normal impact velocity.

$$K_c = Oh.Re^{1.25} = 57.7 \qquad (1.12)$$

They noticed in their experiments that the transition from deposition to splash occurs when K_c =*57.7*. So, when K_c is above *57.7* splash occurs, on the contrary, below this value the deposition is observed.

Vander Wal et al. (2006) also developed a study to determined empirical correlations for the splash/non-splash boundary for dry smooth surface and also for thin liquid films. Their experiments considered an aluminum disk with very low surface roughness, less than *0.01*μm. The transition criteria proposed for these authors is presented in equation 1.13.

$$K_c = Oh.Re^{0.609} = 0.85 \qquad (1.13)$$

According to their results, this correlation fits very well for large Reynolds numbers. However, does not fit well when the Reynolds number decreases (particularly for Re<*4000*). In this last case, the viscous and the wetting effects become more important.

Most of these correlations presented above refer to the normal impact and/or only considered the normal component of velocity.

Regarding the inclined surface, the transition criteria are still not well understood. According to Stow and Hadfield (1981) the splashing threshold on an inclined surface was not studied in detail. They also noticed the importance of the tangential impact velocity and the asymmetric splash.

Bird et al. (2009) presented the splashing threshold of oblique impact, having the tangential velocity in consideration.

$$We\sqrt{Re}\left(1-\frac{u_t k}{u_n\sqrt{Re}}\right)^2 = K_c \qquad (1.14)$$

In their experiments, it was used ethanol droplets impacting obliquely on smooth glass, considering K_c=*5700* and k=*2.5*. Regarding the equation 1.14, the sign of tangential velocity, u_t is taken with respect to the spreading direction of the lamella. Thus, u_t is negative for the upper side, and positive for the lower side, which spreads in the same direction as the surface's motion, considering an inclined surface. This means that this empirical correlation takes into account the asymmetric splash. It is also important to mention that when there is no tangential velocity the droplets either spread or splash in all directions.

This transition criterion was compared with another that established a splashing threshold of oblique droplet impacts on surfaces of various wettability. This study was performed by Aboud and Kietzig (2015) and six different sample surfaces were tested: two substrate materials of different inherent surface wettability (PTFE and aluminum), each prepared with three different surface finishes (smooth, rough, and textured to support superhydrophobicity).

According to Aboud and Kietzig (2015) the splashing threshold (ST), could be given by equation 1.15.

$$ST = u_{n0} + mu_t \qquad (1.15)$$

where u_{n0} is the critical velocity for splashing at a normal angle of incidence, m defines a slope with respect to u_t and splashing occurs for cases in which $u_n > ST$. To support this information the following figures were provided. Figure 1.20 a) is an illustration of how equation 1.15 can be interpreted graphically.

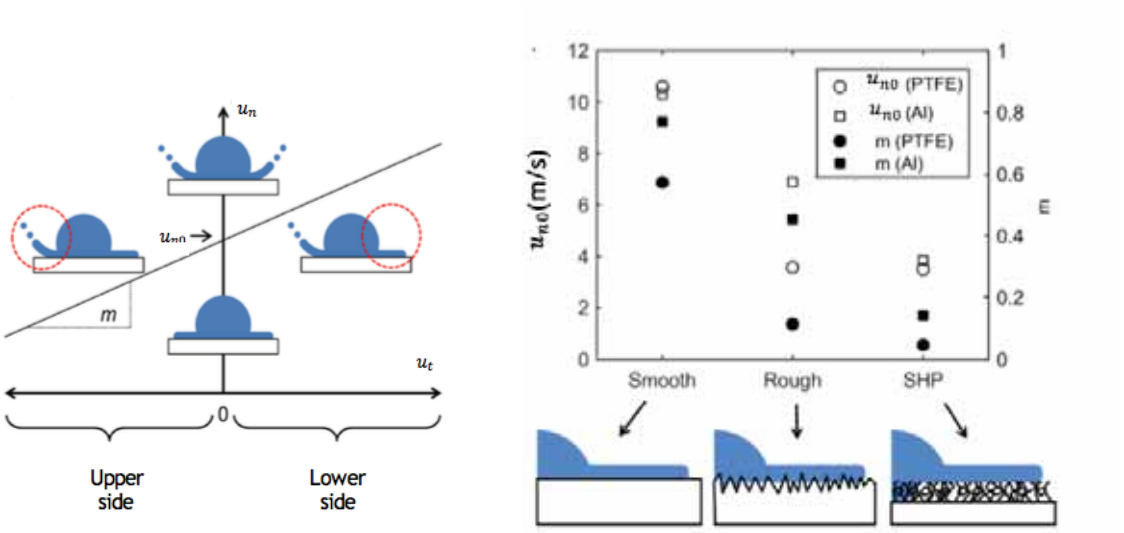

(a) (b)

Figure 1.20 - a) Illustration of the types of splashing behavior adapted from Aboud and Kietzig (2015); b) Dependence of modeling parameters from equation 1.15 on surface finish adapted from Aboud and Kietzig (2015).

The results obtained with this study were grouped and are demonstrated in Figure 1.20 b) and table 1.4. Through these data, it is possible to notice the influence that the different surfaces has on the various parameters. According to table 1.4, these results strongly contracted with Bird et al (2009) statement, which refers that k is expected to be order one and K_c much greater than one, between 1180 and 19200.

Table 1.4 - Modeling parameters adapted from (Aboud and Kietzig, 2015).

		model [95% CI]		Bird's model	
surface	D (mm) ± 2 st. dev.	v_{n0}	m	K	k
s-PTFE	0.93 ± 0.04	11.33 [10.23; 12.43]	0.69 [0.54; 0.84]	197,000	72.8
r-PTFE	0.97 ± 0.02	3.57 [3.35; 3.79]	0.13 [0.10; 0.16]	9,930	8.77
t-PTFE	0.97 ± 0.09	3.51 [3.43; 3.59]	0.053 [0.019; 0.087]	9,420	4.18
s-Al	0.94 ± 0.02	11.42 [10.32; 12.52]	0.83 [0.64; 1.02]	163,000	94.9
r-Al	0.94 ± 0.02	6.64 [6.35; 6.93]	0.47 [0.41; 0.53]	51,900	47.2
t-Al	0.97 ± 0.06	3.86 [3.74; 3.98]	0.13 [0.10; 0.16]	11,810	9.40

1.3 Objectives

The present work is devoted to an experimental study regarding the dynamic behavior of a single droplet impinging onto a sloped surface. Currently, the work developed on this subject is scarce and the scientific community has been struggling to understand this theme. As reviewed in the literature, hardly any work developed adopts Jet-Fuel and biofuel mixtures. Therefore, the main objective is to verify the influence of the physical properties of the fluids in the droplet impinging onto a surface. To achieve this objective, a comparative study of droplet impact onto a sloped surface versus a droplet impact onto a surface with the influence of a crossflow was performed. The work regarding the influence of a crossflow was performed by Cunha (2018). Accomplishing it requires several procedures:

- Design, built and validate an experimental facility, as well as conceiving a mechanism that aims to change the surface inclination;
- Recreate the same conditions as Cunha (2018) and visualize the phenomena;
- Report the similarities and differences between the phenomena derived from the comparison and verify the conditioning factors of these results;
- Compare the experimental results with a few splashing thresholds that are reported in the literature.

1.4 Organization

The present document is organized in four main chapters denominated by Introduction, Experimental Study, Results and Discussion, and Conclusions and Future Work.

This chapter provides the motivation, the main objectives and the overview of this dissertation. The literature review is also presented in this chapter in order to supply the knowledge regarding this theme. A summarized chronological review is crucial to understand the relevant concepts required for the comprehension of this work.

The second chapter is dedicated to the experimental study, where all the components and requirements are presented. Then, the work methodology will be explained in detail in order to provide the procedures of this work. The fluid properties are also listed and summarized. Finally, it is shown how to perform image processing data for this study.

The third chapter presents a detailed description of the experimental results. Firstly, the results concern a comparison between droplet impacts onto a sloped surface and droplet impacts upon a dry surface with the influence of a crossflow. Then the similarities and

differences will be analyzed. The visualization regarding the normal impact will be shown and compared for the two impact surfaces. At the end of this chapter, the experimental data will be compared with transition criteria presented in the literature.

Finally, the last chapter summarizes the most important conclusions of this dissertation and several suggestions for future works.

Chapter 2

2. Experimental Study

The current chapter is dedicated to the experimental study where all the details and specifications will be presented.

Firstly, the experimental arrangement will be introduced. In the first section, it will be presented several components that were used and the most relevant characteristics for the arrangement of the experimental work. The methodology addressed in this dissertation will be demonstrated in order to simplify the understanding of the work. Another important detail is the physical properties of the fluids which condition the dynamic behavior of a droplet impinging upon a surface. Finally, image data processing will be explained in order to achieve the droplet characteristics.

2.1 Experimental Arrangement

To achieve the predefined objectives, an experimental facility was designed to allow testing with an inclined surface and with the presence of a crossflow. Therefore, in this experimental facility, it is indispensable to have the impact surface, the wind tunnel, the image acquisition system, the illumination set and also the droplet dispensing system. During the experiments, the relative humidity and temperature of the air in the laboratory were kept approximately constant. To facilitate the experiments, a structure was required in order to support all of the essential elements. This structure is represented by the green iron beams displayed in figure 2.1.

The droplets are generated by a droplet dispensing system, which is composed of a syringe pump and a syringe attached to a needle with the aid of a circular tube. This system is controlled by the computer, which allows the fluid to be released with a specific pumping rate. A high-speed digital camera was required for the image acquisition and a set of LEDs was installed to facilitate the visualization. The impact surface is placed onto the trajectory of the needle, so the droplet impacts in the center of the plate.

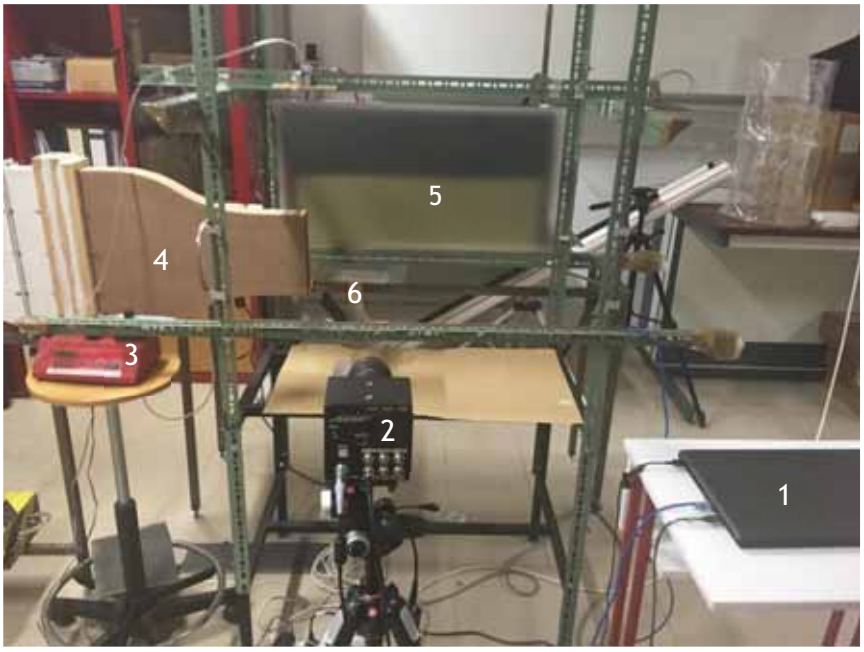

Figure 2.1 - Experimental facility: 1- Computer; 2- High-speed digital camera; 3- Syringe Pump; 4- Wind tunnel; 5- Illumination; 6- Impact surface

2.1.1 Image acquisition system

To acquire the images with a certain accuracy, a high-speed digital camera was used. The camera used in this dissertation was a Photron FASTCAM mini UX50, with 1.3 Megapixel image resolution at frame rates up from 2000fps and frame rates up to *160000fps* at reduced image resolution. It was connected to a computer and was manually triggered. A Macro Lens Tokina AT-X M100 AF PRO D with a minimum focus distance of *300mm*, a focal length of *100mm*, a macro ratio of 1:1 and a filter size of *55mm* was coupled to the camera (figure 2.2).

The visualization of the different phenomena required certain care, hence when the experiments were using the sloped surface the high-speed digital was tilted at maximum 10º. This enabled the complete observation of the outcome. The image acquisition was pursued with *4000fps* (frames per second), leading to a resolution of 1280x512, and three different exposure times, *1/10000*s, *1/12800*s and *1/20840*s.

Figure 2.2 - High-speed digital camera Photron FASTCAM mini UX50 with the Tokina lens coupled

2.1.2 Wind Tunnel

One of the main goals of this work is to establish a comparison between the single droplet impact onto a sloped surface with a droplet impact onto a surface with the influence of a crossflow. Therefore, the knowledge and the use of a wind tunnel is indispensable in this study. In order to recreate the same phenomena as Cunha (2018), the tests were performed with the same wind tunnel. This wind tunnel is composed of a diffuser, a settling chamber, and a contraction.

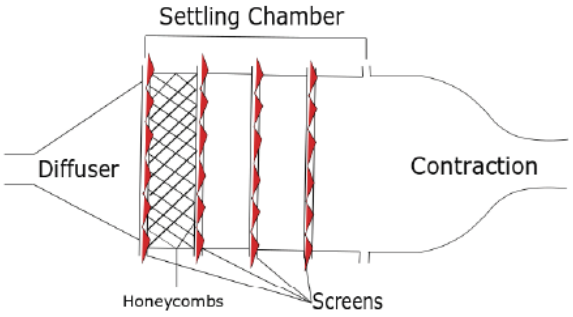

Figure 2.3 - Schematic of the wind tunnel with the elements placing.

The purpose of the diffuser is to decelerate the crossflow. The diffuser used has the following specifications: a length of *335mm* and an angle of *48,24º* (Cunha, 2018).

According to Mehta and Bradshaw (1979), the setting chamber is composed of two components: a honeycomb and screens.

The honeycombs are effective to remove swirl and lateral mean velocity variations, providing that the flow yaw angles are lower than 10^o. The screen allows a more uniform velocity profile of the flow and reduces the boundary layer thickness, giving the flow an increased ability to withstand a pressure gradient.

The contraction is required to accelerate the flow allowing the placement of the screens and honeycombs in a low-speed area reducing pressure losses. The length of the contraction is an important factor given that if it is long enough it would be possible to avoid separation, however, besides the space requirements, this would increase the exit boundary layer thickness (Mehta and Bradshaw, 1979). The exit has *200x40mm* (figure 2.4).

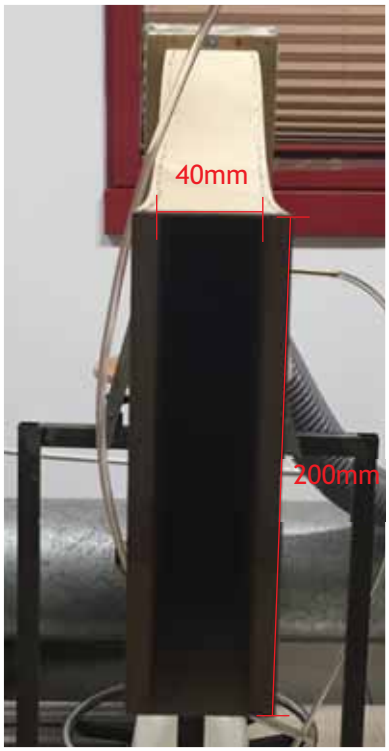

Figure 2.4 - Contraction designed and built by Cunha (2018).

In the work developed by Cunha (2018) the experiments were performed with three different crossflow velocities: $7m/s$, $10m/s$ and, $15m/s$. Furthermore, most of the results obtained by Cunha (2018) have been verified in the presence of $7m/s$. Due to this, in this dissertation, it was only considered a crossflow velocity of $7m/s$.

2.1.3 Droplet Dispensing System

The injection system is composed of a syringe pump NE-1000 that allows the release of droplets with the aid of a computer to be more effective and practical (figure 2.5).

Figure 2.5 - Syringe Pump NE-1000.

This system has the capacity of *1.459μl/hr* for a *1ml* syringe and *127.2ml/min* for a *60ml* syringe. In this dissertation, the pumping rate established was *0.5ml/min* for a *50ml* syringe.

The droplet is originated at the tip of the needle and detaches when the gravity exceeds the surface tension force. In the work developed by Cunha (2018), the water exhibited the largest diameter of all the fluids due to the higher surface tension value. In order to obtain similar diameters between the water and the remaining fluids, different needles were tested.

These needles have unique characteristics with their inner diameters being *1.50mm* and *0.5mm*. The water droplet was released with the *0.5mm* inner diameter needle to exhibit a similar diameter as the diverse fluids, as shown in figure 2.6. For each fluid, different needles with straight tips were used to avoid contamination.

Figure 2.6 - Stainless steel needles. The inner diameter (D_{in}) for the olive needle is 1.50mm and the light blue needle is 0.5mm.

Through this difference in the diameters, it is possible to obtain different values for the impact velocity and, consequently, various dimensionless parameters. Table 2.1 shows the maximum and minimum values of diameters, impact velocity, Reynolds, Weber, Ohnesorge, Laplace, Capillary, Bond, and Froude numbers.

Table 2.1 - Range of the impact conditions.

	Minimum	**Maximum**
Diameter [*mm*]	*3.0*	*4.03*
Impact velocity [*m/s*]	*1.9*	*6.0*
Reynolds number	*3265*	*24339*
Weber number	*333*	*1854*
Ohnesorge number (*Oh*x10^3)	*1.8*	*7.3*
Laplace number	*18645*	*317189*
Capillary number	*0.044*	*0.281*
Bond number	*2.0*	*2.9*
Froude number	*119*	*521*

2.1.4 Impact Surface

The study of the droplet dynamics impinging onto a surface depends on several factors. One of them corresponds to the characteristics of the impact surface. As already mentioned, it was considered a sloped surface.

For this reason, a mechanism was designed with the possibility of varying the surface angle, which can range from *0º* to *80º* with a precision error of *±1.3º*. A smooth dry aluminum plate with *160x80mm was* placed above this mechanism, shown in figure 2.7 a).

The results obtained were not the same as the previous work. Due to this, for an amount of experiments, the impact surface used by Cunha (2018) was considered. This surface was attached to the top of the mechanism. As described in Cunha (2018), this surface is a smooth aluminum plate with 700x80mm, demonstrated in figure 2.7 b).

To answer a few questions that were relevant to understand the difficulties in this work, it was necessary to perform experiments using the wind tunnel. In this case, the aluminum plate is placed across the exit nozzle and is equidistant to two glasses. To recreate the same conditions as Cunha (2018) the aluminum plate was placed *70 mm* above the base of the exit nozzle to guarantee a stable crossflow influence.

(a) (b)

Figure 2.7 - a) Cunha (2018) impact surface; b) The mechanism for the inclined surface.

Thus, knowing the surface roughness of these impact surfaces is indispensable for this work. The surface roughness analysis was achieved with the aid of a roughness tester, more concretely a Hommel Tester T1000 (figure 2.8).

To measure the roughness of the plate, three tests were performed in which the length of each section of the analysis was *4.8mm*. This roughness tester is connected to a computer to control the operation.

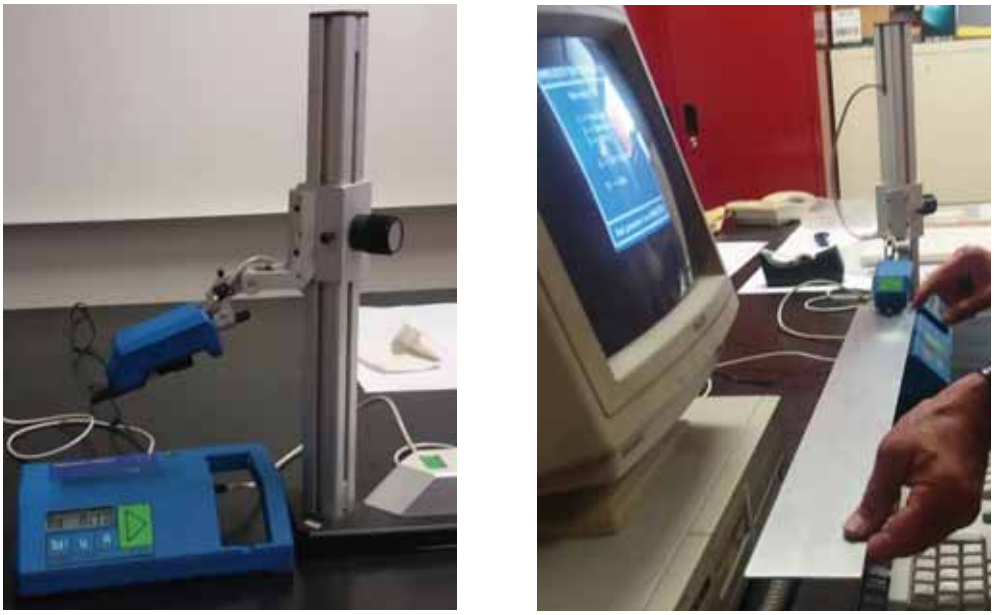

(a) (b)

Figure 2.8 - a) Roughness tester Hommel Tester T-1000; b) Testing the impact surface used by (Cunha, 2018).

As can be seen in figure 2.8, the Cunha (2018) impact surface was analyzed and presented a surface roughness of Ra=$0.19\mu m$, while the surface developed for this dissertation presents a slightly lower value of Ra=$0.13\mu m$. To achieve this characteristic, the plate was polished several times. It is also important to mention that, between the tests, the plates were properly cleaned in order to not condition results.

2.1.5 Illumination

In order to clearly observe the different phenomena, proper illumination is required. To achieve this, a 96 W LEDs ribbon was attached to a wooden panel, as can be seen in figure 2.9. This panel of LEDs is powered by a power supply. The function of the power supply is to transform the alternating current into direct current with the intention of obtaining a more efficient and uniform illumination.

To intensify the contrast and to improve the visualization of the images, the room was completely dark with only the LED lights on. This illumination was parallel to the droplet falling plane. To provide a uniform illumination, a diffusion glass was placed between the lighting and the impact surface.

(a) (b)

Figure 2.9 - a) Power supply; b) Panel of LEDs.

2.2 Methodology

As any work, it is necessary to plan the methodology to follow. Therefore, it is required a detailed explanation of how the work will be developed. This section is dedicated to the methodology used in this experimental study.

The main goal of this dissertation is the comparison between the droplet impact onto a sloped surface and the droplet impact onto an horizontal surface with the influence of crossflow, the latter being conceived previously by Cunha (2018). So, all the information about this previous work is required. This information regards the observed phenomena, incident angles, impact velocities, diameters, and fluid properties. Thus, for each fluid, the experiments were performed with the same incident angle and approximately the same impact velocity.

In the work developed by Cunha (2018), the crossflow effect was crucial to study the behavior of the droplet impinging onto a surface. Due to this, the droplet suffers a certain deformation. It is important to mention that, in this case, the droplet does not have the same direction as the gravitational acceleration. When the gravitational acceleration and the movement of the droplet have the same direction, it is considered an impact onto an inclined stationary surface, which does not verify the presence of crossflow. Although both of these impacts are considered an oblique impact, it does not necessary mean that they provide the same results.

Therefore, the same phenomena were attempted to be observed as Cunha (2018). For each fluid, three tests were performed, which in two of them spreading occurs and in the other splash. However, as will be explained in more detail in the next chapter, not all the fluids describe the same outcomes observed as Cunha (2018).

Firstly, for these tests, the impact surface developed for this study was used. However, the results were not similar to Cunha (2018). Therefore, it was important to use the same plate as Cunha (2018) in order to verify if the results were being influenced by the characteristics of the impact surface, whereby a surface roughness analysis was mandatory. Nevertheless, the phenomena observed was still different. Due to this, several conditions were changed. For these cases that the phenomena observed were not the same as Cunha (2018), two or three phases were planned. In the first phase, it was considered the same impact velocity and the incident angle was varied. For the second phase, the inverse occurs. The third phase only occurs for water. One detail taken into account in the work developed by Cunha (2018) was the fact that the diameters of the fluids were not the same. The water exhibited a larger droplet. So, it was required to find a needle that generates a water droplet with *3mm* diameter. Therefore, in this dissertation, experiments were carried out in order to all the fluids present the same diameter. The normal impact was also compared with Cunha (2018) and the impact velocity, as well as the dimensionless numbers, were analyzed.

When the tests with the sloped surface were performed, the high-speed digital camera was leaning in order to better visualize every phenomena detail. The camera was tilted at a maximum angle of 10^{o} and this fact was taken into account in the impact velocity measurements. Regarding droplet diameter and impact velocity measurements, these were determined with the aid of image processing data, which will be explained in more detail in section 2.4.

2.3 Description of Fluid Properties

The dynamic behavior of single droplets impinging onto a surface depends on the physical properties of the fluid, which was reported by Mundo et al.(1995) and Stow and Stainer (1977).

In this present work, four fluids were considered:

- 100% Jet-Fuel;
- 75%JF - 25%HVO;
- 50%JF - 50%HVO;
- H_2O (Water).

The conventional Jet-Fuel chosen was Jet A-1 and the Biofuel was NEXBTL (Neste Renewable Diesel), which is an HVO (Hydroprocessed Vegetable Oil).

A few specifications, such as density and others properties regarding these fluids are presented in Springer Handbook of Aviation Fuel Properties, (1983) and Neste Renewable Diesel Handbook (2015).

The only fluid that has their properties reported in the literature is H_2O (pure water). Several researchers use this fluid as a reference. However, not all fluids have their characteristics well established and it is imperative to measure the properties of the other three fluids before the experiments. Three properties were presented: Density, surface tension, and viscosity.

Regarding the mixtures, the portions used were followed current legislation that admits 50% in volume for alternative fuels, consequently, it was only considered 75%JF - 25%HVO and 50%JF - 50%HVO.

2.3.1 Density

Density (ρ) is defined in terms of mass per unit volume of a substance or object at a particular temperature. It is usually expressed in kg/m^3 (Springer Handbook of Aviation Fuel Properties, 1983).

In equation form, density is represented by:

$$\rho = \frac{m}{V} \quad (2.1)$$

where *m* is the mass and *V* is the volume occupied by the substance.

2.3.2 Surface tension

Surface tension (σ) is defined as the specific free energy of a liquid surface at the interface with another fluid. Regularly, values for surface tensions are given when the surface of the liquid is in contact with air (Springer Handbook of Aviation Fuel Properties, 1983).

2.3.3 Viscosity

According to Springer Handbook of Aviation Fuel Properties (1983) the viscosity (μ) is defined as a measure of the fluid internal resistance to motion created by the cohesive forces among the fluid molecules.

2.3.4 Summary of fluid properties

This subsection is dedicated to the fluid properties. The table 2.2 presents the fluids properties used in this experimental work. These values were adapted from Cunha (2018).

Table 2.2 - Summary of fluid properties.

	100%JF	75%JF - 25%HVO	50%JF - 50%HVO	H_2O
$\rho[\mathbf{kg}/m^3]$	798	795	792	1000
$\sigma[mN/m]$	25.4	25.5	24.6	72.8
$\mu[mPa.s]$	1.12	1.44	1.79	1.0

Regarding the density, the water exhibits the higher value. The density values decrease with the increase of the percentage of HVO, so the 100% Jet-Fuel presented the higher value. The surface tension values are almost similar for 100% Jet-Fuel and mixtures. However, the H_2O surface tension is approximately three times higher than the other fluids. For the viscosity, 100%Jet-Fuel and H_2O are approximately the same whereas, for the mixtures, the value increases as HVO percentage increase.

2.4 Image data processing

The technological development of high-speed digital cameras in engineering and scientific applications have facilitated research in terms of visualization. As mentioned in section 1.3, the objectives of this dissertation refer to a comparison in which it is fundamental to acknowledge the droplet diameters, impact velocities and, consequently, the dimensionless numbers. This information was acquired through image data processing. Using MATLAB software, several algorithms were developed. The MATLAB software provides a comprehensive set of reference-standard algorithms and a few programs for image processing, analysis, and visualization. To finalize, this section is devoted to the image data processing and adopted methodology. Thus, Image Processing Toolbox, pixel sizing, binarization and others will be explained.

2.4.1 Pixel sizing

To study the dynamic behavior of a single droplet impinging onto a surface, it was acquired the images with the aid of a high-speed digital camera. This present work is regarding a sloped surface, so this feature was taken into consideration.

Firstly, it is crucial to measure the pixel size. Thus, it was made correspondence between the number of pixels and the value in millimeters using a reference. In this present work, the reference was a needle with an outer diameter of D_{ou}= *1.26mm*.

Figure 2.10, shows an image of the reference that is captured before any test. This reference corresponds to the impact surface inclined approximately *20º*. In order to avoid any error, it is important to count the pixels when the needle is vertical. The image is read using *imread* command and it is stored in a two-dimensional array. In the first lines of the MATLAB algorithm, figure 2.10 a) is rotated the same angle as the surface inclination and the result is demonstrated in figure 2.10 b). Then, the image is binarized. This step consists of replacing the pixels taken into consideration the grey scale. More concretely, the pixels are transformed into zeros and ones. The black pixels correspond to zeros, inversely white pixels to ones. Thus, the contour of the needle is clearly represented in white which is essential for this analysis. Considering approximately fifteen lines of the image, the algorithm counts how many pixels exist between the boundaries of the needle. So, the pixel size is obtained by the ratio between the outer diameter of the needle (D_{ou}) and the number of pixels.

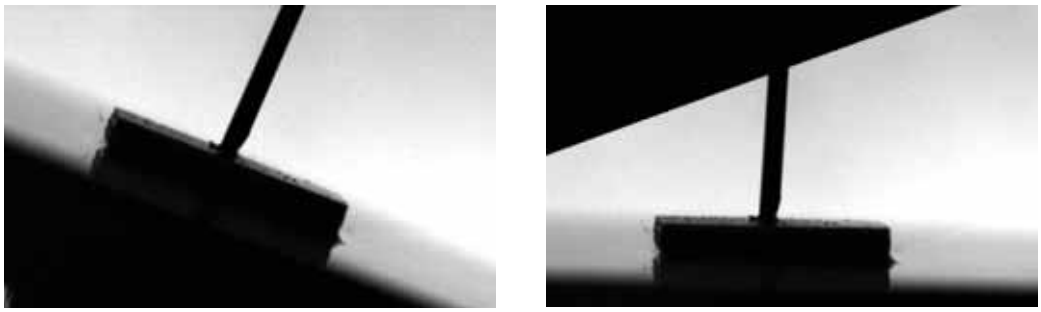

(a) (b)

Figure 2.10 - a) Reference D_{ou}= 1.26mm when the impact surface is inclined;) Rotation of the image about 20º and presentation of the respective reference.

During the experiments, the surface inclination changes and due to this the position of the camera suffered some alterations, which affects the pixel sizes. In this present work, the pixel size range between 26 and 32 pixels, which corresponds to a minimum pixel size of *39.5μm* and a maximum of *48.4μm*. A representation of the reference used to determine the pixel size is shown in figure 2.11.

Figure 2.11 - Reference used to determine the pixel size

According to Springer Handbook of Aviation Fuel Properties (1983), the measurements of a body presented in a image with gray values associated to the pixel positions can only be determined with an accuracy of ± 0.5 pixel, which in this case correspond to $\pm 24.2 \mu m$.

2.4.2 Diameter droplet

As mentioned before, experiments were performed, which had the purpose of obtaining a water droplet with diameter of *3mm*. To achieve it, several needles were used and consequently various diameters were measured. It was elaborated an algorithm that determines the vertical and horizontal maximum length of the droplet.

Firstly, it was selected approximately 52 frames with the presence of a droplet before impact and the background image without any droplet. This background image is subtracted to the image which appears the droplet (figure 2.12).

Then, occurs the binarization, where the pixels are divided into to zeros and ones, which correspond to black and white pixels, respectively. As can be seen in the following images, it was necessary to fill the droplet diameter to exhibit the droplet perfectly. This result was only achieved through the use of filters that eliminate errors that may arise.

(a) (b)

Figure 2.12 - a) Background image; b) Image analyzed with a droplet.

In the literature review, was described the variation of the droplet shape. Before the impact, the droplet may stretches and contracts. Therefore, the droplet vertical and horizontal length varies from frame to frame. Due to this, for each needle was considered five tests at the same impact height.

To determine the maximum vertical length was considered a matrix that takes was taken into account all the zero values corresponds to black pixels and the ones to white pixels. Thus, the white pixels are count in each column and the maximum value matches the maximum vertical length. The maximum horizontal length is obtained by the subtraction between all the columns with black pixels and the value of the image total horizontal pixels, more concretely, 1280 pixels.

After collecting the values of the length was necessary to obtain the mean values for the vertical and horizontal maximum length. As described in subsection 2.4.1, the real value in millimeters is achieved by the multiplication between the pixel size and the value of the droplet maximum length in pixels.

2.4.3 Impact velocity

The impact velocity is one of the most important features in the study of the dynamic behavior of a single droplet impinging onto a surface. Through this, it is possible to determine the dimensionless numbers, such as Reynolds, Weber, Laplace, Ohnesorge, and Froude numbers. It is important to mention that one of the recreated conditions taking into account the previous work was the impact velocity.

Similarly to pixel sizing and droplet diameter measurements, an algorithm for the impact velocity was developed. In this case, for each test was considered 3 images. These three images were the background, an image with the droplet right before impact and other with the droplet *1.75ms* before impact (figure 2.13).

(a) (b) (c)

Figure 2.13 - Impact velocity measurement of a 100% droplet; a) Background image; b) Droplet image 1.75ms right before the impact c) Droplet image right before the impact.

This algorithm was designed to determine the centroid position of the droplet right and *1.75ms* before impact. The difference between these two images represents the distance traveled by the falling droplet between these two instants. So, the impact velocity is calculated by the division of the distance of the centroid position and the time between the two frames. The time was selected considering the camera frame rate. As described in subsection 2.1.1 the image acquisition was pursued with *4000fps*. The two images have 7 frames of interval, hence the time period considered was *1.75ms*.

After the images had been defined, the binarization occurred. Similarly, to the droplet diameter measurement, the background image was used to the subtraction. Therefore, the subtraction occurs between this image and the other two images that presents a droplet. To avoid any error, the droplet perimeter is filled.

One of the main problems was the reflex of the droplet due to the illumination and the impact surface. So, a reflex appears as it was expected. It was added a few lines to the algorithm which label connected components in a binary image. Therefore, due to a different coloration, it was possible to identify the real droplet and the reflex (figure 2.14).

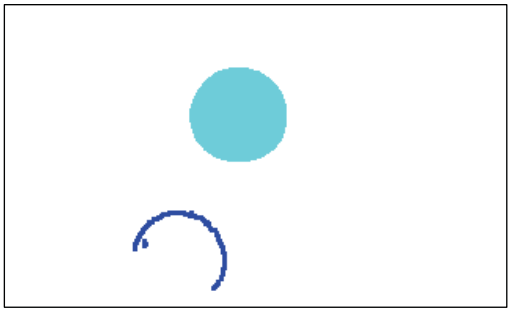

Figure 2.14 - In dark blue is represented the reflex, and light blue the droplet to measure.

To obtain the distance between the centroid positions was added to the algorithm a command *regionprops* that provides all information regarding measure properties of image regions such as area and coordinates.

Through this command, correct centroids positions were achieved. Regarding the impact velocity error, it can be determined by the ratio between half of the highest pixel and the time period. So, this value is calculated with an accuracy of $\pm 0.014 m/s$.

Chapter 3

3. Results and Discussion

This chapter is dedicated to experimental results regarding a single droplet impinging vertically onto a sloped surface. The first section describes the visualization referring to the comparison between a droplet impact onto a sloped surface and a droplet impact onto a surface with the influence of a crossflow. Through this observation, it was tried to verify if there is similarities in the phenomena occurring between the two activities. However, the results were not similar for the two activities, so several questions arose about what is causing the different outcomes on oblique impacts. In this study, it was considered the same conditions as Cunha (2018) in order to achieve similar impact characteristics.

The second section is devoted to the normal impact visualization. The purpose of this study was to observe the phenomena that occurred in this kind of impact. Therefore, it was possible to obtain the impact velocity and consequently the dimensionless numbers. These results were also compared with the previous study reported by Cunha (2018).

In the third section, several splash thresholds are presented. The deposition/splash transition was studied. The experimental results were compared with empirical correlations developed by others researches.

Finally, the last section is referent to the summary. Briefly, it is presented the most important conclusions of this chapter.

3.1 Visualization

The visualization regarding droplet impingement onto a sloped surface was based in a previously developed work by Cunha (2018). Therefore, this work aims to analyze the phenomena obtained by the impact of a single droplet on a dry surface with and without the influence of a crossflow. Four different fluids were used: 100% Jet-Fuel, 75%JF - 25%HVO, 50%JF - 50%HVO and H_2O, as a reference. The droplet diameter is a relevant characteristic in this study. Therefore, the droplet diameters for the different fluids used in Cunha (2018) are shown in table 3.1.

Table 3.1 - Fluids diameters according to Cunha (2018).

Fluids	Diameter [mm]
100%JF	3.0
75%JF - 25%HVO	3.1
50%JF - 50%HVO	3.1
H_2O	4.1

To produce these diameters, it was used needles with an inner diameter of *1.50mm*. As shown in table 3.1, the 100% Jet-Fuel, 75%JF - 25%HVO, and 50%JF - 50%HVO exhibit approximately the same diameter. On the other hand, H_2O exhibits the largest diameter. Regarding the impact surface, it was used a smooth dry aluminum surface with a mean surface roughness of Ra=$0.19\mu m$. According to Cunha (2018), in the normal impact of a single droplet upon a dry wall, three phenomena were spotted: deposition, prompt splash, and fingering.

To provide a better understanding of the previous work (Cunha, 2018), Figure 3.1 displays the influence of a crossflow on droplet behavior.

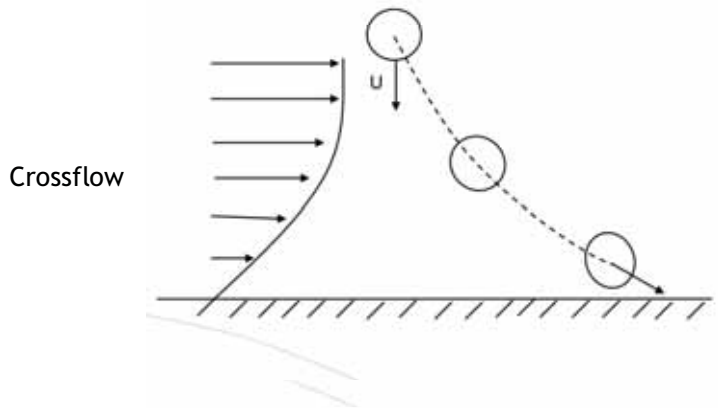

Figure 3.1 - Representative diagram regarding Cunha (2018) experimental activity.

In this previous work, Cunha (2018) designed and built a wind tunnel that allowed variations in the droplet impact velocity, which enable the visualization of different phenomena. All the tests considered in this dissertation were performed with a crossflow velocity, U_{cf}, of *7m/s*. As represented in Figure 3.2, the droplet suffers a certain deformation due to the influence of the crossflow. This effect conditions the impact. So, the droplets impacts the surface with a certain angle, defined as the incident angle (θ). The incident angle represents the angle between the absolute impact velocity and the surface.

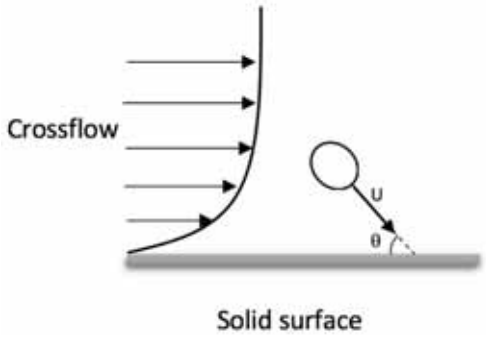

Figure 3.2 - Representation of the velocity vector and incident angle.

According to the previous work performed by Cunha (2018), the table 3.2 presents the incident angle and the phenomena, as a result of the crossflow influence, for each fluid. These results correspond to three tests performed at different conditions. For each fluid, in all the tests carried out, the spreading was verified on the two first cases of table 3.2, as intended. However, the same did not happen for the third line. The first cases corresponds to the conditions used in normal impact when splash occurred. However, this outcome did not appear under the influence of a crossflow. The second case is the spreading immediately before splash. The third case with (*) is when the splash appears.

Table 3.2 - Summary phenomena for each fluid according to the incident angle.

Fluids	Cases	Incident angle (θ^o)	Phenomenon
100% JF	1º Case	55	Spreading
	2º Case	60	
	3º Case	62(*)	Splashing
75%JF- 25% HVO	1º Case	73	Spreading
	2º Case	73	
	3º Case	76(*)	Splashing
50%JF - 50% HVO	1º Case	67	Spreading
	2º Case	67	
	3º Case	72(*)	Splashing
H_2O	1º Case	85	Spreading
	2º Case	85	
	3º Case	86(*)	Splashing

In these experiments, H_2O was the fluid that exhibited the biggest incident angle. On the contrary, the 100% Jet-Fuel presented the smallest angle. In order to recreate these different incident angles with a vertical falling droplet onto an inclined stationary surface, it is necessary to understand the dynamic of this kind of impact.

Consequently, the inclined surface will perform an angle that corresponds to 90^o-θ. The gravity acceleration and the movement of the droplet have the same direction and there is no influence of crossflow. Figure 3.3 shows the dynamic of the droplet.

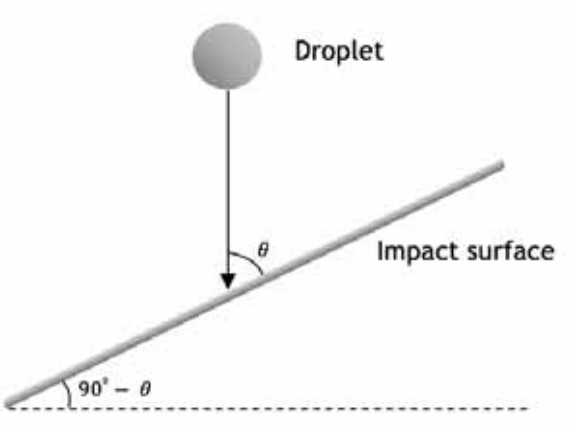

Figure 3.3 - Schematic of droplet impact onto an inclined surface.

Firstly, it was considered the results of the impact affected by the crossflow. The visualization regards the cases where it was supposed to verify splash.

3.1.1 Effect of crossflow

When a droplet is affected by a crossflow, it may deform and be oriented by the gas flow. Deformation is caused by an unequal static pressure distribution over the droplet surface (Guildenbecher et al, 2009). This deformation can be seen in figure 3.4. The effect of a crossflow on the impinging droplets can be attributed to the aerodynamic forces exerted by the gas flow (Silva, 2007).

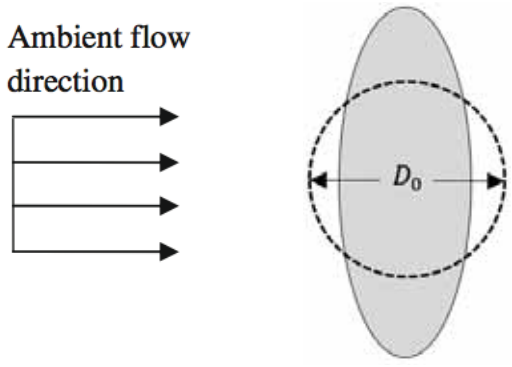

Figure 3.4 - Droplet deformation due to the crossflow adapted from (Guildenbecher et al, 2009).

3.1.1.1 100% Jet-Fuel droplet impinging onto an inclined aluminum surface (Ra=$0.13\mu m$)

Figure 3.5 a) corresponds to the impact on a dry inclined surface with an incident angle (θ) of 62^o. The surface is a smooth aluminum plate with a roughness of Ra=$0.13\mu m$. When the droplet is reaching the surface, the shape is practically spherical. Then, it extends asymmetrically to both the upper and lower sides. This definition has as reference the point of impact, represented by a white cross at the instant $\tau = 0.5ms$, figure 3.5 a) Consequently, the upper side is symbolized by an orange arrow and the lower side by a red arrow. In this figure, it is possible to visualize spreading upon a dry surface. This phenomenon can be also called deposition, and usually occurs for low impact energies without producing any secondary droplets. The instant when the droplet impinges the surface was characterized as the starting moment, at the instant $\tau = 0ms$. After this, the lamella immediately appears, and the droplet began to spread. Then, the droplet extends to its maximum dimension.

Figure 3.5 b) shows a sequence of images that represents the impact on a dry surface with the influence of a crossflow performed by Cunha (2018). So, prompt splash occurs ($\tau = 0.2ms$). This phenomenon occurs when the impact energy is high enough for the droplet to disintegrate in the first moments after impact and small droplets are ejected. Contrary to figure 3.5 a) the droplet is deformed before reaching the surface. This fact clearly influences the phenomenon, and as can be seen, the splash is asymmetrical.

Therefore, recreating the same conditions as Cunha (2018), such as impact velocity and incident angle, it was expected the occurrence of splash, however only spreading was spotted.

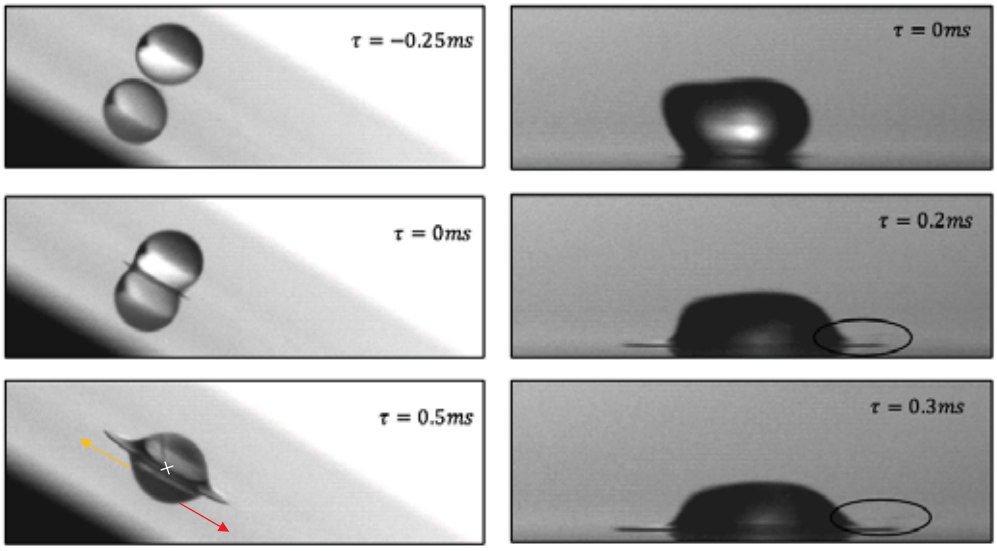

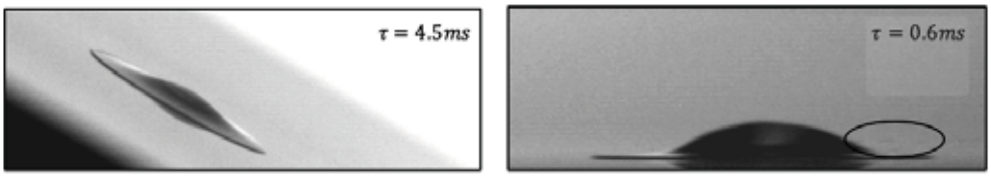

(a) (b)

Figure 3.5 - Image sequences: a) Spreading of 100% Jet-Fuel droplet impact onto an inclined surface (θ=62°, D_0=3.0mm,U=2.1m/s, Ra=0.13μm); b) Prompt splash of 100% Jet-Fuel droplet impact with the influence of a crossflow (θ=62°, D_0=3.0mm,U=2.3m/s, Ra=0.19μm).

3.1.1.2 H_2O (Water) droplet impinging onto an inclined aluminum surface (Ra=$0.13\mu m$)

The figures below correspond to the tests that used H_2O droplets with a diameter of *4.1mm*, where the occurrence of splash would be expected. Figure 3.6 a) shows the fingering originated by a H_2O droplet impinging upon a dry inclined surface with an incident angle of *85º*. The droplet spreading can have instabilities at the outer rim of the lamella that can be called fingering, according to Ribeiro (2018). It is noticeable, in instant $\tau = 0.25ms$ that splash does not occur when the droplet impacts, instead the spreading phase begins. It is possible to observe fingers at the outer rim. These fingers grow as a result of instabilities that were mentioned before. After the lamella reached the maximum diameter, the receding stage began and then the droplet recoil. Similarly, to the 100% Jet-Fuel, splash did not occur.

A H_2O droplet impinging on a dry surface with the influence of crossflow is shown in Figure 3.6 b). The droplet reaches the surface with a certain deformation due to crossflow effect. At the instant $\tau = 0.1ms$, it is possible to observe the occurrence of prompt splash. Prompt splash occurs when the impact energy is high enough for the droplet to disintegrate in the first moments after impact. At the periphery of the liquid lamella, several tiny droplets are ejected, while the crown is still rising or advancing, reported by Ribeiro (2018). Consequently, $\tau = 0.4ms$ shows the creation of a crown-like shape, however the occurrence of crown splash is not considered (Cunha et al. 2018). This crown is formed by the interaction of the crossflow and the impact of the droplet. The crossflow created an upward movement that elevated the satellite droplets in the left and right side of the impact. It was also noticeable that the splash on the left side is more evident than on the right side, due to the direction of crossflow.

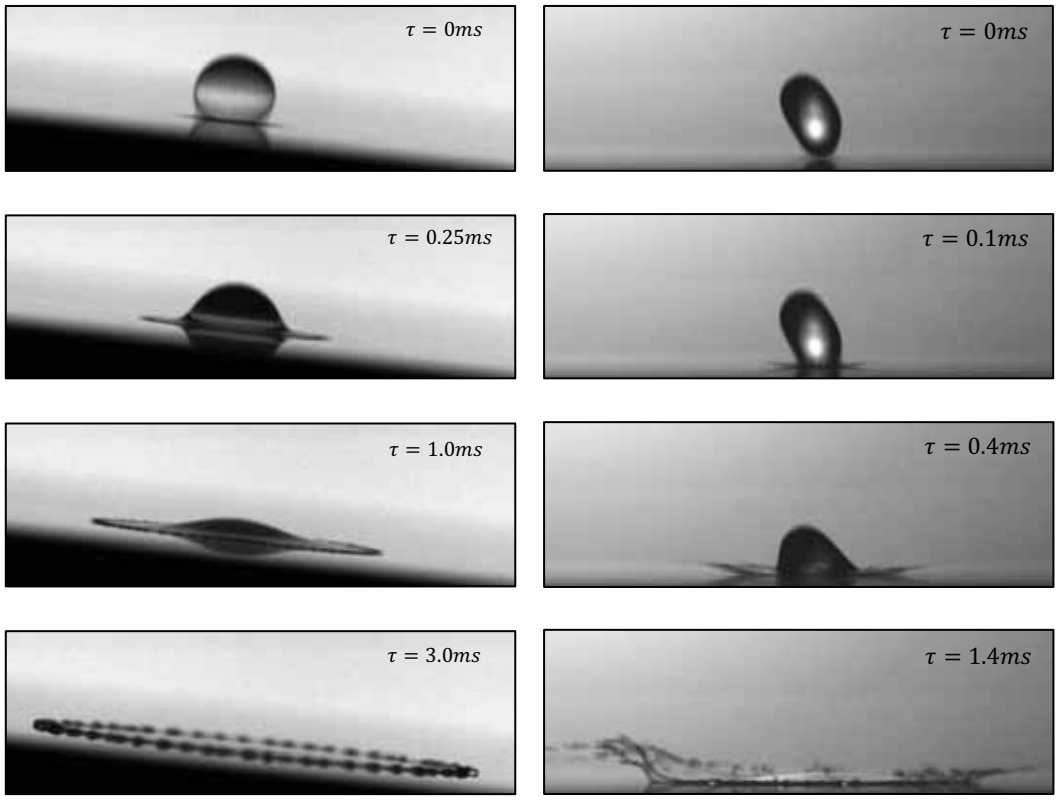

Figure 3.6 - Image sequences: a) Fingering of water droplet impact onto an inclined surface (θ=86°, D_0=4.1mm, U=4.2m/s, Ra=0.13μm); b) Prompt splash of water droplet impact with the influence of a crossflow (θ=86°, D_0=4.1mm,U=4.6m/s, Ra=0.19μm).

3.1.1.3 50%JF - 50%HVO droplet impinging onto an inclined aluminum surface (Ra=$0.13\mu m$)

The sequence of images presented below corresponds to a 50%JF - 50%HVO droplet impinging onto a surface with a roughness value of Ra=0.13μm. In this case, only splash was spotted.

Thus, considering a 50%JF - 50%HVO droplet and a dry smooth aluminum surface, it was verified splash when the impact surface is tilting *20º (θ=70º)*. Figure 3.7 a), corresponds to an impact onto an inclined surface without crossflow. In this image is represented prompt splash. This phenomenon is visible at the beginning of the spreading phase when small droplets appear which requires a high Weber number. After this, the lamella tends to expand, reaching the maximum diameter. In this case, the splash is asymmetrical and occurs in the upper and lower side.

The sequence of frames regarding Figure 3.7 b) corresponds to the impact of a droplet with the influence of a crossflow.

At the moment of impact, the prompt splash was observed. Due to crossflow effect, the droplet presented a certain deformation. The 50%JF - 50%HVO mixture presented the same outcome with the influence of crossflow and when the impact surface is inclined.

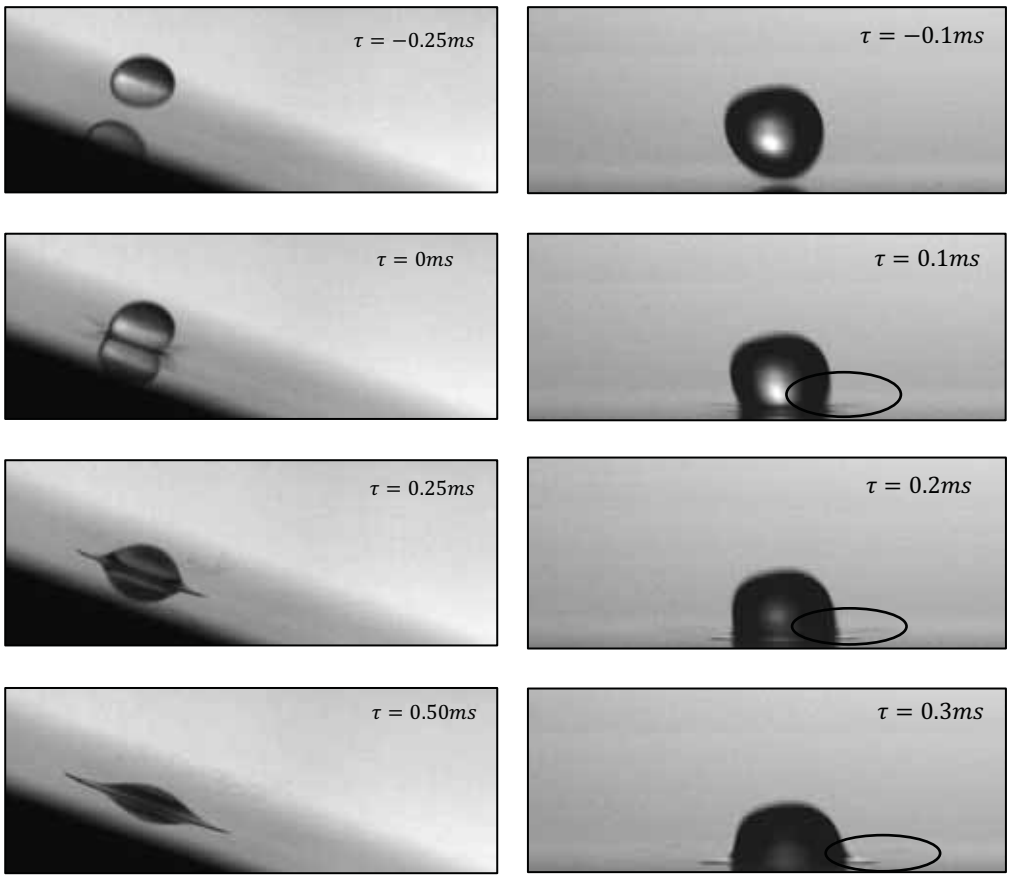

Figure 3.7 - Image sequences: a) Prompt splash of 50%JF - 50% HVO droplet impact onto an inclined surface (θ=72°, D_0=3.1mm,U=2.9m/s, Ra=0.13μm); b) Prompt splash of 75%JF - 25%HVO droplet impact with the influence of a crossflow (θ=72°, D_0=3.1mm, U=3.1m/s, Ra=0.19μm).

3.1.1.4 75%JF - 25% HVO droplet impinging onto an inclined aluminum surface (Ra=$0.13\mu m$)

Figure 3.8 a) corresponds to an inclined impact surface where a 75%JF - 25%HVO droplet is falling. The purpose is to recreate an incident angle of *75º* and analyze if the outcome is the same as Cunha (2018).

When the droplet reaches the surface, prompt splash occurs, and secondary droplets appear. The same phenomenon is presented in Figure 3.8 b). At the moment of impact, it is visible prompt splash with a crossflow velocity of $7m/s$.

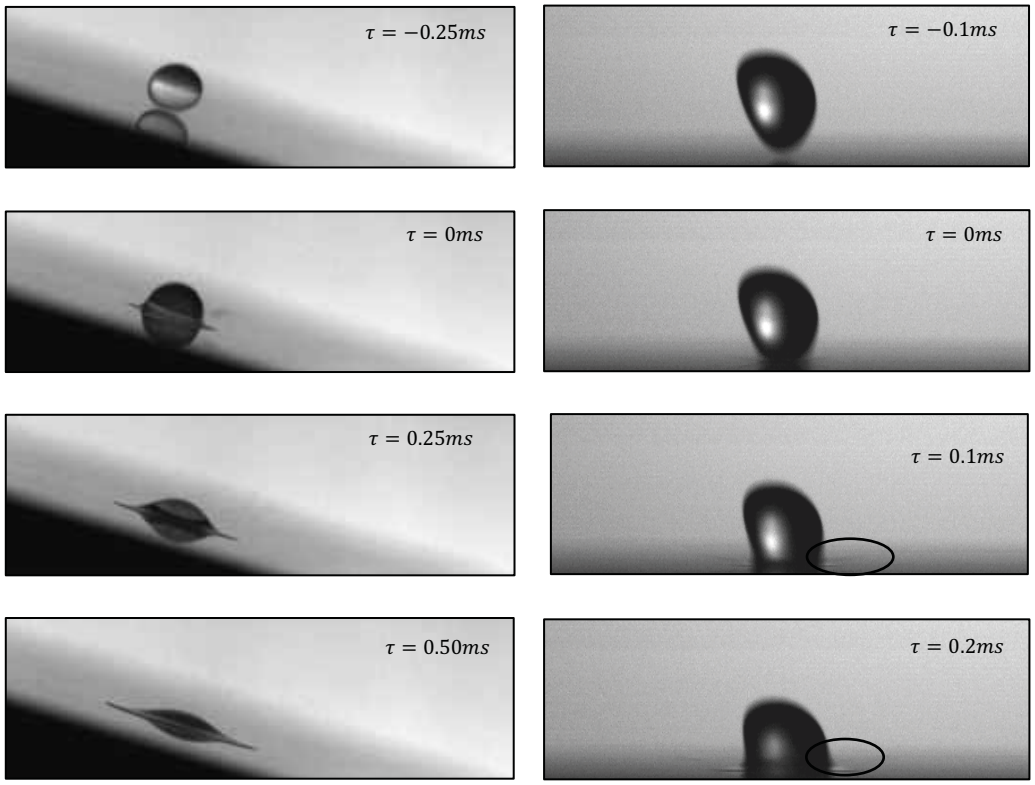

Figure 3.8 - Image sequences: a) Prompt splash of 75%JF - 25% HVO droplet impact onto an inclined surface (θ=76°, D_0=3.1mm,U=3.4m/s, Ra=0.13μm); b) Prompt splash of 75%JF – 25%HVO droplet impact with a crossflow (θ=76°, D_0=3.1mm ,U=3.5m/s, Ra=0.19μm).

For 50%JF - 50%HVO mixture, the observed phenomenon due to the influence of the crossflow is the same when it recreates the incident angle with the aid of an inclined surface. The visualization presented above is carried out with the impact surface developed for this dissertation.

Thus, a question arose if these results could be conditioned by the difference of the surface roughness between this plate and Cunha (2018) plate. After analyzing the surface roughness, it was concluded that the values were Ra=$0.13\mu m$ and Ra=$0.19\mu m$. Due to this, the following results were performed with a roughness plate of Ra=$0.19\mu m$.

3.1.1.5 100% Jet-Fuel droplet impinging onto an inclined aluminum surface (Ra=$0.19\mu m$)

The impact of a 100% Jet-Fuel droplet onto a slope surface is shown in figure 3.9. So, it was considered an inclination of *30º (θ=60º)* and a surface roughness of Ra=0.19μm. For this set of conditions, it was only spotted spreading, which indicates impact without the production of any secondary droplets. This sequence of images that represents droplet impacts onto a sloped surface show that the shape of the droplet distorts and spreads asymmetrically relative to the point of impact, with no evidence of secondary atomization. Elongation and upper-to-lower asymmetry increases with time, due to gravity. These images can be compared with figure 3.5 b). As can be seen in figure 3.5 b) the droplet presented a deformation due to the crossflow. As already referred the occurrence of splash is detected at the instant $\tau = 0.2ms$. This phenomenon is not clearly visible through the images. However, it can be affirmed that it is an asymmetrical splash.

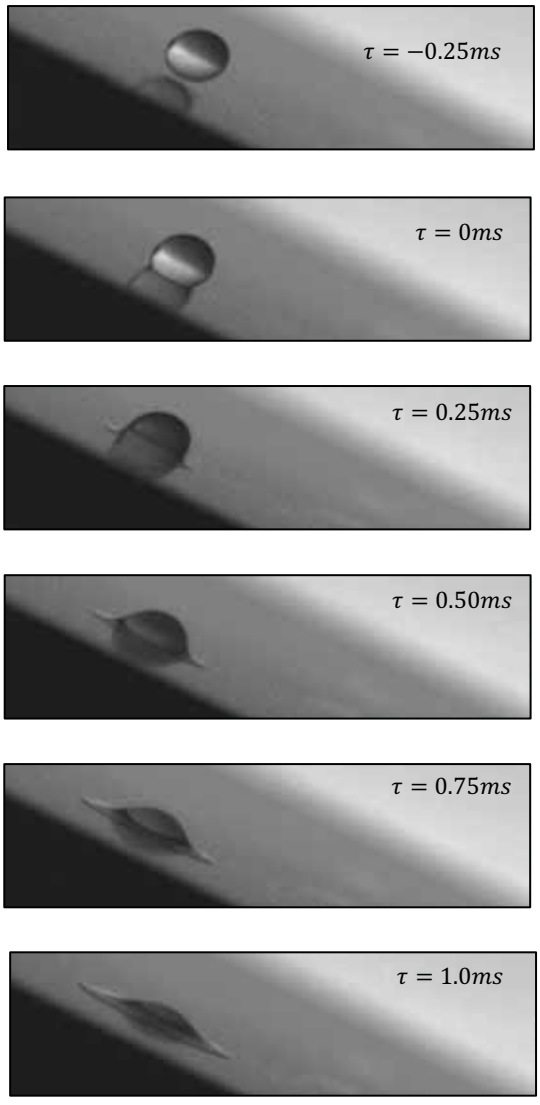

Figure 3.9 - Spreading of 100% Jet-Fuel droplet impact onto an inclined surface (θ=62°, D_0=3.0mm, U=2.2m/s, Ra=0.19μm).

Therefore, with the purpose of understanding what promote this kind of phenomenon, several questions appear. Thus, the experimental work was divided into two phases. In the first phase, it was considered a variation of the incident angle, using a sloped surface, and maintaining the same impact velocity as Cunha (2018). On the contrary, in the second phase, it was considered a constant incident angle and the impact velocity was increased through the variation of the impact height.

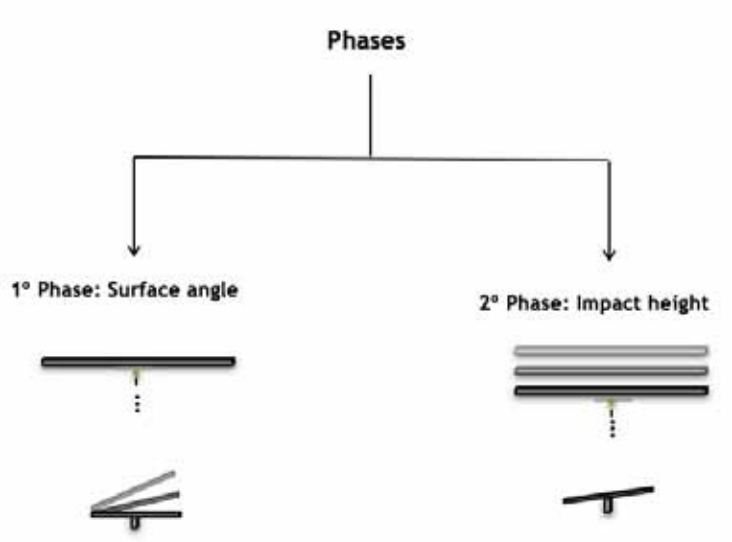

Figure 3.10 - Schematic of phases regarding 100% Jet-Fuel droplet.

Regarding the first phase, to keep the velocity constant the impact height should be the same. However, the impact surface angle changes, due to this the distance between the target surface and the dispensing needle varies. Thus, extreme careful was needed to assure that the impact velocity was kept constant. Therefore, every test had their own specifications. The impact surface angle was varied between *0º* and *30º*, with intervals of *5º*. In this case, the impact velocity was *2.1m/s*. With this experimental work, it was possible to observe that the splash occurred only for normal impact. The study regarding the variation of the incident angle, keeping the impact velocity constant emphasizes a notorious feature on the impingement onto an inclined surface. The increase of the incident angle leads to a change in the behavior of the wetted area.

So, this behavior is different from the normal impact. This indicates that the effect of gravity appears as slippage of the liquid element. Šikalo et al. (2005) noticed in their experiments that an increase of the impact velocity leads to an increase of the spreading in upper and lower directions.

Kang and Lee (1999) reported that the inclination of surface might provide a much wider area that the horizontal surface even though the normal impact momentum is decreased. They also observed that the increase in the surface inclination leads to a larger spreading diameter.

In the three sequences below is shown the influence of the variation of the incident angle. The first corresponds to an inclination of the surface approximately *25º (θ=65º)*.

As can be seen, the spreading diameter is much larger than the others, which coincide with the reported in the literature.

Regarding the other sequences, it is noticeable the difference between the diameter and the spreading velocity. The lower side velocity is larger than the upper side velocity for all the inclined surfaces.

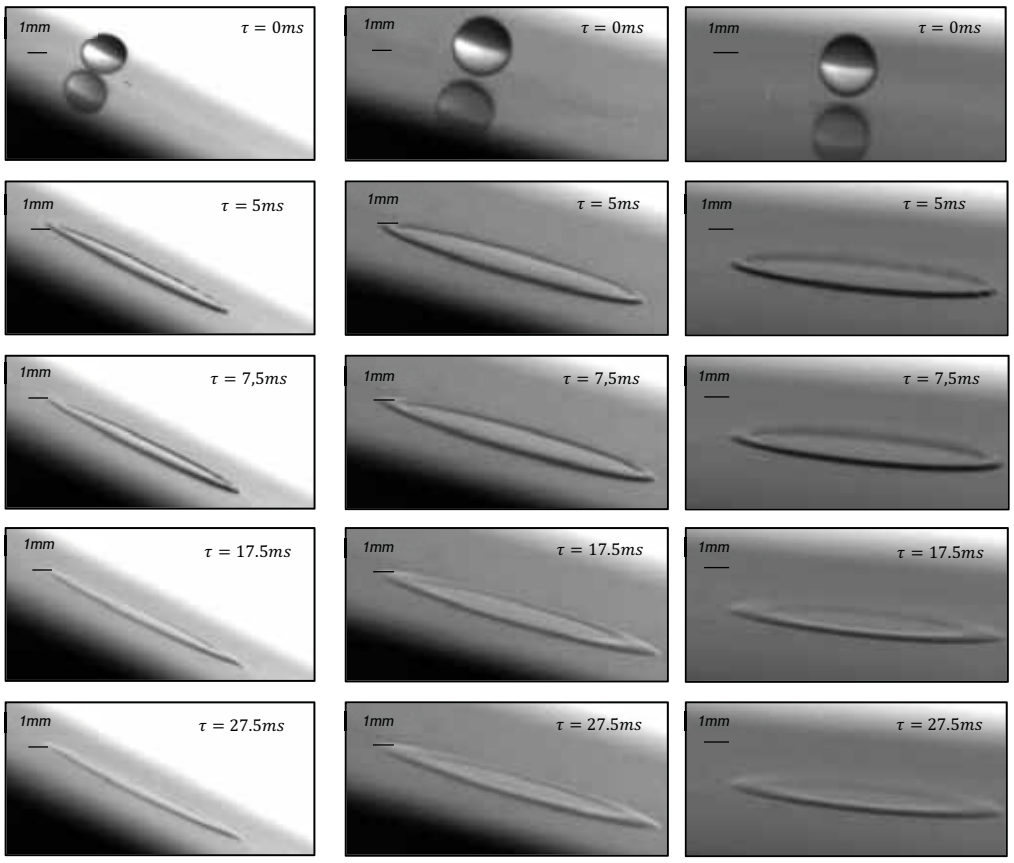

Figure 3.11 - Image sequences: a) Spreading of 100% Jet-Fuel droplet impact onto an inclined surface (θ=65º, D_0=3.0mm,U=2.1m/s, Ra=0.19μm); b) Spreading of 100% Jet-Fuel droplet impact with a crossflow (θ=75º, D_0=3.0mm,U=2.1m/s, Ra=0.19μm); c) Spreading of 100% Jet-Fuel droplet impact with a crossflow ($\theta = 85º$, $D_0 = 3.0mm$, $U = 2.1m/s$, $Ra = 0.19\mu m$).

In the second phase, it was considered a constant incident angle of *62º*. In this phase, only the impact velocity was changed. Table 3.3 shows the variation of the impact velocities maintaining the incident angle.

Table 3.3 - Results regarding the second phase for 100% Jet-Fuel droplet.

Incident angle (θ°)	Height (cm)	Velocity (m/s)
62°	29	2.2
	34	2.4
	39	2.5
	52	3.0
	56	3.1 (*)

Cunha (2018) observed splash when the impact velocity reached $2.3m/s$. However, it was noticed that the occurrence of splashing in this phase of studies only happen when the impact velocity is approximately $3.1m/s$, as represented by (*).

These results agree with Liu et al. (2010) saying that increasing oblique impact angles, the spreading velocity increase, but splashing reduces. This fact was verified in the first phase. As expected in the second phase, increasing the impact velocity, the probability of visualize splash is higher, as already been referenced by several authors.

3.1.1.6 H_2O (Water) droplet impinging onto an inclined aluminum surface (Ra=$0.19\mu m$)

Figure 3.12 represents a H_2O droplet impinging onto an inclined surface. In work developed by Cunha (2018) it was verified splash for this fluid. Therefore, it was recreated an incident angle of 85^o and only fingering was spotted. This phenomenon that presents finger-like shapes can be identified at the instant $\tau = 0.25ms$. After impact, the lamella diameter increased, and no secondary atomization was produced. Then, the lamella reached the maximum diameter and the receding stage started, so the droplet recoiled.

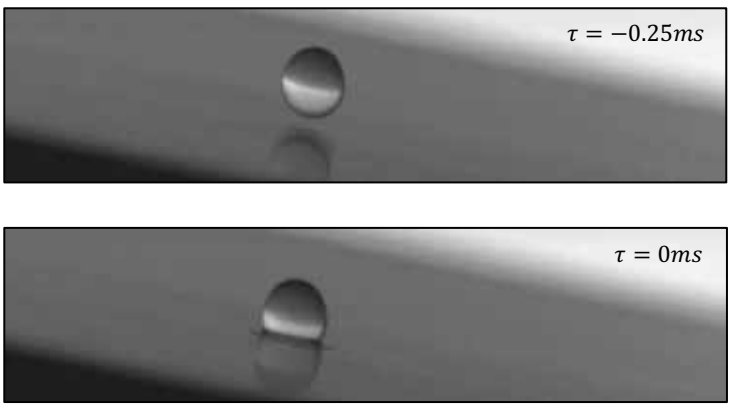

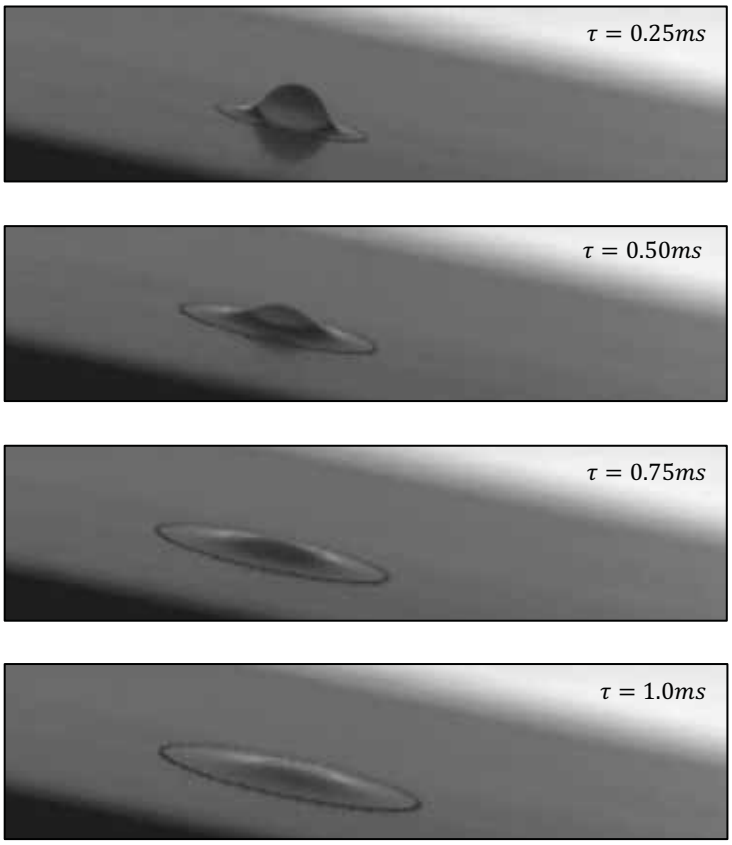

Figure 3.12 - Fingering of H_2O droplet impact onto an inclined surface (θ=86°, D_0=3.0mm, U=4.5m/s, Ra=0.19μm).

As already mentioned, this result were not similar to Cunha (2018).So, it was necessary to understand what parameters influence the producing splash. Therefore, the same procedure was used as 100% Jet-Fuel. However, in this case, it was considered three phases of studies.

At the first phase, the incident angle was constant, and the impact velocity was increased. On the contrary, in the second phase, the impact velocity was maintained, and it was considered a variation of the incident angle. Analyzing the table 3.1, all diameters are approximately *3mm*, except the H_2O. So, in the third phase, it was studied the dynamic of a single droplet impinging onto a dry surface with a smaller diameter, involving the normal impact and the impact with a crossflow. Consequently, it was possible to compare all the results obtained by Cunha (2018) with the same droplet diameter for the different fluids.

In the first phase, it was tested three different incident angles, and it was used an impact velocity of $4.3m/s$. In these experiments, the three incident angle (θ) were 90^o, 87.5^o, and 85^o. This case did not exhibit splash for any incident angle.

Regarding the second phase, the incident angle was kept at 85^o, and the impact velocity was increased.

According to Cunha (2018) due to the influence of crossflow, the splash occurred when the impact is *4.61m/s*. In this case, without crossflow and the droplet falling vertically the splash occurred when the impact velocity reached *5.2m/s (table 3.4)*.

Table 3.4 - Results regarding the second phase for H_2O droplet.

Incident angle (º)	Height (cm)	Velocity (m/s)
85º	135	4.5
	139	4.9
	146	5.2 (*)

As previously mentioned, in the third phase the experiments were performed with a smaller droplet diameter. So, it was used a water droplet with a diameter of *3.0mm*. To achieve this diameter, several tests were made. Before starting these tests, it was necessary to define certain parameters such as the impact height, the needle inner diameter, and others. Therefore, Ribeiro (2018) reported that the droplet diameter does not change significantly with the impact height. Ribeiro (2018) elaborated the table 3.5 that shows the relation between the needle inner diameter and the droplet diameter that is relevant for this study.

Table 3.5 - The H_2O droplet diameter according to (Ribeiro, 2018).

Needle Inner Diameter	H_2O Diameter [mm]
0.51	3.2
0.25	2.8

Through these conclusions, it was performed five different tests at the same height. The needle used had an internal diameter of *0.3mm*, thus giving rise to water droplet diameter of *3mm*. After achieving this diameter, it was executed experiments with and without the influence of the crossflow. The behavior of a droplet on the influence of crossflow is quite different from a normal impact. At a normal impact the droplet falls down vertically, and its shape is spherical before impacting onto the surface. For the inclined impacts, the droplet shape is also spherical before the impact. However, when a droplet is influenced by a crossflow it is noticed a certain deformation before the impact, shown in figure 3.13 represented by droplet (2).

Figure 3.13 – H_2O droplet shape (D_0=3mm), which (1) corresponds to normal impact and (2) to crossflow impact (U_{cf}=7m/s).

Figure 3.14 is a sequence of images regarding the water droplet impacting onto a dry surface with the influence of the crossflow, where the droplet presents a certain deformation. The purpose of this test was to study the dynamic behavior of a water droplet with *3mm* diameter. To achieve this goal, the wind tunnel built by Cunha (2018) was used and it was considered the same crossflow velocity, $U_{cf} = 7m/s$. Fingering was the only phenomena spotted. This outcome can be verified at the instant $\tau = 0.75ms$. This phenomenon occurs when the lamella formed has surface perturbations that extended radially creating what is called "fingers" (Yarin, 2006).

Unfortunately, due to several constraints in the experimental setup, it was not possible to verify splash for this condition. Due to the high impact velocity, the image is not displayed with the desired sharpness.

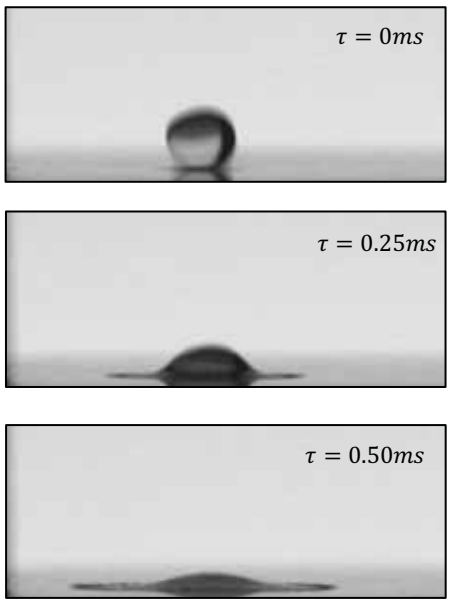

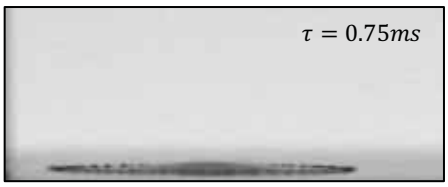

Figure 3.14 - Fingering of water droplet impact onto an inclined surface (D_0=3.0mm, U=5.2m/s, Ra=0.19μm).

These results agreed with the literature. Stow and Stainer (1977) reported that the number of droplets produced by splash increases with the impact velocity and droplet size. So, using a smaller diameter it was expected to be more difficult the visualization of splash.

3.1.1.7 50% JF - 50% HVO droplet impinging onto an inclined aluminum surface (Ra=$0.19\mu m$)

In this case, it was reproduced an incident angle of *72º*. As it was expected for a 50%JF - 50%HVO droplet it can be noticed splash at the moment of impact. This phenomenon is defined as prompt splash and can be detected at the instants $\tau = 0ms$ and $\tau = 0.25ms$. Due to inclination, the lamella continues to increase its diameter till reach the maximum value. This sequence of images is compared to figure 3.7 b)) where the droplet is influenced by the crossflow. Through these images, it is concluded that the phenomena visualized were similar when the droplet is influence by the crossflow and when it is impinging onto a sloping surface.

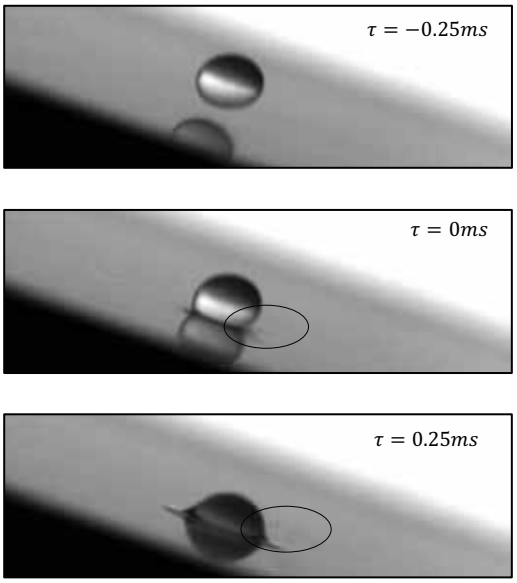

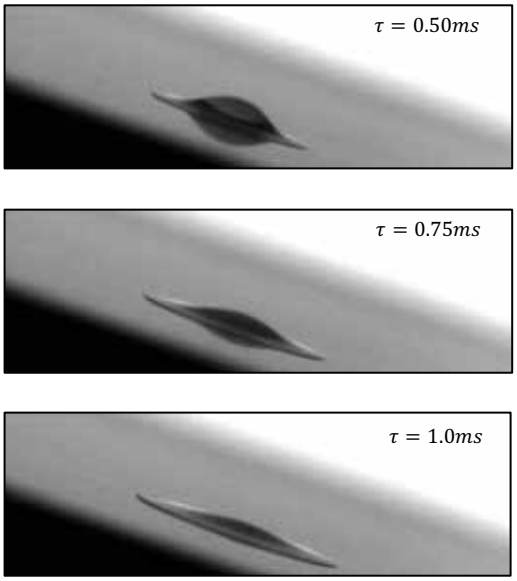

Figure 3.15 - Prompt splash of 50%JF - 50% HVO droplet impact onto an inclined surface (θ=72º, D_0=3.1mm, U=2.9m/s, Ra=0.19μm);

3.1.1.8 75%JF - 25% HVO droplet impinging onto an inclined aluminum surface (Ra=$0.19\mu m$)

For the 75%JF - 25%HVO mixture the phenomenon is shown in Figure 3.16. At the moment of impact, few secondary droplets can be detected as well as the asymmetric splash. Consequently, it is clearly perceptible that on the lower side the splash is more intense. According to Zen et al. (2010), the instability of the lower side is relatively higher than the upper side. The hypothesis is that the component of gravity, which is parallel with the inclined surface, promotes the instability of downward flow in the spreading stage. On the other hand, the same forces acting on the upward flow will suppress this instability. In this case, it was used an impact surface with Ra=*0.19μm* and approximately $\theta = 75º$.

This case is compared with Figure 3.8 b) where a 75%JF - 25%HVO droplet is deformed due to crossflow. Thus, it was verified that recreating the same incident angle and the same impact velocity can achieve splash.

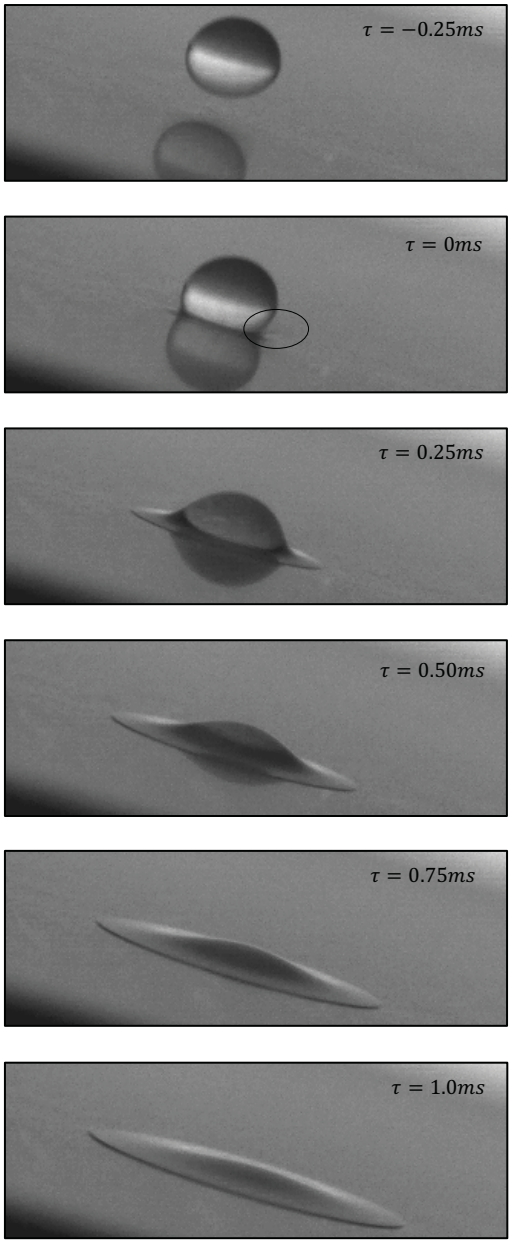

Figure 3.16 - Prompt splash of 75%JF - 25% HVO droplet impact onto an inclined surface (θ=75°, D_0=3.1mm, U=3.2m/s, Ra=0.19μm).

Through these results, it is concluded that although an inclined impact and an impact with the influence of crossflow are considered oblique impacts, which does not imply that the phenomena visualized are the same. In all cases, only the mixtures presented the same outcomes as in Cunha (2018). Thus, several doubts arose about what will be the parameter that most conditions the similarity of the phenomena. In this way, the parameters that are conditioning can be the deformation of the drop, the fluids physical properties, and components of the impact velocity.

3.2 Normal impact

The normal impact happens when the droplet impacts perpendicularly onto a surface. Figure 3.17 shows the dynamic of this kind of impact.

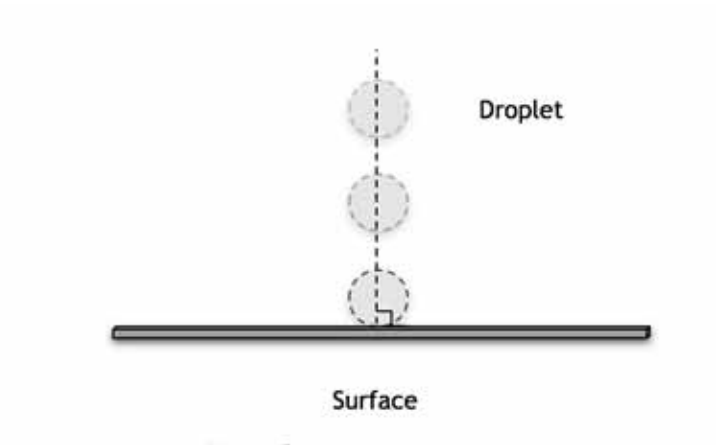

Figure 3.17 - Schematic of the normal impact.

In this present work, it was also recreated the normal impact using the same conditions as Cunha (2018). It will be presented several images regarding the normal impact. Firstly, it will be shown the results obtained with the impact surface developed for this dissertation (Ra=$0.13\mu m$), demonstrated in 3.2.1. The remaining results shown correspond to plate used by Cunha (2018), which are presented in 3.2.2.

3.2.1 100% Jet-Fuel, 75%JF - 25% HVO and 50%JF - 50% HVO droplets impinging onto an aluminum surface (Ra=$\mathbf{0.13\mu m}$)

At normal impact, the 100% Jet-Fuel, 75%JF - 25%HVO and 50%JF - 50%HVO presented the same behavior. Due to this, the three sequences presented below show the normal impact when the impact surface has no inclination. In the presented sequences the splash becomes more perceptible at instant $\tau = 0.25ms$. A few secondary drops are visible, so it can be affirmed the occurrence of prompt splash and consequently the diameter of the lamella increases. Unlike the results on a sloped surface, in these cases the phenomenon is symmetrical. This fact is verified due to the inexistence of tangential velocity.

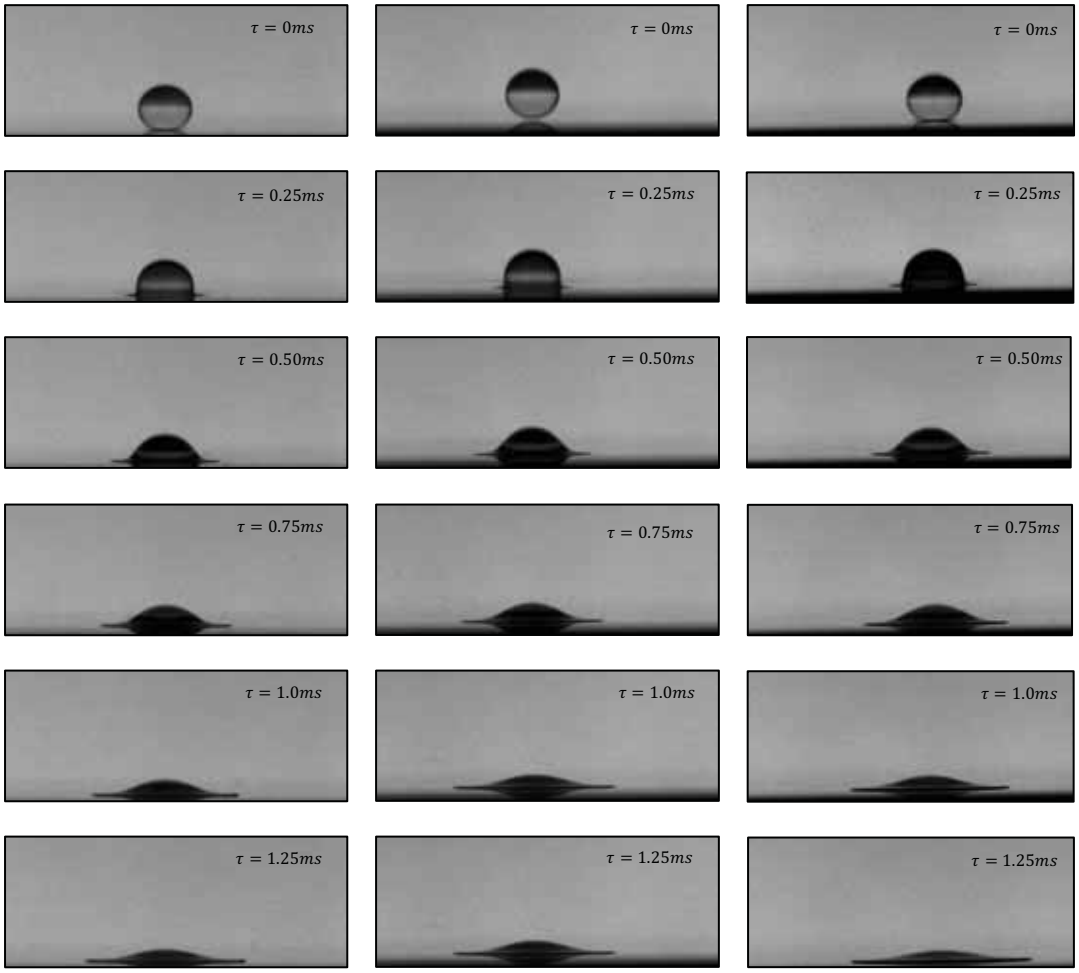

(a) (b) (c)

Figure 3.18 - Image sequences: a) Splash of 100% Jet-Fuel droplet that occurs for the normal impact ($D_0 = 3.0mm, U = 2.1m/s, Ra = 0.13\mu m$); b) Splash of 75% JF - 25% HVO droplet that occurs for the normal impact ($D_0 = 3.1mm,\ U = 2.9m/s,\ Ra = 0.13\mu m$); c) Splash of 50%JF - 50% HVO droplet that occurs for the normal impact ($D_0 = 3.1mm,\ U = 2.8m/s,\ Ra = 0.13\mu m$).

3.2.2 100% Jet-Fuel, 75%JF - 25% HVO and 50% JF - 50% HVO impinging onto an inclined aluminum (Ra=$0.19\mu m$)

In the present work, the surface was stationary, and the droplets fall vertically. The same dynamics of impact were also carried out by Cunha (2018). This means that applying almost the same impact velocity as Cunha (2018), the three fluids verified the presence of splash. At these experiments, the impact surface used by Cunha (2018) was placed above the mechanism that is performing a *0º* angle. Thus, the sequence of frames below shown the correspondent tests.

The first sequence is regarding 100% Jet-Fuel. In the figure 3.19 a), the occurrence of splash is not clearly noticeable. At the instants $\tau = 1.25ms$ and $\tau = 1.75ms$, very fine secondary droplets are ejected from the rim immediately after impact. Then the length of the lamella increased. This kind of splash can be defined as prompt splash. After the lamella reaches the maximum extension, the 100% Jet-Fuel droplet does not contract back and there is not evidently noticeable the receding contact line motion. The appearance of splash is also visible in the other two cases sequences b) and c). The dynamic behavior of the impinging droplet is practically the same as 100% Jet-Fuel. The occurrence of secondary drops right after the impact evidences the splash phenomenon, as can be seen at the instants $\tau = 0.25ms$ of sequence b) and c). After this happened, the droplet reaches the maximum diameter and the contraction of the lamella does not occur.

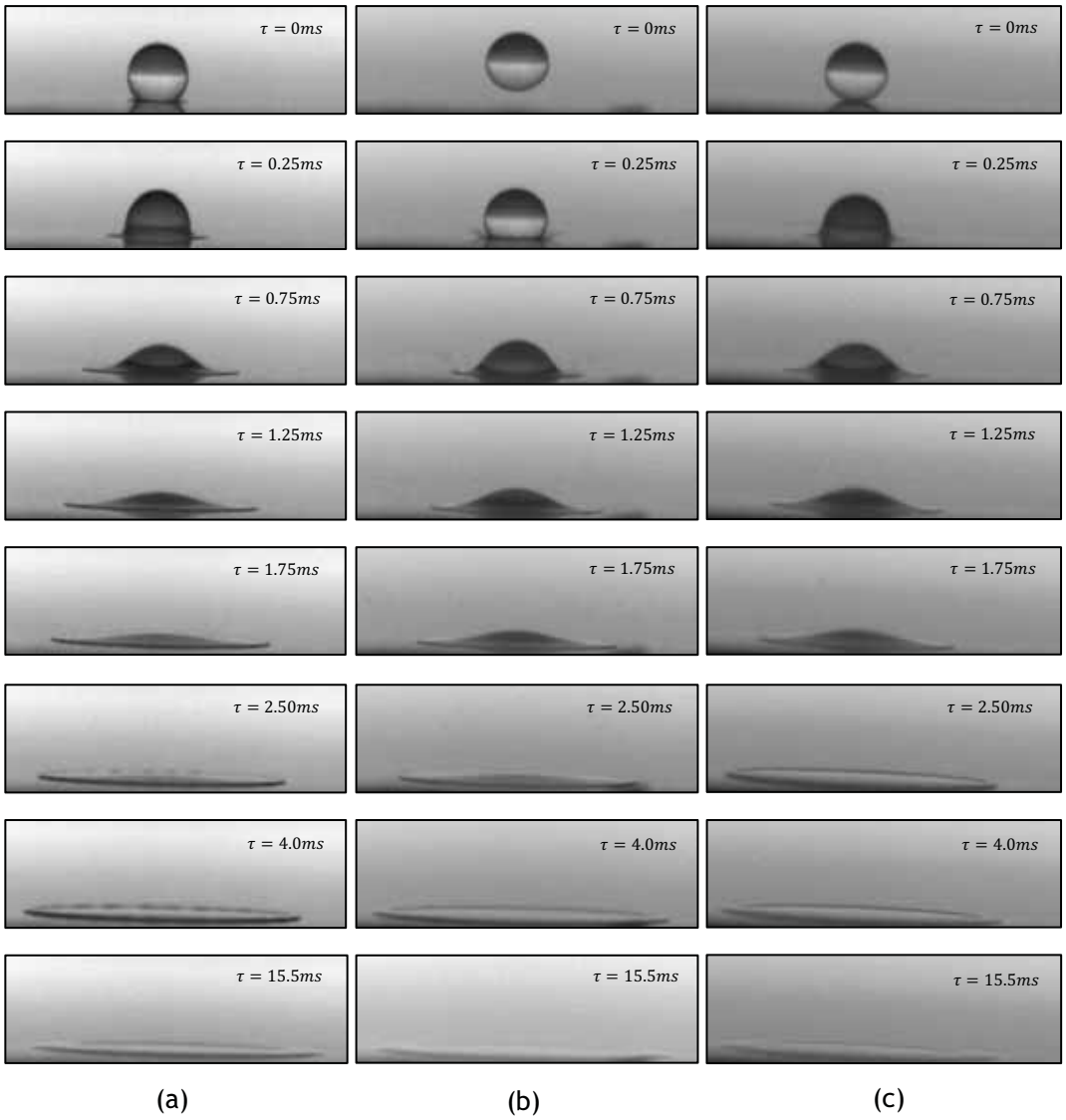

Figure 3.19 - Image sequences: a) Splash of 100% Jet-Fuel droplet that occurs for the normal impact ($D_0 = 3.0mm,\ U = 2.1m/s,\ Ra = 0.19\mu m$); b) Splash of 75%JF - 25% HVO droplet that occurs for the normal impact ($D_0 = 3.1mm,\ U = 3.2m/s,\ Ra = 0.19\mu m$); c) Splash of 50%JF - 50%HVO droplet that occurs for the normal impact ($D_0 = 3.1mm,\ U = 3.0m/s,\ Ra = 0.19\mu m$)

At the impact onto an inclined surface, the shape of the droplet deforms usually asymmetrically. This fact indicates that is notable a certain difference in the lower and upper side after the impact. However, at the normal impact the phenomenon is equal for each side.

3.3 Splash-Threshold

As described in the literature, several transition criteria were presented in order to establish a boundary between the splash and the deposition regime. Thus, in this section is demonstrated the results obtained for several criteria.

The criteria considered were proposed by Bai and Gosman (1995), Mundo et al. (1995), Vander Wal et al. (2006), Bird et al. (2009), and Aboud and Kietzig (2015). However, the criteria presented do not have the same characteristics. Bai and Gosman (1995), Mundo et al. (1995) and Vander Wal et al (2006) only considered one component of the impact velocity, while Bird et al. (2009) and Aboud and Kietzig (2015) take into account both of the components more concretely the normal and tangential velocity.

The aim of this section is to verify if the results obtained in this dissertation fit properly in the presented empirical correlations.

Firstly, the subsection 3.3.1 will be dedicated to the normal impact, using only three criteria Bai and Gosman (1995), Mundo et al. (1995), and Vander Wal et al. (2006).Then, in the subsection 3.3.2 are the results regarding the sloped surface with the presentation of the most relevant characteristics and transition criteria developed by Bai and Gosman (1995), Mundo et al. (1995), Vander Wal et al. (2006), Bird et al. (2009) and Aboud and Kietzig (2015).

3.3.1 Normal impact

In this subsection, the transition between deposition and splash for the normal impact is presented. The difference between these phenomena is obtained through the variation of the impact height which depends on the conditions of the experimental facility, as described in section 2.1. Due to this, for each fluid, the transition deposition/splash was studied. To provide a better understanding of this boundary it was elaborated the table 3.6. In this table is shown all the results regarding the impact velocity, droplet diameter, dimensionless numbers, and fluids physical properties.

Table 3.6 - Results regarding normal impact which includes present work's surface (Ra=0.13μm) and Cunha (2018) surface (Ra=0.19μm).

	100% JF		75%JF-25%HVO		50%JF-50%HVO		H_2O $(D_{in} = 1.5mm)$		H_2O $(D_{in} = 0.5mm)$		
	D	S	D	S	D	S	D	S	D	S	
$U_0[m/s]$	2.0	2.1	2.7	2.9	2.5	2.8	6.0	-	5.3	-	Present work' s surface
Re	4333	4593	4492	4896	3336	3825	24339	-	15767	-	
We	389	436	674	800	595	782	1854	-	1053	-	
$Oh\mathbf{x10^3}$	4.5		5.8		7.3		1.8		2.1		
La	49081		29949		18706		319550		236121		
$D_0\ [mm]$	3.0		3.1		3.1		4.1		3.0		
$\rho[Kg/m^3]$	798.3		795.0		792.4		1000		1000		
$\sigma[mN/m]$	25.4		25.5		24.6		72.8		72.8		
$\mu[mPa.s]$	1.1		1.4		1.8		1.0		1.0		
$U_0[m/s]$	1.8	2.1	2.9	3.0	2.7	2.8	6.0	-	5.2	-	Present work with Cunha (2018) surface
Re	3929	4507	5000	5182	3725	3904	24255	-	15655	-	
We	317	417	835	897	742	815	1841	-	1038	-	
$Oh\mathbf{x10^3}$	4.5		5.8		7.3		1.8		2.1		
La	49081		29949		18706		319550		236121		
$D_0\ [mm]$	3.0		3.1		3.1		4.1		3.0		
$\rho[Kg/m^3]$	798.3		795.0		792.4		1000		1000		
$\sigma[mN/m]$	25.4		25.5		24.6		72.8		72.8		
$\mu[mPa.s]]$	1.1		1.4		1.8		1.0		1.0		

The first lines corresponds to results obtained for the surface with Ra=$0.13\mu m$ and the second lines to the surface used by Cunha (2018) with Ra=$0.19\mu m$. The dynamic behavior of a droplet impinging onto a surface is extremely dependent on the physical properties of the fluid. The surface tension influences the droplet size. This means that a higher surface tension leads to a higher droplet diameter. The surface tension and density values for the mixtures and the 100% Jet-Fuel are almost similar. However, for the mixtures, the transition between deposition and splash requires a higher impact velocity, comparatively to 100% Jet-Fuel. Due to the limitations in the experimental facility, it was not possible to visualize splash for H_2O. This outcome did not occur for any impact surface.

Therefore, there is no transition velocity between deposition and splash for this fluid. These results are relevant to elaborate the empirical correlations, which predict the occurrence of secondary atomization.

According to Bai and Gosman (1995), for a dry surface, the transition between deposition and splash take into consideration the A coefficient, which depends of the surface roughness (Ra). This means that each impact surface has a different coefficient A that can be obtained in table 1.3.

As already mentioned, in this dissertation two different impact surfaces were used with the following surface roughness Ra=$0.13\mu m$ and Ra=$0.19\mu m$. Due to this, to obtain the correct value for A it was created an equation for interpolation of the data provided from table 1.3, which means that for the surface with roughness Ra=$0.13\mu m$, the A coefficient is approximately A= 4447. So, for this criterion, the equation used for the smoother surface is presented below.

$$We_c = 4447.La^{-0.18} \qquad (1.11)$$

The boundary line proposed by Bai and Gosman (1995) is shown in figure 3.20. As can be seen, the dimensionless numbers defined as the variables demonstrated in equation 1.11 are not the same as in figure 3.20. To compare with others criteria, the Weber and Laplace numbers were transformed into Reynolds and Ohnesorge numbers. The equation is represented as:

$$Oh.Re^{1.218} = A^{0.6097} \qquad (3.1)$$

Each fluid has a different color, and when the symbol is filled, splash occurs. For H_2O, it was not visible the transition between deposition and splash, so no reference will be shown in figure 3.20. Regarding the splashing threshold proposed by Bai and Gosman (1995) it can be noticeable a difference between the results for the mixtures and for the 100% Jet-Fuel. For 75%JF - 25%HVO and 50%JF - 50%HVO the transition between deposition and splash fits well for this criterion. This means that in these fluids the is below the boundary line and splash is above. However, to 100% Jet-Fuel, the deposition, and splash are plotted in the deposition area of the graphic.

Figure 3.20 also displays more two lines. These lines correspond to the criteria presented by Mundo et al. (1995) and Vander Wal et al. (2006). The equations regarding these splash thresholds are presented in subsection 1.2.5. These expressions only depend on Reynolds and Ohnesorge numbers.

Mundo et al. (1995) also proposed a splashing threshold for droplets impinging upon a dry stainless-steel surface.

In their experiments, it was used three different fluids (Water, ethanol, and water-ethanol-sucrose) with a droplet diameter between 60 μm and 150μm. Their experiments focused on the interaction between droplet and air boundary layer which was formed by the disk rotation.

This correlation is presented in equation 1.12.

$$K_c = Oh.Re^{1.25} = 57.7 \qquad (1.12)$$

Comparing the results with their empirical correlation it can be noticeable that none of the fluids is close to the boundary line. All the results are draw in the splash area of the graphic. One of the reasons for this discrepancy is the fact that Mundo et al. (1995) used a rotating disk. Due to this, the droplets collide with a certain angle upon the surface, this could be a possible explanation for this difference.

In the same graphic, it is also shown another line that corresponds to Vander Wal et al. (2006) criterion. These authors determined an empirical correlation for the splash/ non-splash boundary for dry surfaces and thin liquid films. These splash/non-splash regions of behavior were determined using the *Oh* and *Re* numbers. Their empirical correlation is presented in

$$K_c = Oh.Re^{0.609} = 0.85 \qquad (1.13)$$

Considering the results presented in the graphic, it can be seen that the mixtures are spotted in the splash area and the 100% Jet-Fuel in the deposition area. However, this criterion seems to provide an acceptable correlation due to the proximity to the boundary line. Although all the results do not fit as expected in the boundary lines which does not mean that these criteria are not taken into account. Considering the criterion presented by Bai and Gosman (1995) it was shown that the mixtures perfectly fit, unlike the 100% Jet-Fuel. Vander Wal et al. (2006) criterion provides a great adjustment for all the fluids. In their experiments, it was used an aluminum disk with a mean surface roughness of less than *10* nm which could explain the proximity of the experimental data with their correlation. However, Mundo et al. (1995) presented the criteria that none of the results are near to the boundary line. That fact can be explained by the behavior of the droplet due to the rotating surface. This means that could be adjusted for others experimental studies.

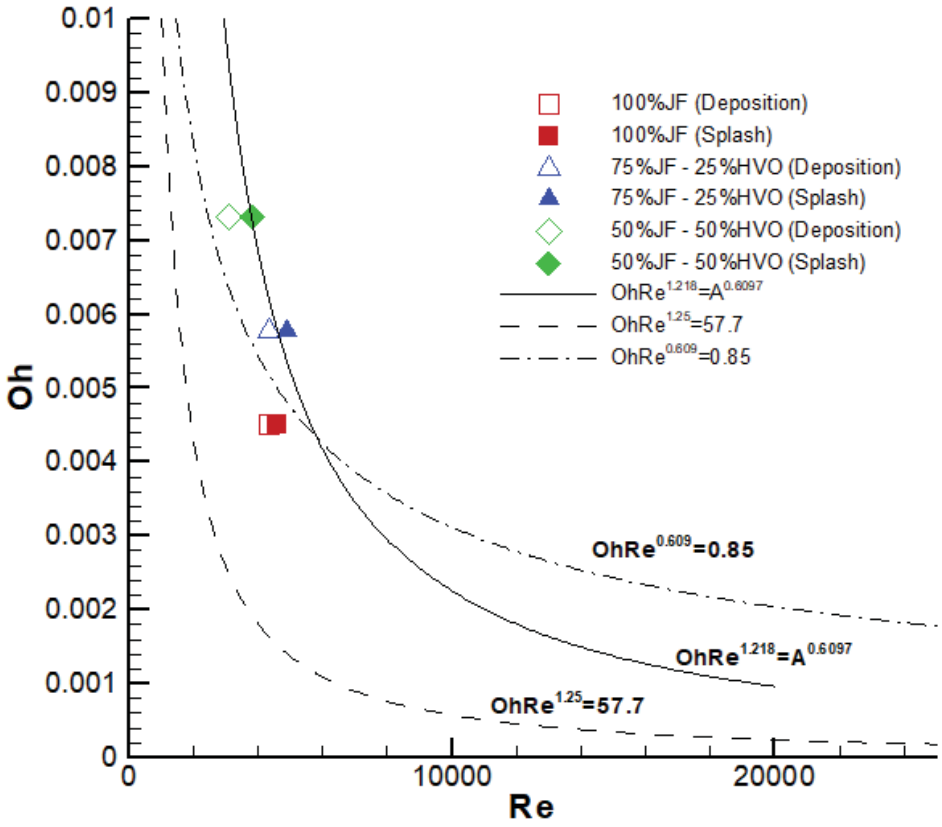

Figure 3.20 - Graphic comparing the experimental results with Bai and Gosman (1995), Mundo et al. (1995) and Vander Wal et al. (2006) splashing threshold, regarding the present work's surface and the normal impact.

The graphic presented above corresponds to the experimental data using an impact surface with a mean roughness of Ra=$0.13\mu m$. As already referred, the experiments were performed with two impact surfaces. So, figure 3.21 shows the results for all the fluids using the same impact surface as Cunha (2018). This plate has a surface roughness Ra=$0.19\mu m$ and it was considered for the normal impact.

The same criteria presented before were also compared for this surface. In this case, each fluid has a different color and the splash has the symbol filled. Regarding Bai and Gosman (1995) criterion, it was necessary to determine the A coefficient for this impact surface. So, following the methodology described above, the value for the A coefficient is 4194, when the surface roughness is $0.19\mu m$. For each fluid, the results are near to the boundary line. However, do not fit so well as in figure 3.20. Cunha (2018) suggested that the empirical correlation proposed for a lower surface roughness, could be used to predict the transition criteria for the mixture. This fact was verified through these images. Besides this, the boundary line proposed by Mundo et al. (1995) is still the most furthest from the results.

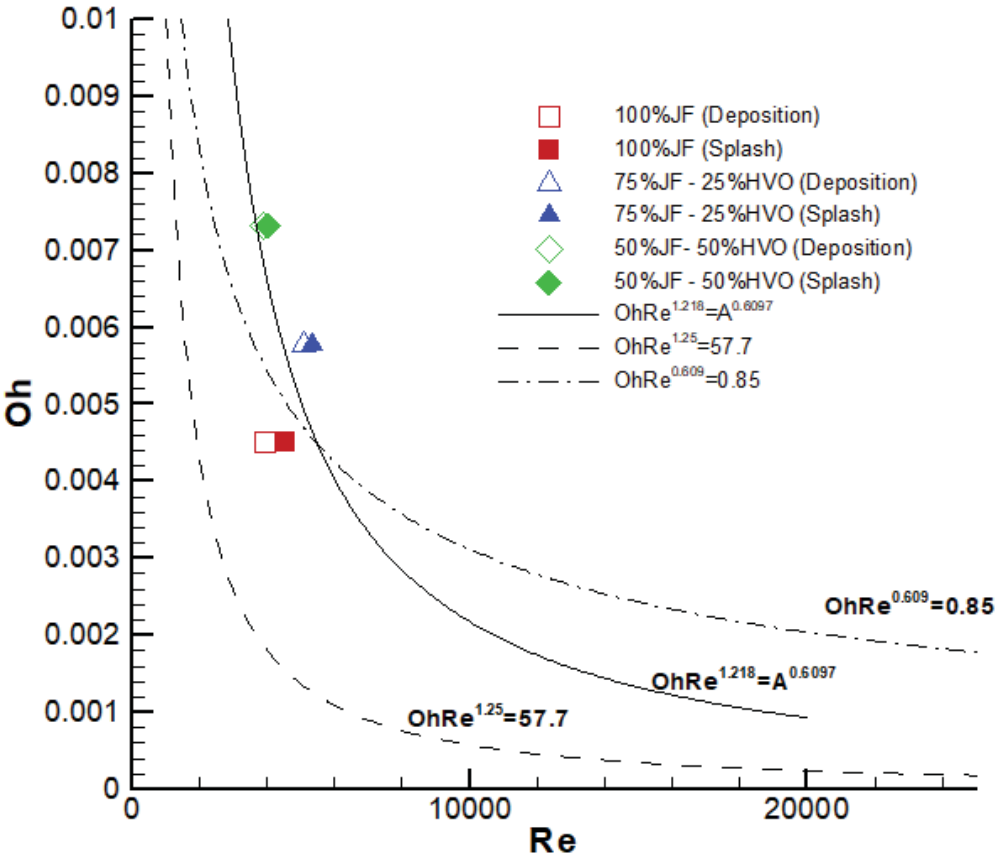

Figure 3.21 - Graphic comparing the experimental results with Bai and Gosman (1995), Mundo et al. (1995) and Vander Wal et al (2006) splashing threshold, regarding the Cunha (2018) surface and the normal impact.

There is no proximity to any of the fluids. Considering the Vander Wal et al. (2006) criterion the results are close to the boundary line, however, the 100% Jet-Fuel (deposition and splash) are in the deposition area, and the mixtures (deposition and splash) are spotted in the splashing area.

3.3.2 Oblique impact

In this present work, it was performed a comparison between a droplet impact onto a sloped surface and a droplet impact onto a surface with a crossflow. The purpose was to recreate some conditions for an inclined surface and verified if the outcomes obtained were the same when a droplet is influenced by the crossflow. These outcomes are shown in table 3.2. The results were obtained for the droplet impacts onto a surface with $U_{cf} = 7m/s$. For each fluid, three tests were performed, and it was expected spreading and splash, as already mentioned. However, some fluids do not present similar outcomes as Cunha (2018). This difference in the visualization of the outcome occurs for two cases where splash was expected to be observed, which corresponds to 100% Jet-Fuel and H_2O. Table 3.7 shows the impact velocity and the dimensionless numbers regarding the inclined surface. The table 3.7 is divided for the two impact surfaces used in this dissertation. The results regard the cases where splash was expected.

The tests were performed for the two plates, which had almost the same surface roughness, so the values of the impact velocities and dimensionless numbers are approximately identical. Through these results, it is possible to compare with some transition criteria reported in the literature.

Figure 3.22 is presents Bai and Gosman (1995), Mundo et al. (1996) and Vander Wal et. al (2006) criteria. Each fluid has a different symbol and each test has a different color. The color red and blue is for the first and second test, respectively, and only spreading was noticed. The color green represents the cases where the splash was visible in Cunha (2018). However, as already mentioned the results shown in figure 3.22 are regarding the sloped surface and not all the fluids exhibited splash. Due to this, in the cases where splash occurred the symbol was filled, such as 75%JF - 25%HVO and 50%JF - 50%HVO. This figure demonstrates the results for the sloped surface which has a mean surface roughness of Ra=$0.13\mu m$. Thus, the A coefficient is 4447 for Bai and Gosman (1995) criterion. Comparing with the normal impact it was concluded that only the mixtures fitted well for this criterion. The references to the splash that occurs for 75%JF - 25% HVO and 50%JF - 50%HVO are spotted in the splash area. However, all the results for H_2O are found in this area, which includes deposition and splash. This fact was not the most desired. Regarding the 100% Jet-Fuel, this empirical correlation fits well. As can be seen in the graphic, all the results for this fluid are in the deposition area.

Table 3.7 - Results regarding inclined impact which includes present work's surface (Ra=0.13μm) and Cunha (2018) surface (Ra=0.19μm).

	100% JF	75%JF - 25% HVO	50% JF - 50% HVO	H_2O	
$U_0[m/s]$	2.1	3.4	2.9	4.2	Present work' s surface
$U_n[m/s]$	1.8	3.3	2.8	4.2	
$U_t[m/s]$	1.1	0.9	1.0	0.4	
We	416	1138	870	894	
We_n	312	1065	768	887	
We_t	104	76	102	7	
Re	4501	5827	4034	16903	
Re_n	3898	5647	3790	16838	
Re_t	2251	1513	1380	1473	
$Oh\mathbf{x10^3}$	4.5	5.8	7.3	1.7	
La	49081	29949	18706	319550	
Ca	0.09	0.18	0.21	0.06	
Bo	2.85	2.86	2.97	2.04	
Fr	146	399	293	438	
$U_0[m/s]$	2.2	3.2	2.9	4.5	Present work with Cunha (2018) surface
$U_n[m/s]$	1.9	3.1	2.7	4.5	
$U_t[m/s]$	1.1	0.8	1.0	0.4	
We	434	969	824	1056	
We_n	326	907	730	1048	
We_t	109	65	97	8	
Re	4632	5378	3920	18373	
Re_n	3985	5212	3696	18302	
Re_t	2301	1396	1345	1601	
$Oh\mathbf{x10^3}$	4.5	5.8	7.3	1.7	
La	49081	29949	18706	319550	
Ca	0.09	0.18	0.21	0.06	
Bo	2.85	2.86	2.97	2.04	
Fr	152	340	278	517	

Considering Vander Wal et al. (2006) criterion, all the fluids are near to the boundary line. The empirical correlation presented by these authors had also the same result for the normal impact, which can be explained by the similarities in the characteristics of the impact surface.

The H_2O and the 100% Jet-Fuel are plotted in the deposition area, which is in conformity with the results. For the mixtures, this empirical correlation does not provide a so good adjustment to the boundary.

As observed in normal impact, the Mundo et al. (1995) criterion presents the least satisfactory result. None of the fluids are close to the boundary line, and as can be seen in figure 3.22, all the fluids are spotted in the splashing area. A possible reason is the component of the impact velocity since Mundo et al. (1995) only considered the normal component. Another factor could be the difference in the impact surface characterizes. Analyzing figure 3.22, it was noticed that none of the transition criteria perfectly fits in the experimental data. Only the criterion presented by Bai and Gosman (1995) provided a good relation for the mixtures. For the 100% Jet-Fuel and H_2O, the empirical correlation that fits properly in these experimental data is the one proposed by Vander Wal et al. (2006).

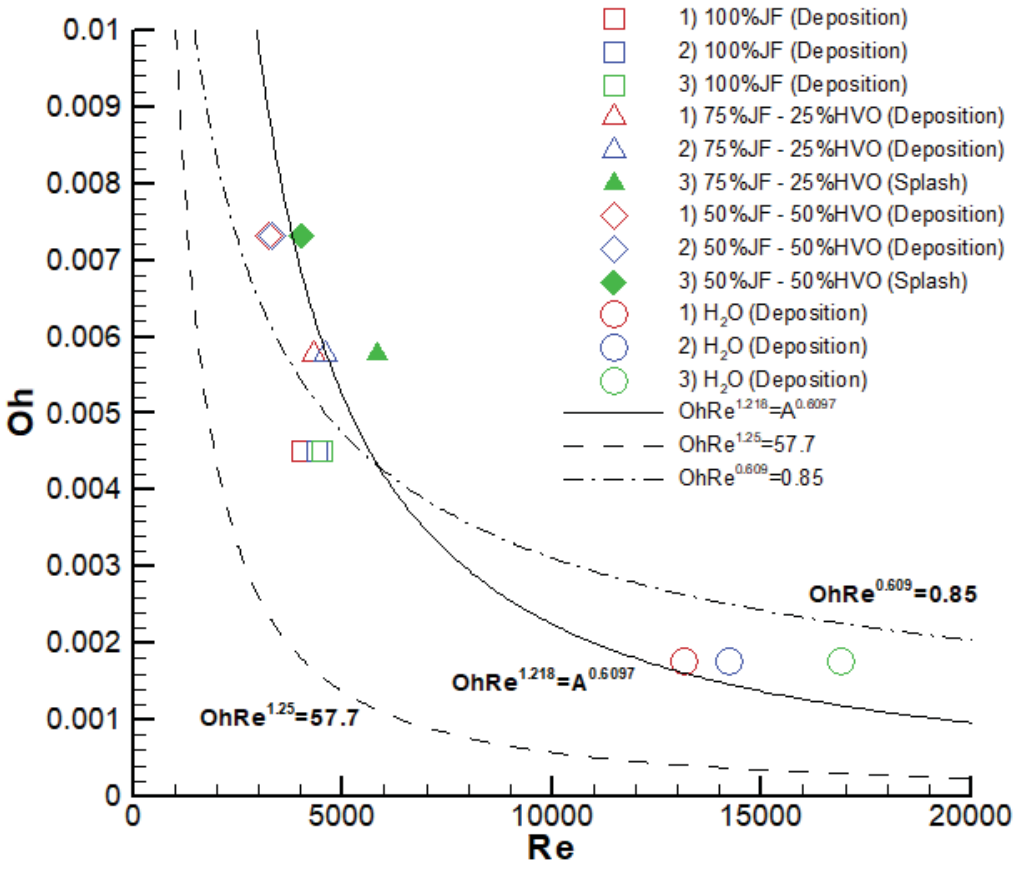

Figure 3.22 - Graphic comparing the experimental results with Bai and Gosman (1995), Mundo et al. (1995) and Vander Wal et al. (2006) splashing threshold, regarding the present work surface and the inclined impact.

Figure 3.23 shows the results obtained for the surface used by Cunha (2018). Comparing with figure 3.22 the relation between the experimental data and the transition criteria is the same.

According to Bai and Gosman (1995) criterion, the splash observed in the mixtures are spotted in the splashing area. Taking into consideration that A coefficient is 4194. The transition criteria provided by Vander Wal et al. (2006) fits properly for the H_2O and 100% Jet-Fuel. Mundo et al. (1995) criterion continues to be the furthest from the experimental data.

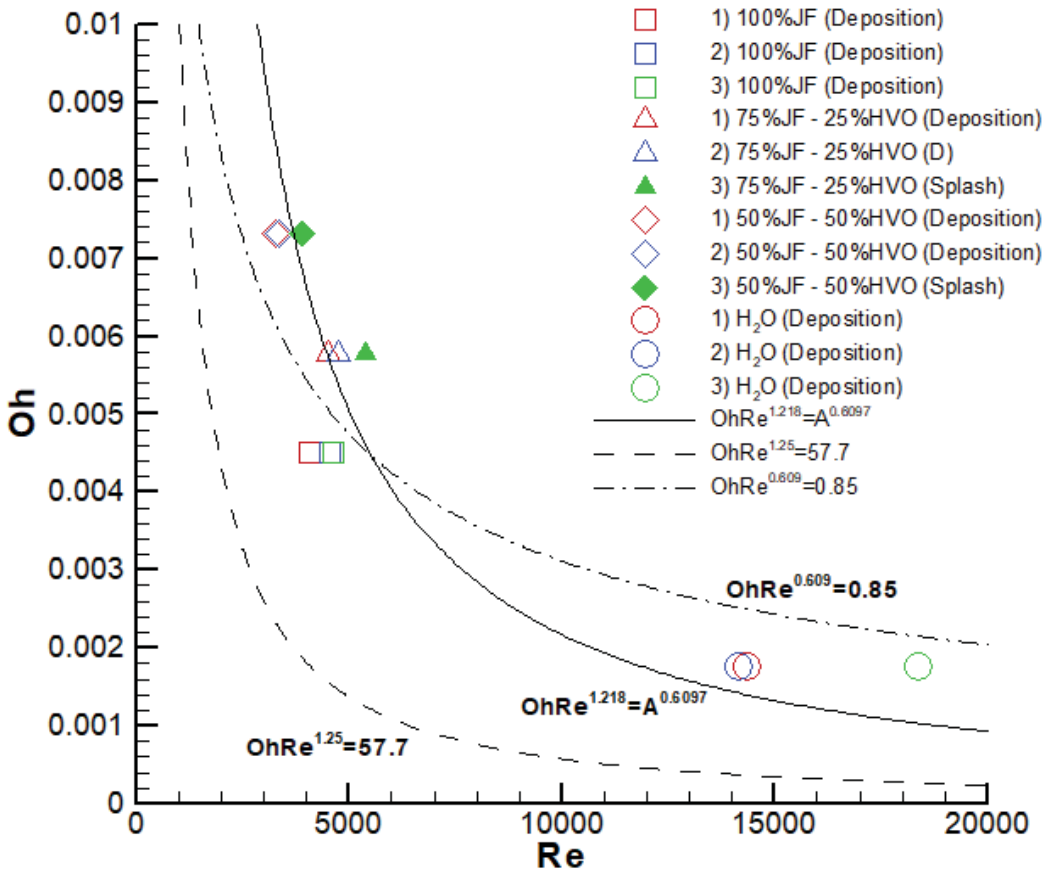

Figure 3.23 - Graphic comparing the experimental results with Bai and Gosman (1995), Mundo et al. (1995) and Vander Wal et al. (2006) splashing threshold, regarding the Cunha (2018) surface and the inclined impact.

When a droplet impacts onto an inclined surface, the impact velocity is composed of two components. The normal (u_n) and tangential (u_t) components. Several authors proposed splashing threshold, which only take into consideration one of the velocity components.

The criterion developed by Mundo et al. (1995) is regarded an oblique impact and, only the normal impact was considered in their splashing threshold, whereas the significance of the tangent velocity was unrecognized.

Bird et al. (2009) determined an empirical correlation for the splash/non-splash boundary, which takes into consideration the tangential velocity. In their experiments, it was used ethanol droplets impacting on a moving aluminum surface,

$$We\sqrt{Re}\left(1-\frac{u_t k}{u_n\sqrt{Re}}\right)^2 = K_c \quad (1.14)$$

where $k = 2.5$ and $K_c = 5700$ which were found out with their experimental data. This empirical correlation considered the asymmetric splash, and the sign of the tangential velocity, u_t, is taken with respect to the spreading direction of the lamella.

Figure 3.24 a) shows the Bird et al. (2009) boundary, an empirical correlation for the results obtained with the impact surface developed for this experimental work. Similarly to the others graphics, each fluid has a symbol, and each test has a color.

All the experimental data are above the boundary line proposed by Bird et al. (2009). The only fluid that as results nearly to this line is the 100% Jet-Fuel. The same conclusion was achieved in figure 3.24 b), where the experimental data are regarded the surface used by Cunha (2018). A possible explanation for this could be the values for k and K_c, which only depended on Bird et al. (2009) activities. So, these values may not be the most appropriate for the present work.

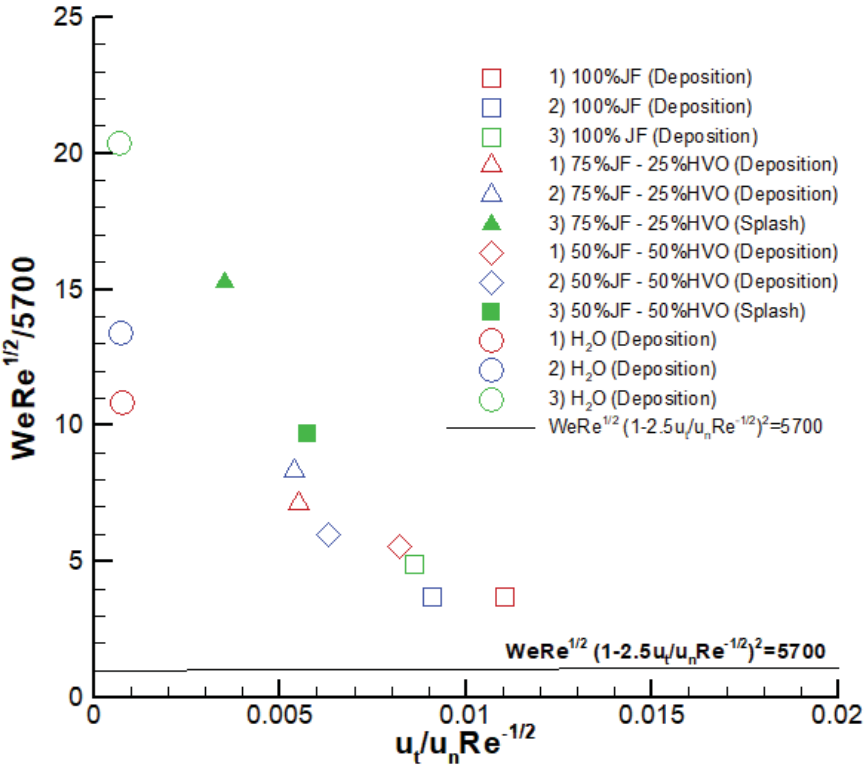

Figure 3.24 - Graphic comparing the experimental results with (Bird et al. 2009) splashing threshold considering the present work' surface

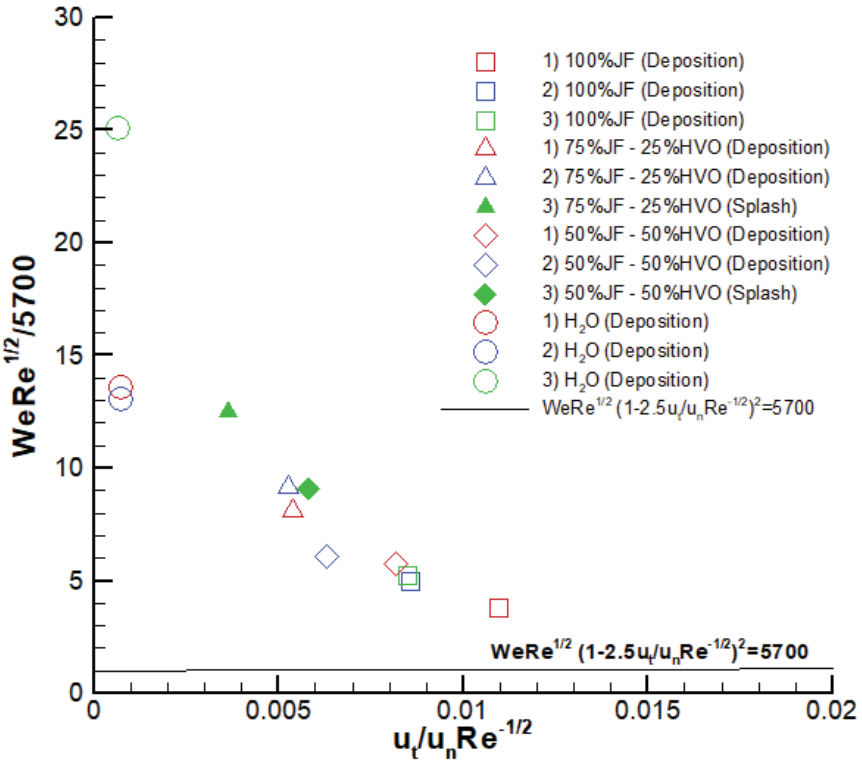

Figure 3.25 - Graphic comparing the experimental results with Bird et al. (2009) splashing threshold, considering Cunha (2018) surface.

The parameter k is related to the lamella's spreading dynamics, such that $k = 1/c$, where c is a constant relating the lamella's spread radius. This constant depends on the normal impact velocity, the elapsed time since the moment of impact and the diameter of the droplet.

Aboud and Kietzig (2015) also elaborated a splashing threshold regarding oblique droplet impacts on surfaces of various wettability. This splashing threshold could be given by equation 1.15.

$$ST = u_{n0} + mu_t \qquad (1.15)$$

where u_{n0} is the critical velocity for splashing at a normal angle of incidence, m defines a slope with respect to u_t, and splashing occurs for cases in which $u_n > ST$. This means that each fluid has an equation. The u_{n0} values for each fluid are presented in table 3.6. The sloped could be achieved by a relation between tangential and normal velocity, these values can be found in table 3.7.

To provide a better understanding of this criterion, table 3.8 summarizes the relation between the u_t, u_n and ST values for each impact surface used in this dissertation. The organization of these parameters allows a better comprehension.

Table 3.8 provides the comparison between the Aboud and Kietzig (2015) criterion and the experimental results. When the normal component of the impact velocity is higher than ST the splash occurs. In the experimental results, the splash was only noticed for 75%JF - 25%HVO and 50%JF - 50%HVO mixtures. For H_2O, it was not possible to observe the deposition/splash transition, so this fluid did not count in the analysis of this criterion.

It was previously reported that each test has its equation, which depends on critical velocity for splashing at a normal angle of incidence, and tangential and normal velocity, whose values are presented in table 3.6 and table 3.7. Thus, through this data, for each fluid it is possible to obtain the correct ST value, applying the equation 1.15.

Considering the surface developed for this dissertation, the Aboud and Kietzig (2015) criterion only presented splash 75%JF - 25%HVO mixture, which is consistent with the experimental results presented. However, 50%JF - 50%HVO mixture also verify this phenomenon and according to Aboud and Kietzig (2015) criterion, this outcome was not spotted. This can be the explained by the difference between the normal velocity and ST values.

For 50%JF - 50%HVO mixture, the difference is relatively small, and the deposition/splash transition may not be defined by a simple line or through a small set of data. Thus, this results could not be properly conclusive.

Regarding to the 100% Jet-Fuel, this empirical correlation perfectly fits with the experimental results. The phenomenon observed was spreading and according to Aboud and Kietzig (2015) this outcome occurs when $ST > u_n$ as can be seen in table 3.8.

Due to the similarity of the mean roughness, the results for the two surfaces are almost the same. Except for the 75%JF - 25%HVO mixture. In this case, the criterion indicates that deposition occurred and the only phenomenon observed was splash.

As can be seen in table 3.8, for the mixtures, the difference between the ST and u_n is slightly small. The explanation given previously can be also applied to this situation.

Table 3.8 - Results regarding Aboud and Kietzig (2015) splashing threshold.

	Aboud and Kietzig (2015) splashing threshold				Phenomena observed	
	u_t [m/s]	u_n [m/s]	ST	Conclusion		
100% JF	1.1	1.8	2.7	$ST>u_n$	Spread	Present work' surface
75%JF - 25%HVO	0.9	3.3	3.1	$ST<u_n$	Splash	
50%JF - 50%HVO	1.0	2.8	3.1	$ST>u_n$	Splash	
100% JF	1.1	1.9	2.7	$ST>u_n$	Spread	Present work with Cunha (2018) surface
75%JF - 25%HVO	0.8	3.1	3.4	$ST>u_n$	Splash	
50%JF - 50%HVO	1.0	2.7	3.3	$ST>u_n$	Splash	

3.4 Summary

This chapter presented the results regarding the experimental work. The purpose of this present work was a comparison between droplet impact onto an inclined surface and an impact onto a surface with a crossflow. Although both are considered oblique impact, it does not imply that the observed phenomena are the same. Thus, in this dissertation, two surfaces with a mean roughness of Ra=0.13μm and Ra=0.19μm were placed above the mechanism that allows a variation of incident angles in order to recreate the same impact conditions.

Table 3.9 presented the phenomena obtained in the present work and, the comparison with the work developed by Cunha (2018), only for the cases where the occurrence of splash was expected.

Table 3.9 - Comparison between the phenomena for each activity considering U_{cf}=7m/s for the work developed by Cunha (2018) and in the present work with an inclined surface.

	Cunha (2018)	**Present work**	
	Impact surface (Ra=0.19μm)	Impact surface (Ra=0.13μm)	Impact surface (Ra=0.19μm)
100% JF	Splash	Non-splash	Non-splash
75%JF - 25%HVO	Splash	Splash	Splash
50%JF - 50%HVO	Splash	Splash	Splash
H_2O	Splash	Non-splash	Non-splash

When a droplet impacts onto an inclined surface, the shape of the droplet distorts, which can condition the phenomena observed. A parameter that influences this kind of impact is the gravity. The component of gravity generates an opposite influence on the lower and upper sides, which influences the phenomenon observed.

Recreating the incident angles and impact velocities, only the 75%JF – 25%HVO and 50% JF – 50%HVO mixtures presented the desired outcome.

As the work progressed, several questions appeared. It was required to understand which could be causing the differences in the phenomena for an inclined surface and for an impact influenced by a crossflow. Thus, various parameters were taken into consideration. For 100% Jet-Fuel and H_2O, spreading was the only visualized phenomenon, so the incident angle and the impact velocity were changed in order to achieve splash. The variation of incident angles does not provide a relevant conclusion, and for the water case, neither in the normal impact or in the inclined impact was observed splash. However, it was possible to observe splash for both cases by increasing the impact velocity.

Regarding the impact surfaces, the difference for the values of surface roughness are practically insignificant. Thus, the results for these impact surfaces are approximately the same. Due to this, considering the five splash thresholds presented, the conclusions are not so different between the two surfaces. In the normal impact, the empirical correlation developed by Bai and Gosman (1995) properly fits for the mixtures. However, Vander Wal et al. (2006) boundary line is relatively closer for all the fluids. Regarding the results for the inclined surfaces, it was achieved the same conclusions as for the normal impact. Mundo et al. (1995) criterion does not fit for every fluid.

All the results are spotted in the splashing area. In their experiments, it was used a rotating disk and it was only considered the normal velocity, which can explain the distance from the boundary line and the results.

It was also presented two splashing thresholds which considered the tangential velocity. For the Bird et al (2009) criterion, no results fit in their empirical correlation. The only fluid close to their boundary line was the deposition for the 100% Jet-Fuel. This could be explained by the values for k and K_c, which are only appropriated for their work. Aboud and Kietzig (2015) developed a splash threshold for oblique impacts and compared it with Bird et al. (2009) criterion. So, Aboud and Kietzig (2015) reported that the values of k and K_c achieved by Bird et al. (2009) are applicable only to their experimental settings, which has been unsuccessfully used by others researchers. This criterion exhibited a properly adjustment for 100% Jet-Fuel. Regarding the mixtures, the comparison with the boundary is not so satisfactory. The water was not considered for this splash threshold due to the fact that it was impossible to observe the deposition/splash transition.

Chapter 4

4. Conclusions and Future Work

In the first section of the last chapter of this dissertation, the relevant conclusions will be presented. Then, the second section is dedicated to future work, where several suggestions will be proposed to improve the knowledge regarding this theme.

4.1 Conclusions

The present work is dedicated to the study regarding the dynamic behavior of a single droplet impinging onto a sloped surface. This dissertation concerns a comparison between the droplet impact onto a sloped surface and the droplet impact onto a surface with the influence of crossflow, the latter being conceived by Cunha (2018). Due to a crossflow, the droplet is susceptible to certain shape deformations that seem to vary the impact conditions. On the contrary, at the impact onto a sloped surface, the droplet is spherical throughout the trajectory and both the gravitational acceleration and movement of the droplet have the same direction. Both studies are considered an oblique impact , which occurs when the droplet impacts onto a surface with a certain angle. However, applying the same impact conditions does not imply similarity for the observed outcomes.

This experimental work recreated several parameters from Cunha (2018) in order to visualize and compare the phenomena, an experimental facility was developed. The reproduction of the incident angles was achieved with a mechanism that allowed the variation of these angles to test the two impact surfaces with approximately the same mean roughness. The fluids used by Cunha (2018) were also a point of interest for this dissertation. Four fluids were considered: 100% Jet-Fuel, 75%JF - 25%HVO, 50%JF - 50%HVO and H_2O, as a reference. The influence of 100% Jet-Fuel and H_2O in impingement processes was already studied and there are only a few studies involving the mixtures. The physical properties of the fluids are essential to understand the dynamic behavior of droplets, which means that density, surface tension, and viscosity influence the impact characteristics. In the work developed by Cunha (2018), the tests performed with a crossflow velocity of $U_{cf} = 7m/s$ provided the visualization of spreading and splash. However, applying the same impact velocity and incident angle in an inclined surface, the 100% Jet-Fuel and H_2O do not present splash as Cunha (2018).

The work developed with the influence of crossflow exhibited splash for the 100% Jet-Fuel and H_2O. On the contrary, in the present work only spreading and fingering occurred, respectively.

Due to this, an effort was made to perceive the reason for not having obtained identical phenomena. Therefore, for these two fluids, the impact velocity and incident angle were varied for the same surface as Cunha (2018). With these results, it was concluded that increasing the incident angle does not promote splash. The variation of the incident angle influences the velocity and the diameter of spreading. Maintaining the impact velocity constant, and only considering the variation of the incident angle, splash only occurs at the normal impact for the 100% Jet-Fuel. However, for H_2O the splash was not observed onto the normal impact. When the impact velocity was increased, and the incident angle was constant, the presence of splash is clearly noticeable for both fluids. When a droplet impacts onto an inclined surface, it can be noticeable asymmetric splash. In this dissertation, the splashes occur on the upper and lower side of the surface. The splash in both sides requires higher impacting energy than the splash in the lower side does. The instability in the lower side is relatively higher than the upper side. In the upper side, the splash is suppressed due to the gravity effect in an inclined surface.

The results obtained by Cunha (2008) revealed that H_2O and the remaining fluids displayed diameters of *3mm* and *4mm*, respectively. In order to compare the dynamic behavior of the fluids, the same diameter is required for an easier comparison. Therefore, the deposition/splash transition of a water droplet ($D_0 = 3mm$) impinging upon a dry surface with and without crossflow was examined. To accomplish this, it was kept a crossflow velocity of $U_{cf} = 7m/s$ and the same surface as Cunha (2018). Due to limitations in the experimental facility, the transition between the phenomena was not achieved. It is also important to mention that the deformation may be a preponderant factor for the understanding of the oblique impacts.

The mixtures were the only fluids that presented the same outcome as the previous work. Recreating the incident angles and the impact velocity for the 75%JF - 25%HVO and 50%JF - 50% HVO mixtures, it is noticeable the occurrence of splash. Therefore, in these fluids, the same phenomenon was observed for an impact onto a sloped surface and an impact with a crossflow. The 50%JF - 50%HVO mixture present splash in the upper and lower side, for the 75%JF - 25%HVO mixture the prompt splash only occurs in the lower side with the respect to the point of impact. Thus, the presence of HVO in these mixtures influences the dynamic behavior of a droplet in an oblique impact.

The outcome analysis provided data regarding impact velocity and consequently dimensionless numbers. The two impact surfaces used for this work have approximately the same mean roughness, meaning that the results are almost the same for an impact onto a sloped surface, it is required an analysis of the components of the impact velocity that also condition the dimensionless numbers. For water it was impossible to observe the transition between deposition and splash in the normal impact.

These experimental results were compared with several splashing thresholds reported in the literature. The empirical correlation developed by Bai and Gosman (1995) takes into consideration the surface roughness.

Regarding the impact normal to the surface with Ra=0.13μm, the mixtures fit perfectly for this criterion. Considering the surface used by Cunha (2018), only the 50%JF - 50%HVO data are coincident with the boundary line. The experimental data for all the fluids are near to the Vander Wal et al. (2006) criterion. On the contrary, in Mundo et al. (1995) criterion, the experimental data are spotted in the splashing area. This divergence in results can be explained by the fact that, in their experiments, a rotating disk was used.

Regarding the impact onto a sloped surface, both surfaces present similar results for the criteria. According to Bai and Gosman (1995), the results for mixtures and 100% Jet-Fuel are in the correct area. However, the deposition verified for water is spotted in the splashing area. The criterion conceived by Vander Wal et al. (2006), similar to the normal impact, provided a boundary line closer to the experimental data. Although for Mundo et al. (1995) criterion, the comparison between empirical correlation and the experimental data do not provide a good agreement . This means that all the results are in the splashing area. Bird et al. (2009) and Aboud and Kietzig (2015) developed two different criterion where the tangential velocity is not despicable. For the Bird et al. (2009) criterion, none of the results are in the correct area for the two impact surfaces. This divergence can be caused by k and K_c values which were obtained in their experiments. Due to this, carefulness is required when considering these variables for comparison with this criterion. Regarding Aboud and Kietzig (2015) criterion, the cases where deposition occurs, this empirical correlations fits perfectly. For the mixtures, the difference between the criterion and the experimental data is narrow. Thus, it is important to mention that the transition between deposition and splash may not be defined by a simple line. There is no comparison to H_2O due to the fact that was not observed the transition deposition/splash for the normal impact.

The researches regarding the oblique impact are scarce. Due to the complexities of this impact an effort is needed to continue to investigate and understand what promotes the different phenomena.

4.2 Future Work

The purpose of this section is to provide several suggestions for future works in order to increase the knowledge regarding this theme.

The first suggestion is regarding a study of droplets impinging onto heated inclined surfaces with the aim of recreating the dynamic in a combustion chamber. The temperature is not the only surface characteristics that could be studied, so the surface roughness is also a point of interest. Through these surface characteristics, it is important to investigate the different outcomes obtained, the size and distribution of the secondary droplets.

There is still a lack of studies regarding oblique impact criteria. It is recommended the development of criteria which takes into consideration the different components of velocity and other characteristics of the experimental work.

References

[1] Worthington, A. M.(1876). “On the Forms Assumed by Drops of Liquids Falling Vertically on a Horizontal Plate” Proceedings of the Royal Society of London , Vol . 25 (1876 - 1877), pp . 261-272 Published by : The Royal Society Stable URL : Society, 25, 261–272.

[2] Engel, O. G.(1955). “Waterdrop collisions with solid surfaces.” Journal of Research of the National Bureau of Standards, 54(5), 281.

[3] Mundo, C., Sommerfeld., M. and Tropea, C.(1995). “Droplet-Wall Collisions: Experimental Studies of the Deformation and Breakup Process”, International Journal of Multiphase Flow, Vol. 21, No. 2, pp. 151-173.

[4] Jayaratne, O. W., and Mason, B. J.(1964). “The Coalescence and Bouncing of Water Drops at an Air/Water Interface.” Proceedings of the Royal Society A: Mathematical, Physical and Engineering Sciences, 280(1383), 545–565.

[5] Levin., Z. and Hobbs., P. V.(1971). “Splashing of Water Drops on Solid and Wetted Surfaces -Hydrodynamics and Charge Separation”, Philosophical Transactions of the Royal Society of London Series A-Mathematical and Physical Sciences, Vol. 269, No. 1200, pp. 555.

[6] Stow., C. D. and Stainer.,, R. D.(1977). “The Physical Product of a Splashing Water Drop”, J. Meteorol. Soc. Jpn., Vol. 55, No. 5, pp. 518-531.

[7] Mehta R. D. and Bradshaw, P.(1979). “Technical Notes Design Rules for Small low Speed Wind Tunnels,” The Aeronautical Journal of the Royal Aeronautical Society , vol. 83, no. 827, pp. 443–449.

[8] Stow, C. D., and Hadfield, M. G.(1981). An Experimental Investigation of Fluid Flow Resulting from the Impact of a Water Drop with an Unyielding Dry Surface. Proceedings of the Royal Society A: Mathematical, Physical and Engineering Sciences, 373(1755), 419–441.

[9] Coordinating Reseach Council Inc.(1983). “Handbook of Aviation Fuel Properties,” Atlanta, p. 122.

[10] Yao, S. C., and Cai, K. Y.(1988). “The dynamics and leidenfrost temperature of drops impacting on a hot surface at small angles.” Experimental Thermal and Fluid Science, 1(4), 363–371.

[11] Bai, C. X., Gosman, A. D.(1995). “Development of a methodology for spray impingement simulation,” SAE Paper 950283.

[12] Marmanis. H and Throddsen. S.(1996). “Scaling of the fingering pattern of an impacting drop” Physics of fluid.

[13] Cossali, G. E., Coghe, A., and Marengo, M.(1997). “The impact of a single drop on a wetted solid surface.” Experiments in Fluids, 22(6), 463–472.

[14] Thoroddsen, S. T., and Sakakibara, J.(1998). “Evolution of the fingering pattern of an impacting drop.” Physics of Fluids, 10(6), 1359–1374.

[15] Kang, B. S., and Lee, D. H.(1999). “On the dynamic behavior of a liquid droplet impacting upon an inclined heated surface”.

[16] Kind, R. J.(2001). “Ice Accretion Simulation Evaluation Test.” North Atlantic Treaty Organization-Research and Technology Organisation-NATO-RTO, Neuilly-Sur-Seine Cedex (Vol. 32).

[17] Rioboo, R., Tropea, C., and Marengo, M.(2001). “Outcomes From a Drop Impact on Solid Surfaces.” Atomization and Sprays, 11(2), 12.

[18] Chen, R. H., and Wang, H. W.(2005). Effects of tangential speed on low-normal-speed liquid drop impact on a non-wettable solid surface. *Experiments in Fluids*, *39*(4), 754–760.

[19] Šikalo, Š., Tropea, C., and Ganić, E. N.(2005). “Dynamic wetting angle of a spreading droplet.” Experimental Thermal and Fluid Science, 29(7 SPEC. ISS.), 795–802.

[20] Šikalo, Š., and Ganić, E. N.(2006). “Phenomena of droplet-surface interactions.” Experimental Thermal and Fluid Science, 31(2), 97–110.

[21] Vander Wal, R. L., Berger. G. M., and Mozes. S. D.(2006). “The splash/non-splash boundary upon a dry surface and thin fluid film,” Experiments in Fluids , vol. 40, no. 1, pp. 53–59.

[22] Yarin, A. L.(2006). “DROP IMPACT DYNAMICS: Splashing, Spreading, Receding, Bouncing…”. Annual Review of Fluid Mechanics, 38(1), 159–192.

[23] Silva, A.(2007). “Experimental and Numerical Study of Physical Aspects of Fuel Processes.” PhD thesis, University of Beira Interior.

[24] Moreira, A. L. N., Moita, A. S., Cossali, E., Marengo, M., and Santini, M.(2007). “Secondary atomization of water and isooctane drops impinging on tilted heated surfaces.” Experiments in Fluids, 43(2–3), 297–313.

[25] Deegan, R. D., Brunet, P., and Eggers, J.(2008). “Complexities of splashing.” Nonlinearity, 21(1).

[26] Bird, J. C., Tsai, S. S. H., and Stone, H. A.(2009). “Inclined to splash: Triggering and inhibiting a splash with tangential velocity.” New Journal of Physics.

[27] Cui, J., Chen, X., Wang, F., Gong, X., and Yu, Z.(2009). “Study of liquid droplets impact on dry inclined surface.” In Asia-Pacific Journal of Chemical Engineering.

[28] Guildenbecher, D. R., López-Rivera, C., and Sojka, P. E.(2009). Secondary atomization. Experiments in Fluids, 46(3), 371–402.

[29] Moita, A. S.(2009). “Thermal and Fluid Dynamics of Droplet Wall Interactions”, Ph. Dissertation.

[30] Liu, J., Vu, H., Yoon, S. S., Jepsen, R. A., and Aguilar, G.(2010). “Splashing Phenomena During Liquid Droplet Impact.” Atomization and Sprays, 20(4), 297–310.

[31] Zen, T. S., Chou, F. C., and Ma, J. L.(2010). “Ethanol drop impact on an inclined moving surface.” International Communications in Heat and Mass Transfer, 37(8), 1025–1030.

[32] Liang, G., Guo, Y., Yang, Y., Zhen, N., and Shen, S.(2013). “Spreading and splashing during a single drop impact on an inclined wetted surface.” Acta Mechanica, 224(12), 2993–3004.

[33] Panão, M. R. O., Moreira, A. L. N., and Durão, D. F. G. (2013). Effect of a cross-flow on spray impingement with port fuel injection systems for HCCI engines. *Fuel*, *106*, 249–257.

[34] Antonini, C., Villa, F., and Marengo, M.(2014). “Oblique impacts of water drops onto hydrophobic and superhydrophobic surfaces: Outcomes, timing, and rebound maps.” Experiments in Fluids, 55(4).

[35] Liang, G., Guo, Y., Shen, S., and Yu, H.(2014). “A study of a single liquid drop impact on inclined wetted surfaces.” Acta Mechanica, 225(12), 3353–3363.

[36] Yeong, Y. H., Burton, J., Loth, E., and Bayer, I. S.(2014). “Drop Impact and Rebound Dynamics on an Inclined Superhydrophobic Surface.” Langmuir, 30(40), 12027–12038.

[37] Aboud, D. G. K., and Kietzig, A. M.(2015). “Splashing Threshold of Oblique Droplet Impacts on Surfaces of Various Wettability”. Langmuir.

[38] Neste Corporation.(2015). Neste Renewable Diesel Handbook. Neste, 1–33.

[39] Rodrigues, C.(2015). “Modelling of a Biofuel Spray Wall Impingement,” Ph.D. dissertation, Universidade da Beira interior.

[40] Sinha, A., Surya Prakash, R., Madan Mohan, A., and Ravikrishna, R. V. (2015). Airblast spray

in crossflow - structure, trajectory and droplet sizing. *International Journal of Multiphase Flow, 72*, 97–111.

[41] Jin, Z., Zhang, H., and Yang, Z.(2016). “The impact and freezing processes of a water droplet on a cold surface with different inclined angles.” International Journal of Heat and Mass Transfer, 103, 886–893.

[42] Josserand, C., and Thoroddsen, S. T. (2016). "Drop Impact on a Solid Surface." Annual Review of Fluid Mechanics, 48(1), 365–391.

[43] Shen, C., Yu, C., and Chen, Y.(2016). “Spreading dynamics of droplet on an inclined surface. “Theoretical and Computational Fluid Dynamics, 30(3), 237–252.

[44] Pizziol, B.(2017). “Design and Experimental Characterization of an Air-Assisted, Impinging-Jets Atomizer for Aeronautical Applications With Biofuel,” Master Thesis, Politecnico di Milano.

[45] Cunha, N.(2018). “Experimental Study of a Single Droplet on Dry Surface with and without a Crossflow : Jet Fuel and Biofuel Mixtures”, Master Dissertation, Universidade da Beira Interior.

[46] Cunha, N., Ribeiro, D., Barata, J., and Silva, A.(2018). “The Splash Deposition Transition Limits of a Biofuel Droplet Wall Impact with a and without Crossflow” ICLASS 2018, 14 th Triennial International Conference on Liquid Atomization and Spray Systems, Chicago, IL, USA, July 22-26, 2018.

[47] Lee, T., and Park, J. E. (2018). Determination of the drop size during atomization of liquid jets in cross flows Arizona State University Department of Mechanical Engineering.

[48] Ribeiro, D.(2018). “Experimental Study of a Single Droplet Impinging upon Liquid Films : Jet Fuel and Biofuel Mixtures”, Master Dissertation, Universidade da Beira Interior.

Annex

Annex 1

Papers accepted to Conferences

Comparative study of droplet impact onto sloped surface versus a droplet impact onto a surface with a crossflow

Inês Ferrão[1], Jorge Barata[2] and André Silva[3]
Universidade da Beira Interior, Covilhã, 6200-001, Portugal

Extended Abstract

The droplet impact is a common phenomenon that occurs multiple times in several applications such as fuel injection in internal combustion engines [1], processes involving spray paints and cooling of electronic equipment or even in nature. Due to the technological advance, it becomes possible to observe in detail the dynamic impingement. The phenomena that are more reported in the literature are deposition, prompt splash, corona splash, receding breakup, partial rebound and complete rebound [2]. However, the outcomes of the impingement depend on the various impact conditions. In the study of droplet impingement, the influencing parameters are the liquid along with its physical properties, the impact surface, the surrounding environment and other conditions. The combination of these terms leads to different and unique effects.

The major goal of our research is to elaborate a comparison that involves an experimental study of the fluid dynamic phenomena occurring during the impact of liquid droplets onto a dry surface with a cross flowing air [3, 4] and an inclined surface was idealized for this activity. In order to maintain the consistency of the results, the conditions regarding the impact surface and the fluids were kept the same. It was considered a combination of a conventional jet fuel and a biofuel (HVO – Hydroprocessed Vegetable Oil) more specifically Jet A-1 and NEXBTL, with the aim to implement new alternatives to reduce the pollution levels. It is through these innovations that it is possible to improve various systems such as piston engines or gas turbines with alternative fuels. Therefore, in this research, four different fluids were used: 100% Jet A-1, 75% Jet A-1 / 25% HVO, 50% Jet A-1 / 50% HVO and pure water that was used as a reference. The droplet diameter of these fluids is approximately *3mm* to the mixtures and 100% Jet A-1. The water droplet diameter is *4mm* [3]. It is only allowed by civil aviation mixtures with a minimum of 50% Jet A-1 in volume [5] and that is why the mixtures above were selected. The study of droplet behavior was on a smooth and dry aluminum surface. It is also important to mention that were used the same droplet diameter.

In Cunha's work [3] was observed that the droplet, initially spherical, descends vertically from a predefined height and it is exposed to the presence of crossflow as can be seen in Figure 1. Through the application of this crossflow, the droplet suffers a certain deformation that seems to vary the condition of impact (Figure 2). Knowing that the crossflow velocity is *7 m/s* and analyzing the movement of the droplet, it is visible that each test describes different incident angles.

The crossflow velocity, U_c, and the height impact influence the impact velocity, U. Therefore, the impact velocity was divided into two vectors, the normal (u_n) and the tangential (u_t) direction.

The angle between the impact absolute velocity and the impact surface is designated as incident angle θ, shown in Figure 3. Thus, the impact velocity and the incident angle are found the most important parameters to consider.

In the past, some investigations were done with a certain effort to understand the influence of the incidence angle on the dynamics of the droplet impact. It is notable that the outcome depends on the incidence angle. This fact was considered by Jayarate and Mason [6] and it is still necessary to mention that this angle also influences the direction of the secondary droplets in the impact with smooth surface. Few years later, Yao and Cai [7] reported that if θ is not *90°*, the tangential velocity component acts to destabilize the spreading liquid film, hence to enhance the fragmentation of the droplet following the impingement.

To analyze all the information with the necessary rigor it was followed a strict methodology. It was designed and elaborated an experimental set-up that has the possibility to vary the surface angles. This mechanism can range from *0°* to *80°*, and it has above it a smooth, dry aluminum plate. In order to achieve a certain quality in the motion capture of droplets and the different phenomena, a high speed camera was used, more concretely a FASTCAM mini UX50. Behind the impact surface were placed several Led to facilitate the visualization and the image acquisition was pursued with *4000fps* and three different exposure times, *1/10000* sec, *1/12800* sec and *1/20840* sec. The impact velocity

[1] Master Student, Aerospace Sciences Department, ines_ferrao_abril_11@hotmail.com.
[2] Full Professor, Aerospace Sciences Department, and Associate Fellow of AIAA, jmmbarata@gmail.com.
[3] Assistant Professor, Aerospace Sciences Department, and Member of AIAA, andre@ubi.pt.

depends on the height of the needle above the surface. The droplets formed leave the needle when the gravity exceed the force due to surface tension. This needle has an inner diameter of *1.5mm* and it is connected to a syringe pump with a pumping rate of *0.5ml/ms*. For the recognition of the outcomes and the characterization of the droplets, it was necessary to carry out the image data processing.

To determine the impact velocity the MATLAB Software was used. An algorithm was developed using a function that determined the droplet centroid, considering two frames with distancing of *1.75ms*. This was only possible through image binarization using subtraction of images and the pixel size value.

In a representative way Figure 4 a) relates the behavior of droplet with the influence of a crossflow and the incident angle. Figure 4 b) is shown the impact surface used in this research. With the purpose to recreate the same angle as the Cunha et al [4] it was necessary to give a certain inclination to the plate. This inclination is given by the angle α. Its value can be achieved by subtraction $90° - \theta$. The angles and velocities used in the activity depended on Cunha et al results [4] and can be found in Table 1.

Table 1 – Comparation between velocity results in present work and velocity results in Cunha et [4], when splash occurs.

	Present Work	**Cunha et al [4]**	
	Inclined surface	U_e=7m/s	
	U [m/s]	U [m/s]	θ [°]
75% Jet A-1 / 25% HVO	3.19	3.48	75.72
50% Jet A-1 / 50% HVO	2.89	3.13	72.14

The results obtained with this comparison demonstrated that it was only registered splash in mixtures, so 100% Jet A-1 and pure water do not present the same outcome following the Cunha et al [4] methodology. This observation suggests that probably the biofuel properties influence the impact result.

In present work, the gravity acceleration and the movement of droplet have the same direction and there is no influence of crossflow. However, in Cunha's work [3] due to crossflow, U_e=7m/s, deformation of the droplet occurs as seen in Figure 2. It is also important to mention that in this case the droplet doesn't have the same direction as the gravity acceleration. In order to have agreement with the results, the same fluid properties and the same droplet diameter were considered.

Figure 5 a) correspond to a 50% Jet A-1/ 50% HVO droplet impinging onto an aluminum plate in a crossflow of *7 m/s*. However in Figure 5 b) represented a 50% Jet A-1 / 50% HVO droplet impinging onto an aluminum plate when θ is *72,14°*.

Another relevant characteristic is the drop deformation after impact. As can be seen in Figure 5 a) and b) after the impact the droplet demonstrated asymmetric splash which is a more intense in one side.

Experimental work on inclined surfaces is scarce. However, this type of impact is important and it is necessary to investigate in order to understand the parameters that most condition it. Thus, with this work several doubts arise. What are in reality the parameters that influence the phenomenon in inclined surface, the fluids properties, the inclination, among others.

Acknowledgments

The present work was performed under the scope of Laboratório Associado em Energia, Transportes e Aeronáutica (LAETA) – activities and it was supported by Fundação para a Ciência e Tecnologia (FCT) through the project UID/EMS/50022/2013.

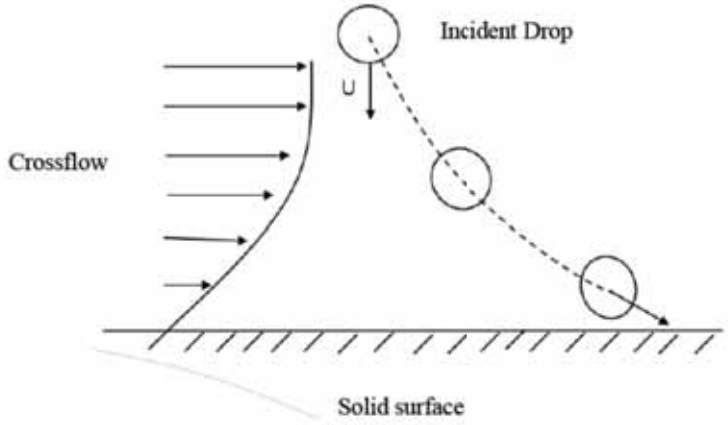

Figure 1 - Representative diagram of Cunha [3] experimental activity

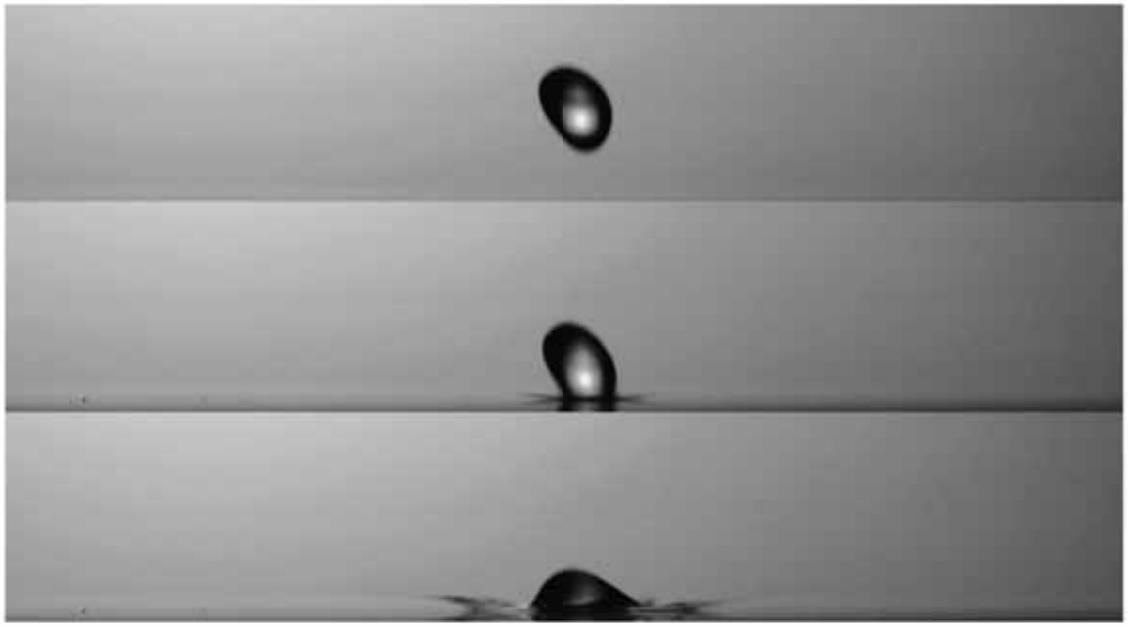

Figure 2 - Droplet deformation with influence of the crossflow adapted from [3]

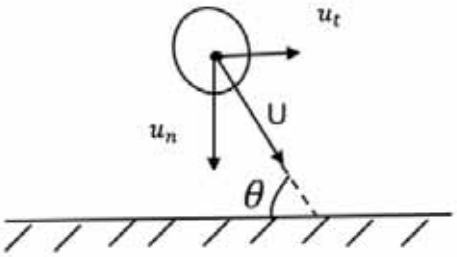

Figure 3 - Representation of velocity vector and incident angle

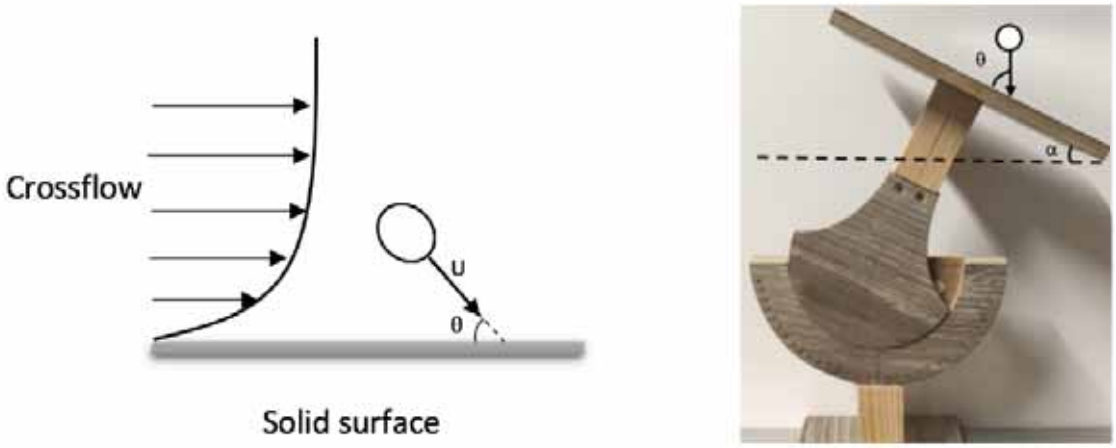

a) b)

Figure 4 - Representation of incident angle in Cunha et al [4] and the impact surface in the present work

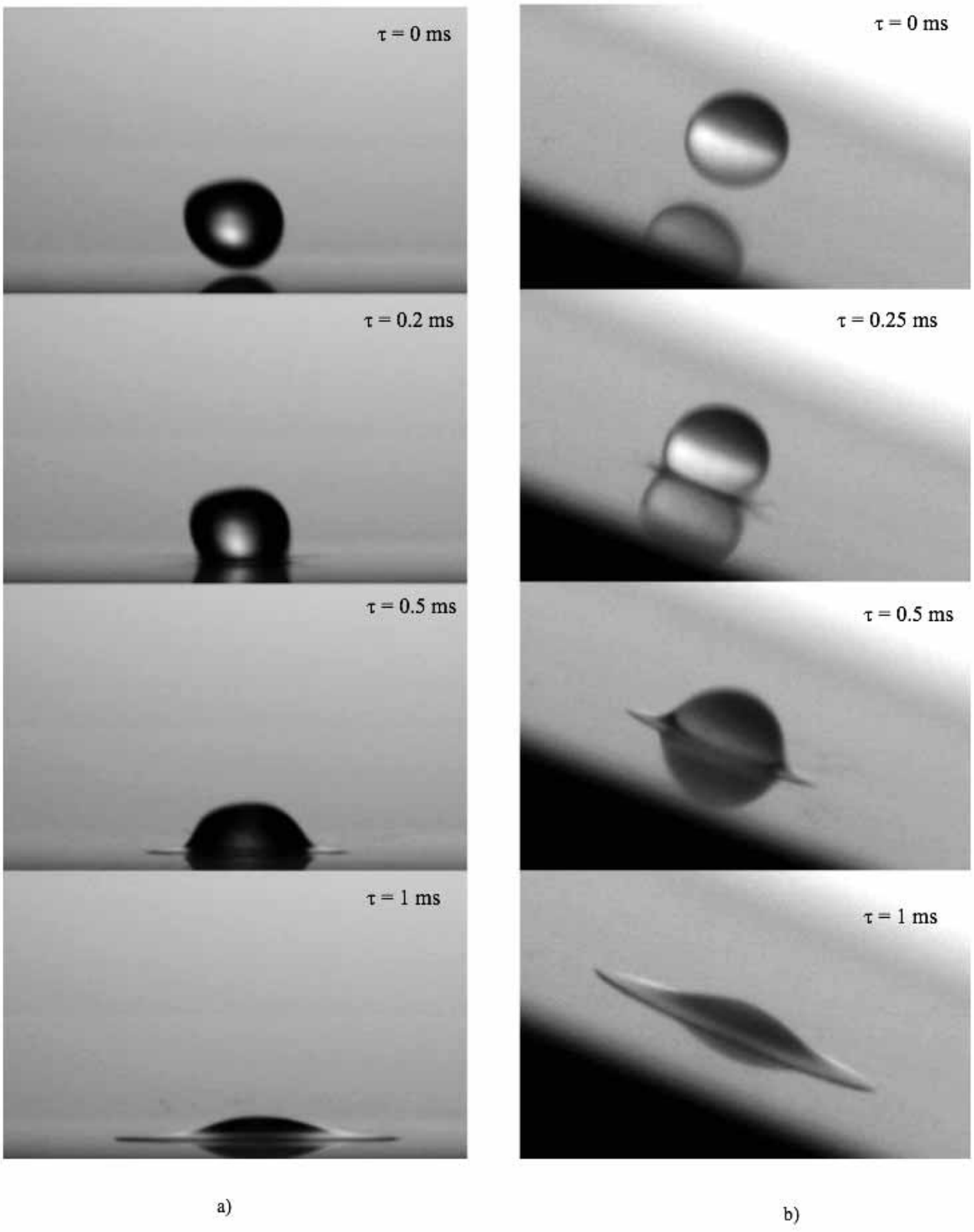

Figure 5 – Visualization of 50% Jet A / 50% HVO droplet impinging onto an aluminum plate D_0=*3mm*, *U=2.4m/s* , a) with a crossflow velocity of *7m/s*, b) with a slope angle of *72.14°*.